

## Supplementary Materials for

### Global hotspots of particulate organic carbon losses under climate change

Siyi Sun<sup>1,2</sup>, M. Francesca Cotrufo<sup>3</sup>, R. A. Viscarra Rossel<sup>4</sup>, Carsten W. Mueller<sup>5,6</sup>, Morimaru Kida<sup>7</sup>, Ailsa G. Hardie<sup>8</sup>, Alec Mackay<sup>9</sup>, Alexander H. Krichels<sup>10,11</sup>, Wulf Amelung<sup>12</sup>, Amit Kumar<sup>13</sup>, Azamat Suleymanov<sup>14,15</sup>, Baoku Shi<sup>16</sup>, Bernard Jackson Cosby<sup>17</sup>, César Plaza<sup>18,19</sup>, César Terrer<sup>20</sup>, Chang Liang<sup>21</sup>, Chang Liao<sup>22</sup>, Christopher Just<sup>23</sup>, Ding Guo<sup>24</sup>, Emanuele Lugato<sup>25</sup>, Enqing Hou<sup>26</sup>, Fan Ding<sup>27</sup>, Fazhu Zhao<sup>28</sup>, Feng Tao<sup>29</sup>, Fernando T. Maestre<sup>30</sup>, Franco Bilotto<sup>31</sup>, Fuzhong Wu<sup>32</sup>, Gisela V. García<sup>33</sup>, Gongwen Luo<sup>34</sup>, Guangxuan Han<sup>35</sup>, Guillermo A. Studdert<sup>33</sup>, Guillermo Hernandez-Ramirez<sup>36</sup>, Guoxiang Niu<sup>26</sup>, Gervasio Piñeiro<sup>37,38</sup>, Gustavo Saiz<sup>39</sup>, Haikuo Zhang<sup>40</sup>, Hamada Abdelrahman<sup>41</sup>, Haodi Xu<sup>42</sup>, Inma Lebron<sup>17</sup>, Irina Kurganova<sup>43</sup>, Jennifer Blesh<sup>44</sup>, Jeppe Å. Kristensen<sup>45,46</sup>, Ji Liu<sup>1</sup>, Jiacong Zhou<sup>1</sup>, Jianping Wu<sup>22</sup>, Jitendra Ahirwal<sup>47</sup>, Junji Cao<sup>48</sup>, Jørgen E. Olesen<sup>49,50</sup>, Karin Kauer<sup>51</sup>, Katerina Georgiou<sup>52</sup>, Kees Jan van Groenigen<sup>53</sup>, Kristof Van Oost<sup>54</sup>, Kwame Agyei Frimpong<sup>55</sup>, Lei Deng<sup>56</sup>, Liane G. Benning<sup>57</sup>, Liang Guo<sup>56</sup>, Lizzie Mujuru<sup>58</sup>, Manuel Delgado-Baquerizo<sup>59</sup>, Maoz Dor<sup>60</sup>, Mehdi Rahmati<sup>61,62</sup>, Min Luo<sup>63</sup>, Olga Kalinina<sup>64</sup>, Olli Hyvärinen<sup>65</sup>, Pablo García-Palacios<sup>18,66</sup>, Paige Hansen<sup>3</sup>, Patra Rounak<sup>67</sup>, Pengpeng Duan<sup>68</sup>, Pengzhi Zhao<sup>69,54</sup>, Peter M. Homyak<sup>11</sup>, Rajan Ghimire<sup>70</sup>, Renaldas Žydelis<sup>71</sup>, Roland Bol<sup>62</sup>, Ronaldo Vibart<sup>9</sup>, Ruiying Chang<sup>72</sup>, Ruyi Luo<sup>73</sup>, Sebastian Villarino<sup>74</sup>, Shuai Xue<sup>75</sup>, Shuli Niu<sup>76</sup>, Shuotong Chen<sup>77</sup>, Tengfei Yu<sup>78</sup>, Steven J. Hall<sup>79</sup>, Thomas Kätterer<sup>80</sup>, Tida Ge<sup>81</sup>, Vusumuzi Erick Mbanjwa<sup>82</sup>, Vyacheslav M. Semenov<sup>43</sup>, Weixing Liu<sup>83</sup>, Weiyu Shi<sup>84</sup>, Wei Zhang<sup>68</sup>, Wolfgang Wanek<sup>85</sup>, Wolfram Buss<sup>86</sup>, Xiangrong Cheng<sup>87</sup>, Xiankai Lu<sup>26</sup>, Xiaojun Shi<sup>88</sup>, Xiaoli Cheng<sup>22</sup>, Xiaorong Wei<sup>56</sup>, Xiaotong Liu<sup>89</sup>, Xuhui Zhou<sup>90</sup>, Yahya Kooch<sup>91</sup>, Yangquanwei Zhong<sup>92</sup>, Yanjiang Cai<sup>40</sup>, Yan Yang<sup>76</sup>, Yiqi Luo<sup>42</sup>, Yixuan Zhang<sup>1</sup>, Yunbin Qin<sup>93</sup>, Yunting Fang<sup>94</sup>, Yuting Liang<sup>95</sup>, Yuyi Li<sup>96</sup>, Zengming Chen<sup>95</sup>, Zhanfeng Liu<sup>26</sup>, Zhaoliang Song<sup>97</sup>, Zhongkui Luo<sup>98</sup>, Zhisheng An<sup>1</sup>, Ji Chen<sup>1,99,100\*</sup>

\*Corresponding author.

Ji Chen, chenji@ieecas.cn

**This file includes:**

Supplementary Notes

Supplementary Methods

Supplementary Table 1 to 5

Supplementary Figure 1 to 39

Supplementary References

## **Supplementary Notes**

### **Different methods for measuring particulate organic carbon and mineral-associated organic carbon**

#### **1 SOC fractionation based on density**

##### **1.1 Fractionation using sodium polytungstate (or sodium iodide)<sup>1</sup>**

The soil samples were air-dried and sieved by 2-mm mesh. Subsequently, the soil samples were placed in a centrifuge tube, with sodium polytungstate (SPT) or sodium iodide (NaI) at a density of 1.60-1.85 g cm<sup>-3</sup>. The centrifuge tube was gently shaken by hand or rotated in an overhead shaker to allow free soil organic carbon (SOC) outside aggregates. The above steps were repeated two to three times. After centrifugation, the floating light fraction (LF) was separated from the heavy fraction (HF) by suction and filtration through a glass fiber/nylon filter and washed thoroughly with deionized water. After drying to constant weight in a 60 °C oven, each fraction was analyzed for carbon (C) content. Here, the C content of LF was considered as POC and the C content of HF was considered as MAOC.

##### **1.2 Fractionation using sodium polytungstate (or sodium iodide) and ultrasonic<sup>2</sup>**

The soil samples were air-dried and sieved by 2-mm mesh. Subsequently, the soil samples were placed in a centrifuge tube, with sodium polytungstate (SPT) or sodium iodide (NaI) at a density of 1.60-1.85 g cm<sup>-3</sup>. The centrifuge tube was gently shaken by hand and centrifuged. Then the free particulate organic carbon (fPOC) was collected, and the remaining suspension was brought back to its initial volume with fresh SPT and ultrasonicated. After centrifugation, the occluded particulate organic carbon (oPOC) was collected. The residues were washed with deionized water three times to remove the residue SPT (or NaI). The residue fraction was mineral-associated organic carbon (MAOC). After drying to constant weight in a 60 °C oven, each fraction was analyzed for C content. Here, the sum of fPOC and oPOC content is calculated as POC.

#### **2 SOC fractionation based on particle size**

(Regarding the size, there are different cut-offs in different publications, for example, 50, 53, or 63 µm.)

##### **2.1 Fractionation using sodium hexametaphosphate<sup>3</sup>**

The soil samples were air-dried and sieved by 2-mm mesh. Subsequently, the soil samples were shaken in dilute (0.5%) sodium hexametaphosphate (HMP) solution (or deionized water, or deionized water with glass balls) for 15 to 18 hours. The dispersed soil was then rinsed onto a 53 µm sieve. We collected the fraction that passed through the sieve as MAOC (< 53 µm) and the fraction that remained on the sieve was POC (> 53 µm). After drying to constant weight in a 60 °C oven, each fraction was analyzed for C content.

## **2.2 Fractionation using water and ultrasonic<sup>4</sup>**

The soil samples were air-dried and sieved by 2-mm mesh. Subsequently, they were dispersed in deionized water with particulate organic matter removal at sonication. The dispersed soil was then rinsed onto the sieve. The fraction that passed through the sieve was collected as MAOC ( $< 53 \mu\text{m}$ ) and the fraction that remained on the sieve was POC ( $> 53 \mu\text{m}$ ). After drying to constant weight in an oven at  $60^\circ\text{C}$ , each fraction was analyzed for C content.

## **3 SOC fractionation based on particle size and density**

### **3.1 Fractionation using sodium polytungstate (or sodium iodide) and sodium hexametaphosphate<sup>5</sup>**

The soil samples were air-dried and sieved by 2-mm mesh. Subsequently, the soil samples were placed in a centrifuge tube, with SPT or NaI at a density of  $1.60\text{--}1.85 \text{ g cm}^{-3}$ . The centrifuge tube was gently shaken by hand or rotated in an overhead shaker. Then, the samples were centrifuged and the LF was collected from the floating fraction. The residual soil sample was dispersed in HMP solution and shaken for 15 to 18 hours. The dispersed soil was then rinsed onto a  $53 \mu\text{m}$  sieve. The fraction that passed through the sieve was collected as MAOC ( $< 53 \mu\text{m}$ ) and the fraction that remained on the sieve was POC ( $> 53 \mu\text{m}$ ). After drying to constant weight in a  $60^\circ\text{C}$  oven, each fraction was analyzed for carbon content. Here, the C content of LF is considered as a part of POC.

### **3.2 Fractionation using sodium polytungstate and ultrasonic<sup>6</sup>**

The soil samples were air-dried and sieved by 2-mm mesh. Subsequently, the soil samples were placed in a centrifuge tube, with SPT or NaI at a density of  $1.60\text{--}1.85 \text{ g cm}^{-3}$ . The centrifuge tube was gently shaken by hand or rotated in an overhead shaker. After centrifuging, the LF was collated from the floating fraction. The residual soil in the centrifuge tube was resuspended and dispersed in the SPT or NaI solution by sonication. The dispersed soil was then rinsed onto a  $53 \mu\text{m}$  sieve. The fraction that passed through the sieve was collected as MAOC ( $< 53 \mu\text{m}$ ) and the fraction that remained on the sieve was POC ( $> 53 \mu\text{m}$ ). After drying to constant weight in a  $60^\circ\text{C}$  oven, each fraction was analyzed for C content. Here, the C content of LF is considered as a part of POC.



## Supplementary Methods

### Biogeochemistry-Informed Neural Network (BINN)

BINN integrates process-based modeling with neural networks to infer soil particulate organic carbon (POC), mineral-associated organic carbon (MAOC), and subsurface processes from observational data. The framework assumes that soil carbon pools are approximately at steady state and that environmental covariates (climate, vegetation, and soil properties) provide sufficient information to predict spatially varying biogeochemical parameters. Specifically, the BINN framework consists of two major components: (1) a neural network that learns the relationships between environmental covariates and biogeochemical parameters, enabling spatially explicit prediction of key process rates, and (2) a process-based model—the Community Land Model version 5 (CLM5) soil carbon module—reformulated in a differentiable matrix form, which simulates SOC dynamics across carbon pools using the parameters predicted by the neural network.

#### 1 Neural Network

We implemented a fully connected neural network to spatially resolve relationships between environmental covariates and biogeochemical parameters. The neural network uses embedding layers to encode categorical covariates, and a spatial positional encoder to compute a vector embedding for each location. We combined these embeddings with the numeric covariates into a vector  $e$ , and passed this through a 4-layer neural network  $f_{NN}$  (Equation 1) with learnable weights/biases  $w$ , which outputs a vector  $z$  with 21 values (one for each parameter in the process-based model):

$$z = f_{NN}(e; w) \quad (1)$$

To ensure compliance with the predefined bounds derived from prior knowledge of biogeochemical parameter ranges, we transformed  $z$  into predicted parameters  $p$  through element-wise application of sigmoid functions  $\sigma$  (Equation 2). This ensures each parameter  $p_i$  stays within these prior ranges:

$$p = \sigma(y_i, \gamma, \theta_{i,max}, \theta_{i,min}) = \frac{1}{1 + \exp(-\frac{z_i}{\gamma})} * (\theta_{i,max} - \theta_{i,min}) + \theta_{i,min} \quad (2)$$

where  $z_i$  is the  $i$ -th output of the neural network,  $\theta_{i,max}$  and  $\theta_{i,min}$  are plausible limits for each biogeochemical parameter  $i$ , taken from previous literature<sup>7</sup>, and  $\gamma$  is a learnable parameter that controls how fast the predictions converge to  $\theta_{i,min}$  or  $\theta_{i,max}$ . The final output of the neural network is  $p$ , a vector of 21 biogeochemical parameters for each location, where each parameter  $p_i$  is constrained to be in its prior range ( $\theta_{i,min}, \theta_{i,max}$ ).

#### 2.2 Process-based Model

In this study, we employed the soil carbon module of the Community Land Model version 5 (CLM5) to represent our knowledge of soil organic carbon (SOC) dynamics. The CLM5 model, iteratively refined over the past decade for SOC dynamics

simulation<sup>8</sup>, mathematically formalizes current biogeochemical understanding through a system of 140 partial differential equations.

The CLM5 simulates SOC dynamics across 20 soil layers extending to 8 m depth. This study focuses exclusively on the 30 cm depth. Each layer contains 7 carbon pools: one coarse woody debris pool, three litter pools (metabolic, cellulose, and lignin), and three SOC pools differentiated by turnover times (fast, slow, and passive). POC was derived from the "fast" pool, while MAOC corresponded to the "slow" and "passive" pools. We incorporated into our neural network framework a differentiable CLM5 model, whose structure can be represented in a matrix form as<sup>9,10</sup>:

$$\frac{dX(t)}{dt} = B(t)I(t) - A\xi(t)KX(t) - V(t)X(t) \quad (3)$$

where  $I(t)$  is the total carbon input from vegetation at time  $t$ ,  $B(t)$  is the allocation of carbon input to different pools.  $A$  is the carbon transfer matrix, quantifying horizontal carbon movement between pools in the same layer.  $K$  is the intrinsic decomposition rate of each carbon pool, which is the same for each pool across layers.  $\xi(t)$  captures how the environment modifies the intrinsic decomposition rate in the  $K$  matrix by temperature ( $\xi_T$ ), water ( $\xi_W$ ), oxygen ( $\xi_O$ ), and depth ( $\xi_D$ ) scalars.  $V(t)$  defines how SOC enters and leaves each layer.  $X(t)$  is carbon pool size. The term  $B(t)I(t)$  represents the vegetation carbon input,  $A\xi(t)KX(t)$  describes the SOC movements among the 7 pools within each layer. The  $V(t)X(t)$  indicates vertical SOC movements along the soil profile. The  $t$  in parentheses means that the corresponding process changes with time.

Equation (3) contains 21 biogeochemical parameters<sup>11</sup> that quantify the strength and reflect properties of different processes (e.g., transformation and stabilization of SOC, temperature sensitivity of soil respiration, and substrate quality) in the soil carbon cycle. Because those processes are highly variable depending on different climate conditions or soil properties, the values quantifying their strength or properties (i.e., the parameter values) should differ with changing environments<sup>12</sup>. We employed the neural network embedded in BINN to dynamically predict these biogeochemical parameter values from environmental covariates. The resultant parameter estimates, combined with environmental forcings, drive Equation (3) to simulate steady-state POC and MAOC stock. Additionally, we predicted POC and MAOC stock from 2081-2100 by integrating these parameter estimates with environmental forcing variables under shared socioeconomic pathway 245 (SSP245).

**Supplementary Table 1 Summary of reported drivers of soil particulate organic carbon (POC).**

Reference	Region	Main conclusions about POC
(Hansen et al., 2024) <sup>13</sup>	Global	Mean annual temperature and soil pH play key roles in global POC.
(Guo et al., 2024) <sup>14</sup>	Global	Edaphic factors are key drivers of global POC.
(Zhou et al., 2024) <sup>15</sup>	Global	Mean annual temperature and net primary productivity are key drivers of global POC.
(García-Palacios et al., 2024) <sup>16</sup>	Global cold regions	POC in cold regions are most vulnerable to warming.
(Zhang et al., 2024) <sup>17</sup>	Global forests	Mean annual temperature and soil pH are the primary drivers of POC content in forest soils.
(Viscarra Rossel et al., 2019) <sup>18</sup>	Australia	Climate factors are the main controlling factors of POC in Australia.

**Supplementary Table 2 Gridded data used in the present study.**

Variables	Data source, resolution
Mean annual temperature (°C)	WorldClim version 2.1, 2.5 minutes
Mean annual precipitation (mm)	WorldClim version 2.1, 2.5 minutes
Temperature seasonality	WorldClim version 2.1, 2.5 minutes
Precipitation seasonality	WorldClim version 2.1, 2.5 minutes
Potential evapotranspiration	GLEAM v3, 0.25°
Background nitrogen deposition	ORNL DAAC, 2017, 5° × 3.75°
Land cover	MODIS MCD12C1 product, 1/12°
Future land cover	(Li et al., 2017) <sup>19</sup> , 1km
Net primary productivity (kg C m <sup>-2</sup> yr <sup>-1</sup> )	MOD17A3HGF v006, 10 km
Leaf area index	(Cao et al., 2023) <sup>20</sup> , 10 km
Soil pH	Harmonized World Soil Database (HWSD), 1 km
Soil clay (%)	Harmonized World Soil Database (HWSD), 1 km
Soil silt (%)	Harmonized World Soil Database (HWSD), 1 km
Bulk density (g cm <sup>-3</sup> )	Harmonized World Soil Database (HWSD), 1 km
Soil cation exchange capacity (mmol(c) kg <sup>-1</sup> )	Soil Grid, 1 km
Mineral type	(Ito and Wagai, 2017) <sup>21</sup> , 2' to 2°
Soil total phosphorus (g m <sup>-2</sup> )	(He et al., 2021) <sup>22</sup> , 0.5°

**Supplementary Table 3 Global future (from 2081 to 2100) carbon changes summarized by land cover types.** POC, particulate organic carbon. MAOC, mineral-associated organic carbon. SOC, soil organic carbon.  $\Delta$ POC,  $\Delta$ MAOC, and  $\Delta$ SOC stocks are the differences between the future and present POC, MAOC, and SOC stocks.

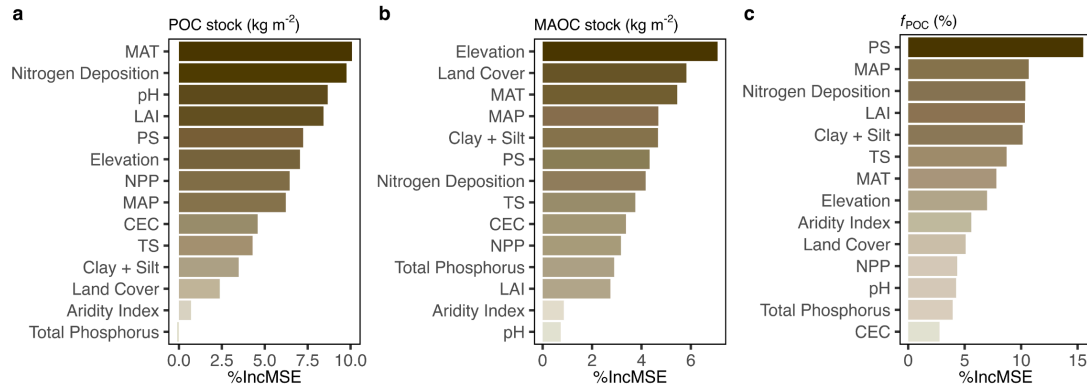
	$\Delta$ POC	$\Delta$ MAOC	$\Delta$ SOC
	(Pg C)	(Pg C)	(Pg C)
<b>Shared Socio-economic Pathway 126</b>			
Global	-29.59	7.39	-22.21
Cropland	-12.08	2.50	-9.57
Forest	-19.75	-4.73	-24.48
Grassland	0.89	5.01	5.90
Shrubland	3.77	5.09	8.86
Tundra	-2.42	-0.49	-2.91
<b>Shared Socio-economic Pathway 245</b>			
Global	-32.17	11.30	-20.87
Cropland	-12.03	3.40	-8.63
Forest	-20.31	-2.76	-23.08
Grassland	-0.80	5.07	4.27
Shrubland	5.20	6.35	11.55
Tundra	-4.22	-0.76	-4.98
<b>Shared Socio-economic Pathway 585</b>			
Global	-22.18	22.54	0.36
Cropland	-7.61	4.82	-2.79
Forest	-16.82	2.47	-14.35
Grassland	0.02	7.82	7.83
Shrubland	6.48	7.97	14.45
Tundra	-4.25	-0.53	-4.77

**Supplementary Table 4 Global future (from 2081 to 2100) carbon changes summarized by latitude.** POC, particulate organic carbon. MAOC, mineral-associated organic carbon. SOC, soil organic carbon.  $\Delta$ POC,  $\Delta$ MAOC, and  $\Delta$ SOC stocks are the differences between the future and present POC, MAOC, and SOC stocks.

	$\Delta$ POC (Pg C)	$\Delta$ MAOC (Pg C)	$\Delta$ SOC (Pg C)
<b>Shared Socio-economic Pathway 126</b>			
High-latitude	-23.10	-7.34	-30.44
Middle-latitude	-9.02	2.18	-6.84
Low-latitude	2.53	12.55	15.07
<b>Shared Socio-economic Pathway 245</b>			
High-latitude	-30.89	-8.52	-39.41
Middle-latitude	-8.20	2.92	-5.28
Low-latitude	6.92	16.90	23.82
<b>Shared Socio-economic Pathway 585</b>			
High-latitude	-32.72	-7.17	-39.88
Middle-latitude	-5.09	3.33	-1.76
Low-latitude	15.62	26.38	42.00

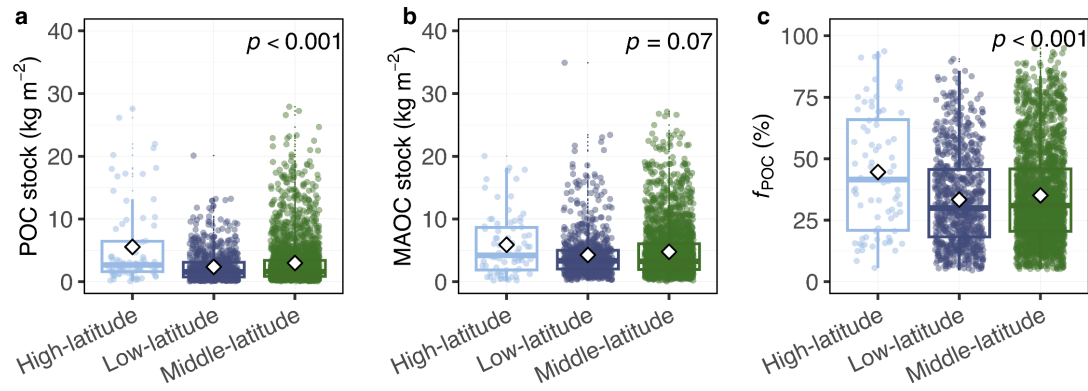
**Supplementary Table 5 Global future (from 2081 to 2100) carbon changes summarized by forest types.** POC, particulate organic carbon. MAOC, mineral-associated organic carbon. SOC, soil organic carbon.  $\Delta$ POC,  $\Delta$ MAOC, and  $\Delta$ SOC stocks are the differences between the future and present POC, MAOC, and SOC stocks.

	$\Delta$ POC (Pg C)	$\Delta$ MAOC (Pg C)	$\Delta$ SOC (Pg C)
<b>Shared Socio-economic Pathway 126</b>			
Boreal forest	-20.96	-6.25	-27.22
Temperate forest	-0.68	-2.02	-2.70
Tropical forest	1.91	3.55	5.46
<b>Shared Socio-economic Pathway 245</b>			
Boreal forest	-23.68	-4.83	-28.51
Temperate forest	-1.78	-2.47	-4.25
Tropical forest	5.16	4.55	9.71
<b>Shared Socio-economic Pathway 585</b>			
Boreal forest	-23.78	-3.19	-26.97
Temperate forest	-2.19	-1.83	-4.02
Tropical forest	9.16	7.50	16.66

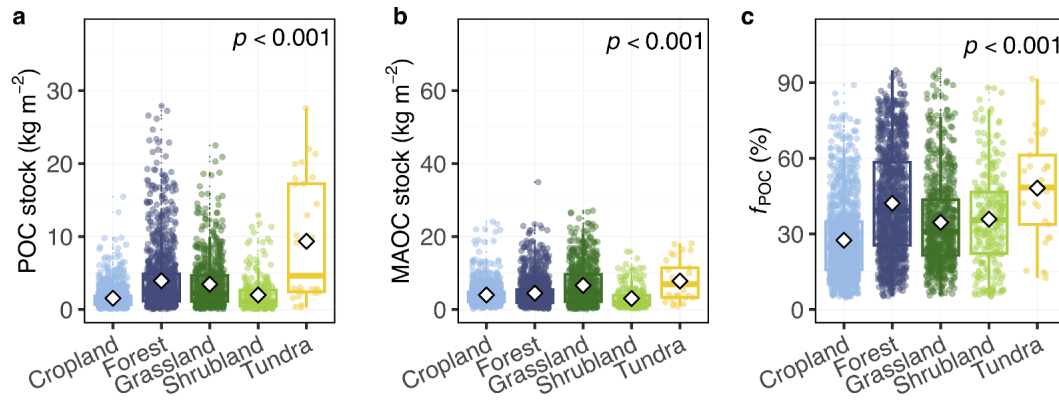


**Supplementary Figure 1 Variable importance of the machine learning random forest model trained exclusively on high-latitude soils for topsoil (a) particulate organic carbon (POC) stock, (b) mineral-associated organic carbon (MAOC) stock, and (c) the proportion of POC relative to soil organic carbon ( $f_{\text{POC}}$ ). Mean annual temperature (MAT), mean annual precipitation (MAP), temperature seasonality (TS), precipitation seasonality (PS), background nitrogen deposition (Nitrogen deposition), aridity index, cation exchange capacity (CEC), percent of clay and silt (clay + silt), total phosphorus, net primary productivity (NPP), soil pH, and leaf area index (LAI) are continuous variables. Land cover is a categorical variable. Variable importance is ranked by the percent increase in mean square error (MSE).**

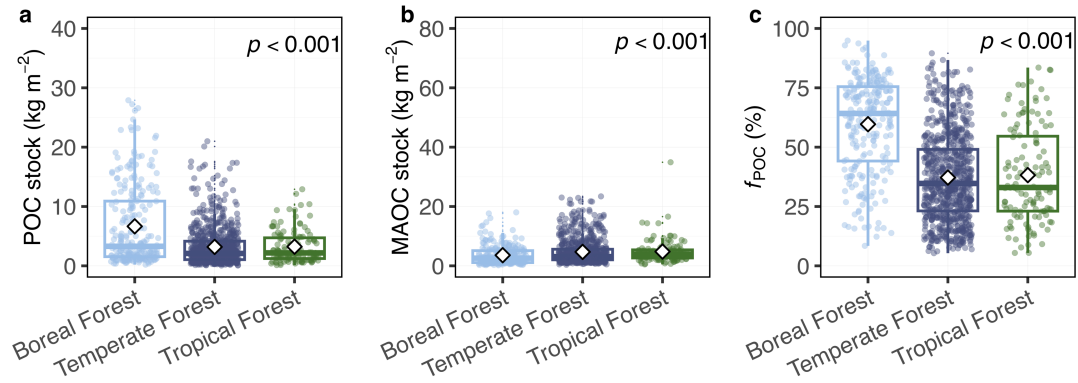




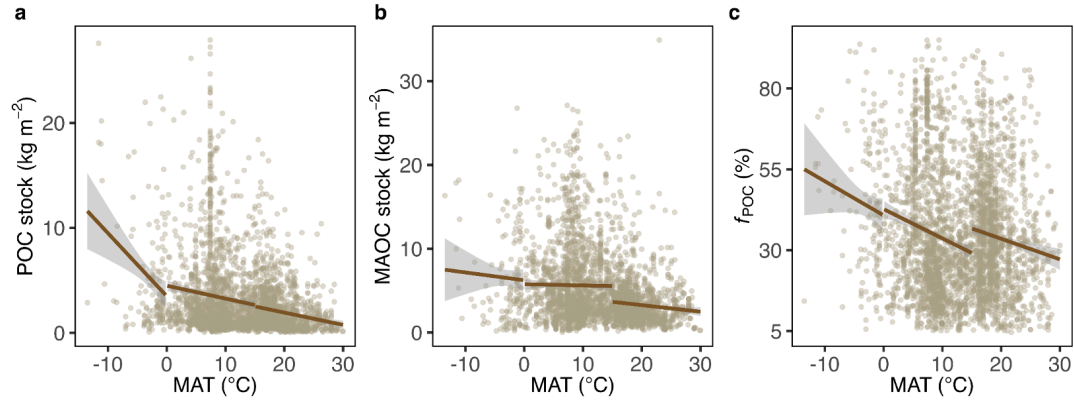
**Supplementary Figure 2** The topsoil (a) particulate organic carbon (POC) stock, (b) mineral-associated organic carbon (MAOC) stock, and (c) the proportion of POC relative to soil organic carbon ( $f_{\text{POC}}$ ) between different latitudes. The dataset was grouped by high-latitude (north of 60° N or south of 60° S;  $n = 78$ ), middle-latitude (south of 60° N and north of 30° N; south of 30° S and north of 60° S;  $n = 2389$ ), and low-latitude (south of 30° N and north of 30° S;  $n = 817$ ). POC and MAOC stocks are standardized values (see “Methods”). Box plots indicate the medians (horizontal lines), 1st and 3rd quartiles (boxes),  $1.5 \times$  interquartile range (whiskers), and means (diamonds). The  $p$ -value indicates the statistical significance between land covers.



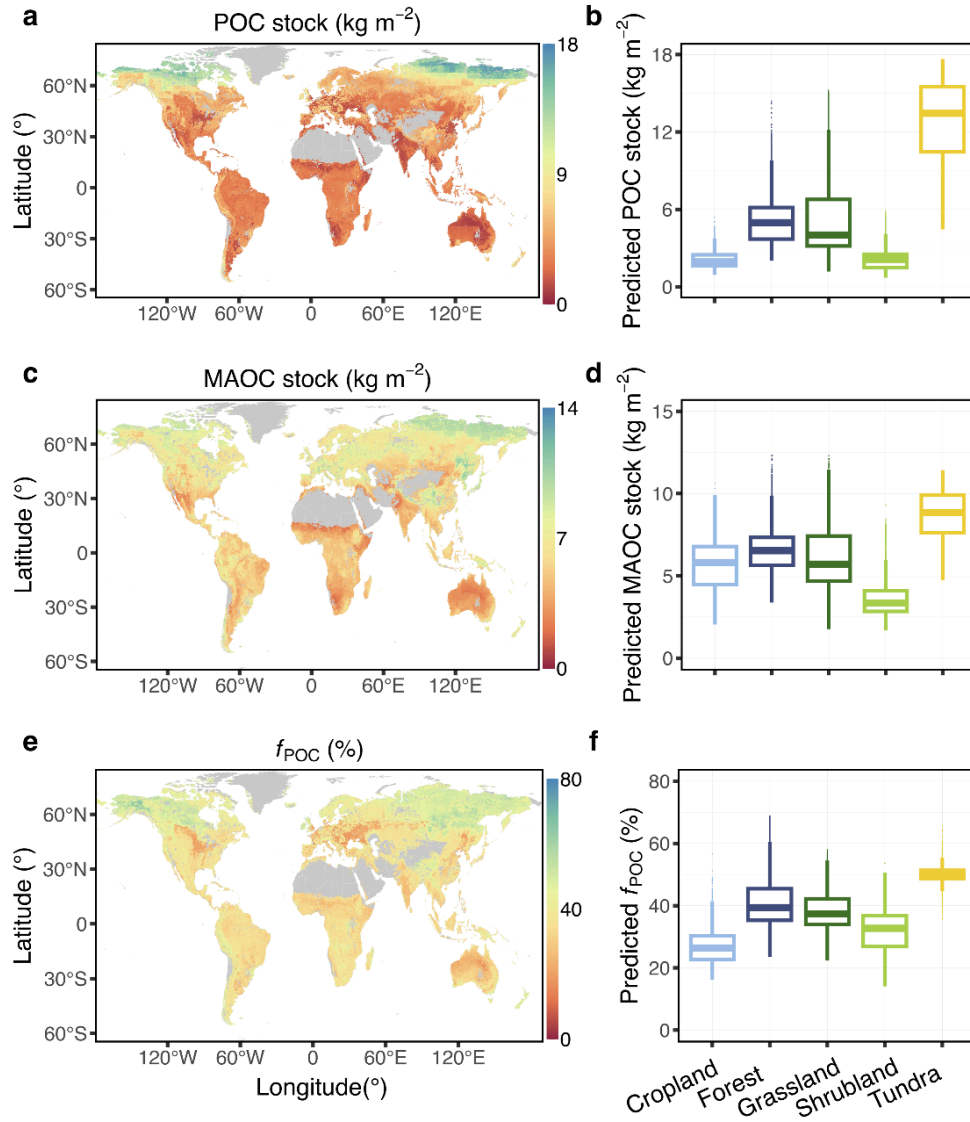
**Supplementary Figure 3** The topsoil (a) particulate organic carbon (POC) stock, (b) mineral-associated organic carbon (MAOC) stock, and (c) the proportion of POC relative to soil organic carbon ( $f_{\text{POC}}$ ) between different land covers. The dataset was grouped by cropland ( $n = 1165$ ), forest ( $n = 1135$ ), grassland ( $n = 693$ ), shrubland ( $n = 262$ ), and tundra ( $n = 29$ ). POC and MAOC stock are standardized values (see “Methods”). Box plots indicate the medians (horizontal lines), 1st and 3rd quartiles (boxes),  $1.5 \times$  interquartile range (whiskers), and means (diamonds). The  $p$ -value indicates the statistical significance between land covers.



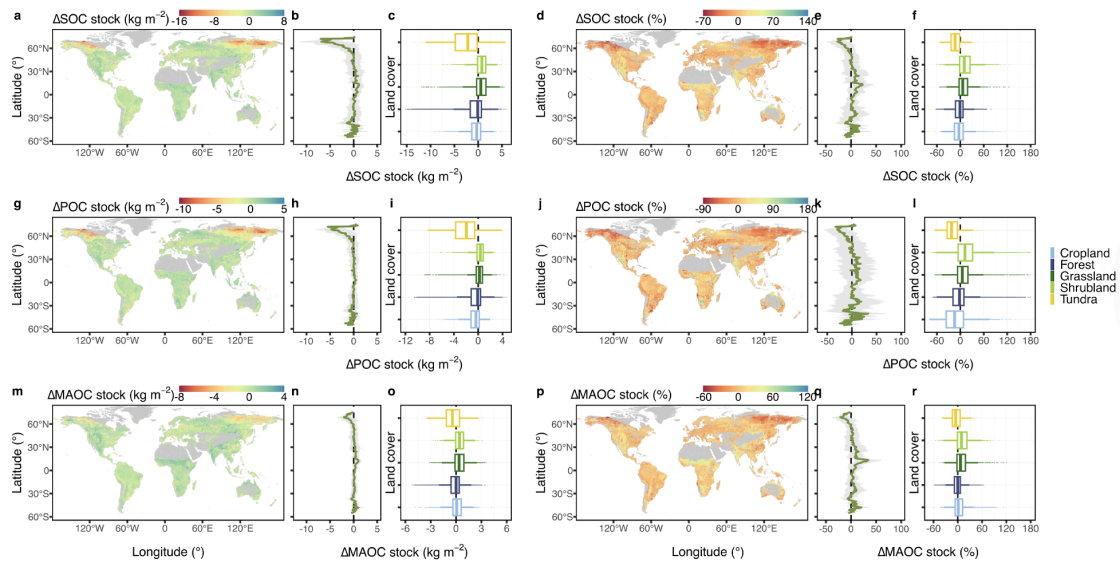
**Supplementary Figure 4** The topsoil (a) particulate organic carbon (POC) stock, (b) mineral-associated organic carbon (MAOC) stock, and (c) the proportion of POC relative to soil organic carbon ( $f_{\text{POC}}$ ) between different forests. The dataset was grouped by boreal forest ( $n = 245$ ), temperate forest ( $n = 767$ ), and tropical forest ( $n = 123$ ). POC and MAOC stocks are standardized values (see “Methods”). Box plots indicate the medians (horizontal lines), 1st and 3rd quartiles (boxes),  $1.5 \times$  interquartile range (whiskers), and means (diamonds). The  $p$ -value indicates the statistical significance between different forests.



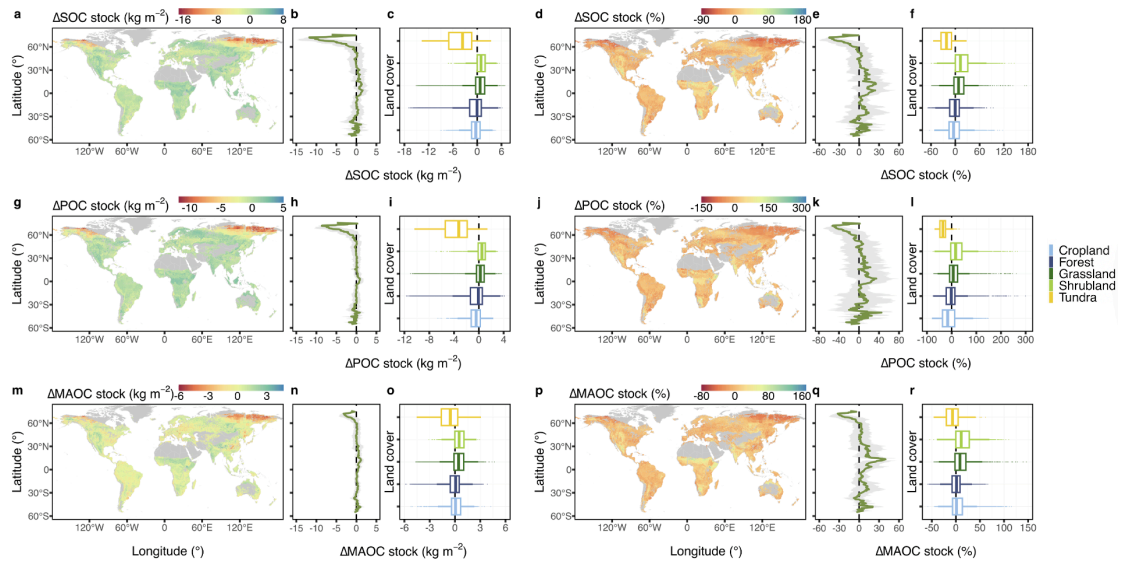
**Supplementary Figure 5** The topsoil (a) particulate organic carbon (POC) stock, (b) mineral-associated organic carbon (MAOC) stock, and (c) the proportion of POC relative to soil organic carbon ( $f_{\text{POC}}$ ) as a function of mean annual temperature (MAT). Linear regressions are shown for cold ( $< 0^{\circ}\text{C}$ ), temperate ( $\geq 0^{\circ}\text{C}$  and  $< 15^{\circ}\text{C}$ ), and warm ( $\geq 15^{\circ}\text{C}$ ) regions, respectively.



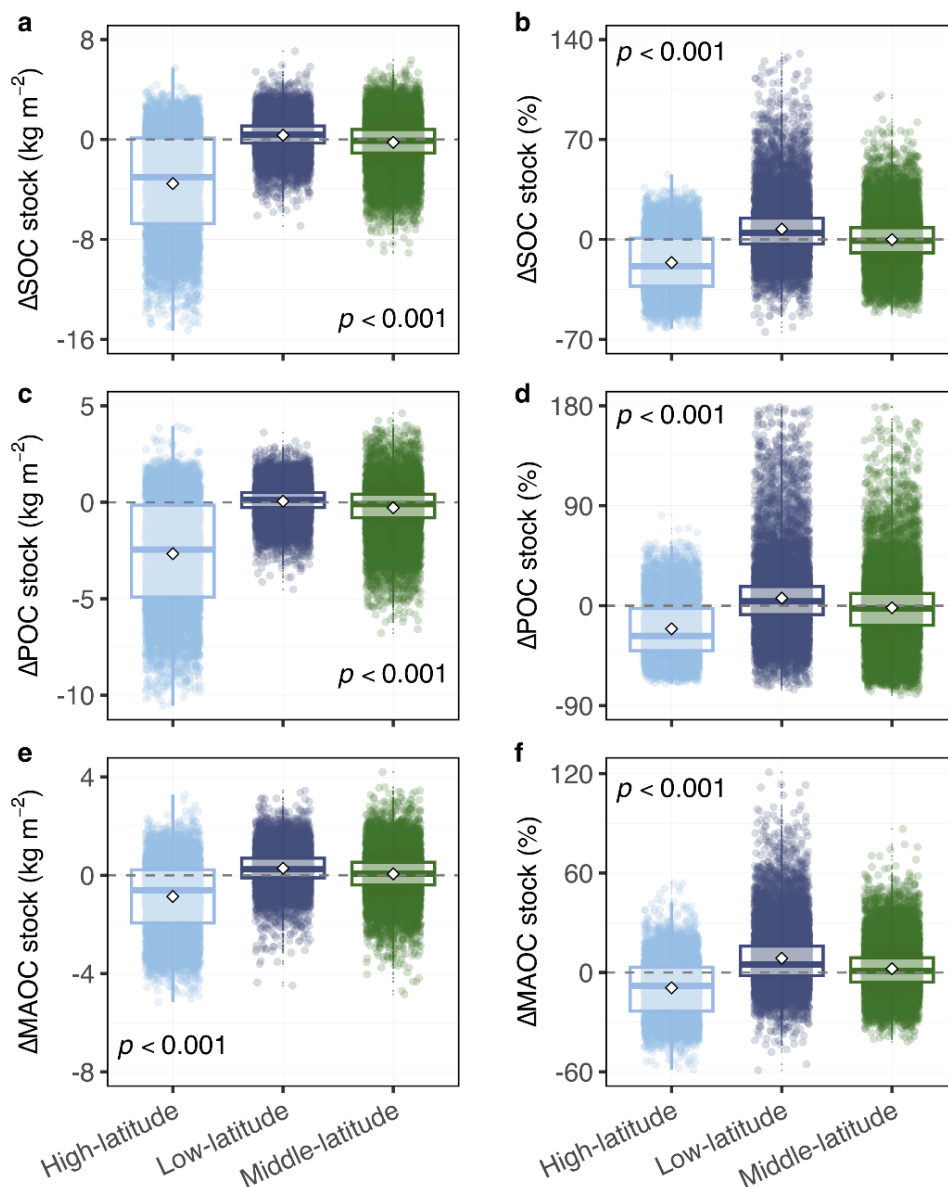
**Supplementary Figure 6** Global distribution of predicted present (a) particulate organic carbon (POC) stock, (c) mineral-associated organic carbon (MAOC) stock, and (e) the proportion of POC relative to soil organic carbon ( $f_{\text{POC}}$ ) in the topsoil (0-30 cm). The POC stock, MAOC stock, and  $f_{\text{POC}}$  were predicted using a random forest model. All maps were at  $0.5^\circ$  resolution. **b, d, f,** The predicted POC stock, MAOC stock, and  $f_{\text{POC}}$  between land cover.



**Supplementary Figure 7 Global distribution of the absolute and relative change of topsoil (a, d) soil organic carbon (SOC) stock, (g, j) particulate organic carbon (POC) stock, and (m, p) mineral-associated organic carbon (MAOC) stock under SSP126 scenario from 2081 to 2100.** SSP, shared socioeconomic pathway. Here, SOC stock represents the sum of POC and MAOC stock.  $\Delta$ POC,  $\Delta$ MAOC, and  $\Delta$ SOC stocks are the differences between the future and present stocks. The POC and MAOC stocks from 2081 to 2100 were calculated using climatic factors of different models under SSP126 scenario. The future mean annual temperature, mean annual precipitation, temperature seasonality, precipitation seasonality, evapotranspiration, and leaf area index were the means of BCC-CSM2-MR, MPI-ESM1-2-HR, and IPSL-CM6A-LR. The future nitrogen deposition background was the mean of ACCESS-ESM1-5, NorESM2-LM, and NorESM2-MM. The future net primary productivity was the mean of IPSL-CM6A-LR, CMCC-ESM2, and CanESM5-1. All maps were at  $0.5^\circ$  resolution. **b, e, h, k, n, q**, Latitudinal profiles of SOC stock, POC stock, and MAOC stock change at  $0.5^\circ$  latitudinal resolution. The green lines represent the absolute or relative change of SOC stock, POC stock, and MAOC stock. The grey shading represents the standard deviation. **c, f, i, l, o, r**, The absolute and relative change of SOC stock, POC stock, and MAOC stock between land covers.

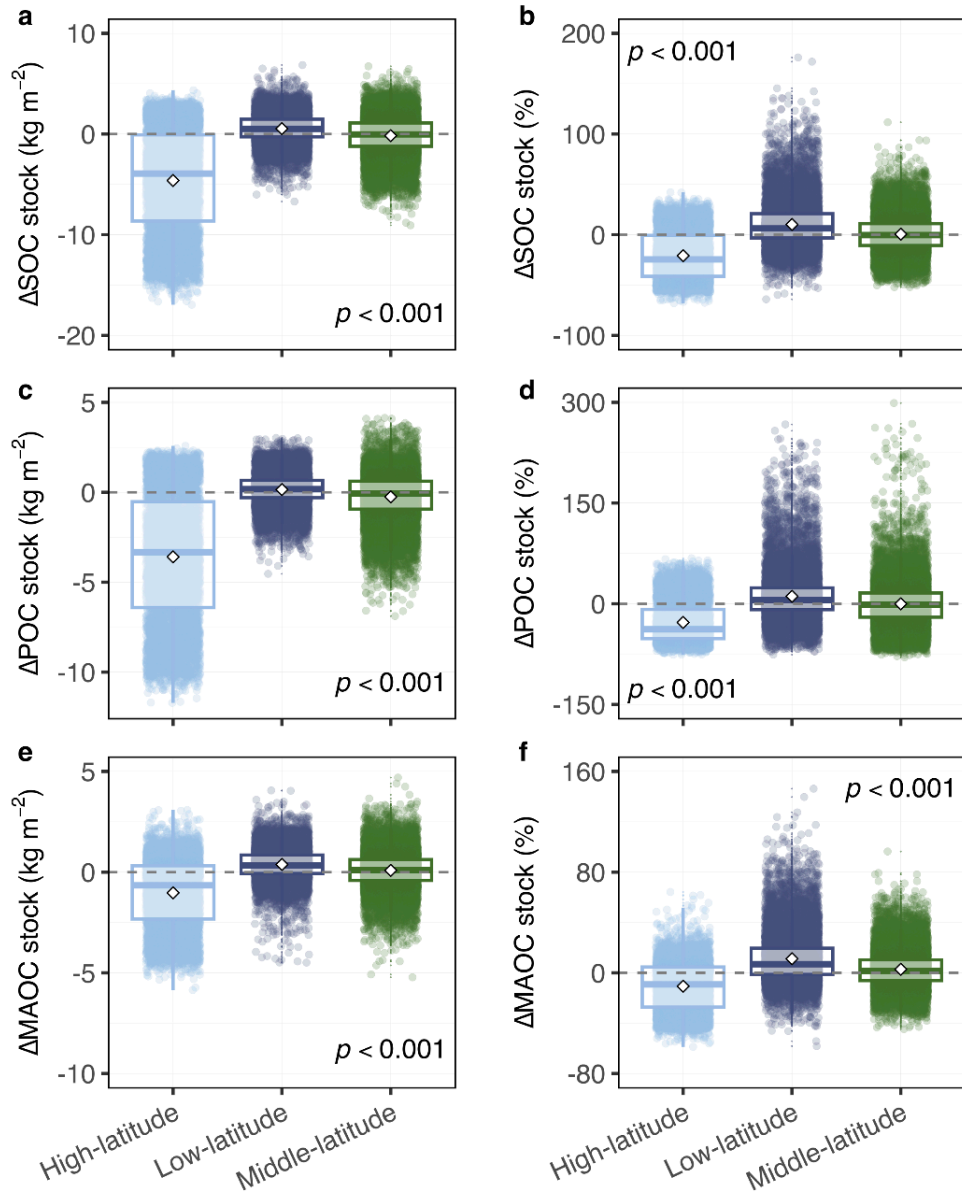


**Supplementary Figure 8 Global distribution of the absolute and relative change of topsoil (a, d) soil organic carbon (SOC) stock, (g, j) particulate organic carbon (POC) stock, and (m, p) mineral-associated organic carbon (MAOC) stock under SSP245 scenario from 2081 to 2100.** SSP, shared socioeconomic pathway. Here, SOC stock represents the sum of POC and MAOC stock.  $\Delta$ POC,  $\Delta$ MAOC, and  $\Delta$ SOC stocks are the differences between the future and present stocks. The POC and MAOC stocks from 2081 to 2100 were calculated using climatic factors of different models under SSP245 scenario. The future mean annual temperature, mean annual precipitation, temperature seasonality, precipitation seasonality, evapotranspiration, and leaf area index were the means of BCC-CSM2-MR, MPI-ESM1-2-HR, and IPSL-CM6A-LR. The future nitrogen deposition background was the mean of ACCESS-ESM1-5, NorESM2-LM, and NorESM2-MM. The future net primary productivity was the mean of IPSL-CM6A-LR, CMCC-ESM2, and CanESM5-1. All maps were at  $0.5^\circ$  resolution. **b, e, h, k, n, q**, Latitudinal profiles of SOC stock, POC stock, and MAOC stock change at  $0.5^\circ$  latitudinal resolution. The green lines represent the absolute or relative change of SOC stock, POC stock, and MAOC stock. The grey shading represents the standard deviation. **c, f, i, l, o, r**, The absolute and relative change of SOC stock, POC stock, and MAOC stock between land covers.

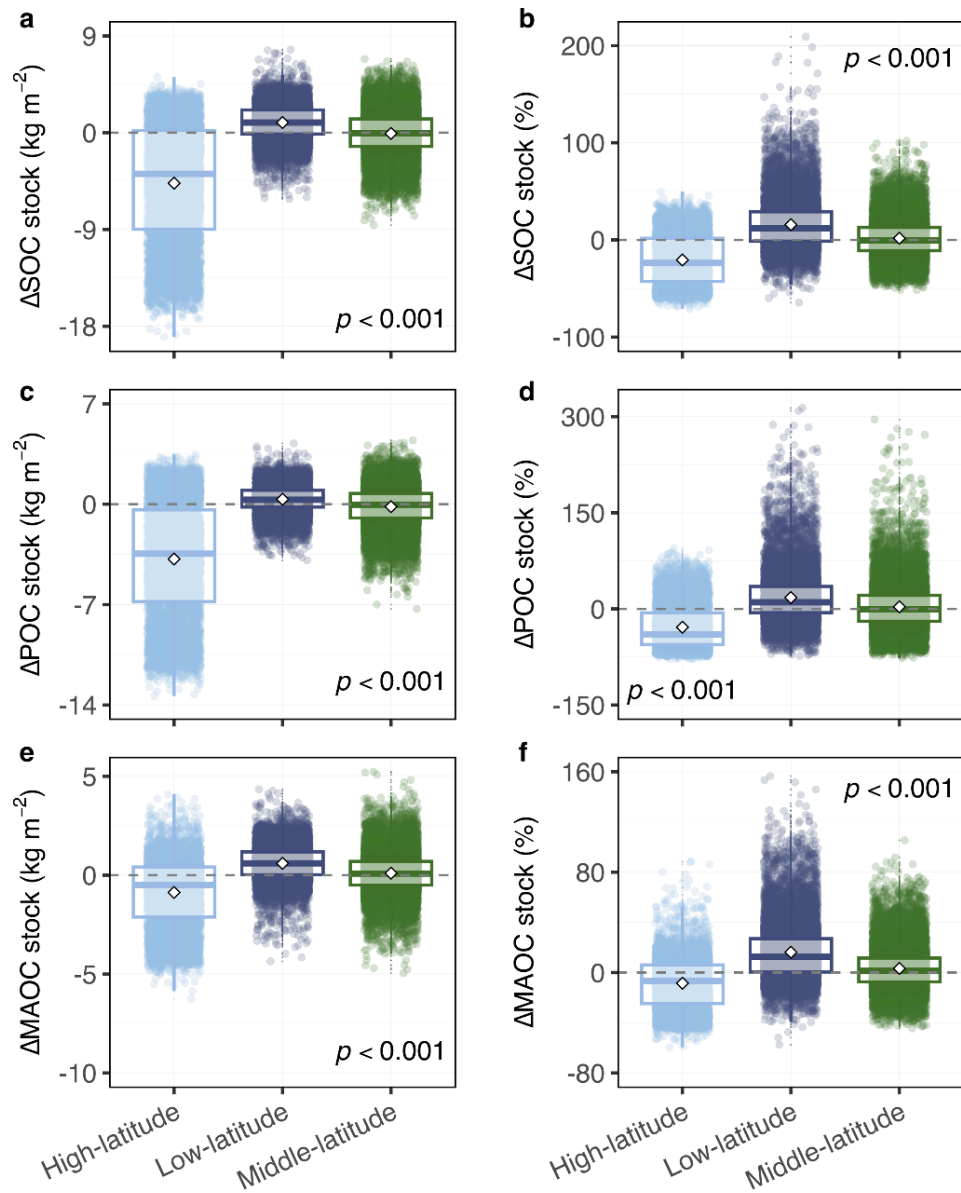


**Supplementary Figure 9** The absolute and relative changes of topsoil (a, b) soil organic carbon (SOC) stock, (c, d) particulate organic carbon (POC) stock, and (e, f) mineral-associated organic carbon (MAOC) stock between different latitude soils under SSP126 scenario from 2081 to 2100. High-latitude: north of 60° N or south of 60° S. Low-latitude: south of 30° N and north of 30° S. Middle-latitude: south of 60° N and north of 30° N; south of 30° S and north of 60° S. Box plots indicate the medians (horizontal lines), 1st and 3rd quartiles (boxes), 1.5 × interquartile range (whiskers), and means (diamonds). The *p*-value indicates the statistical significance between different latitude soils.

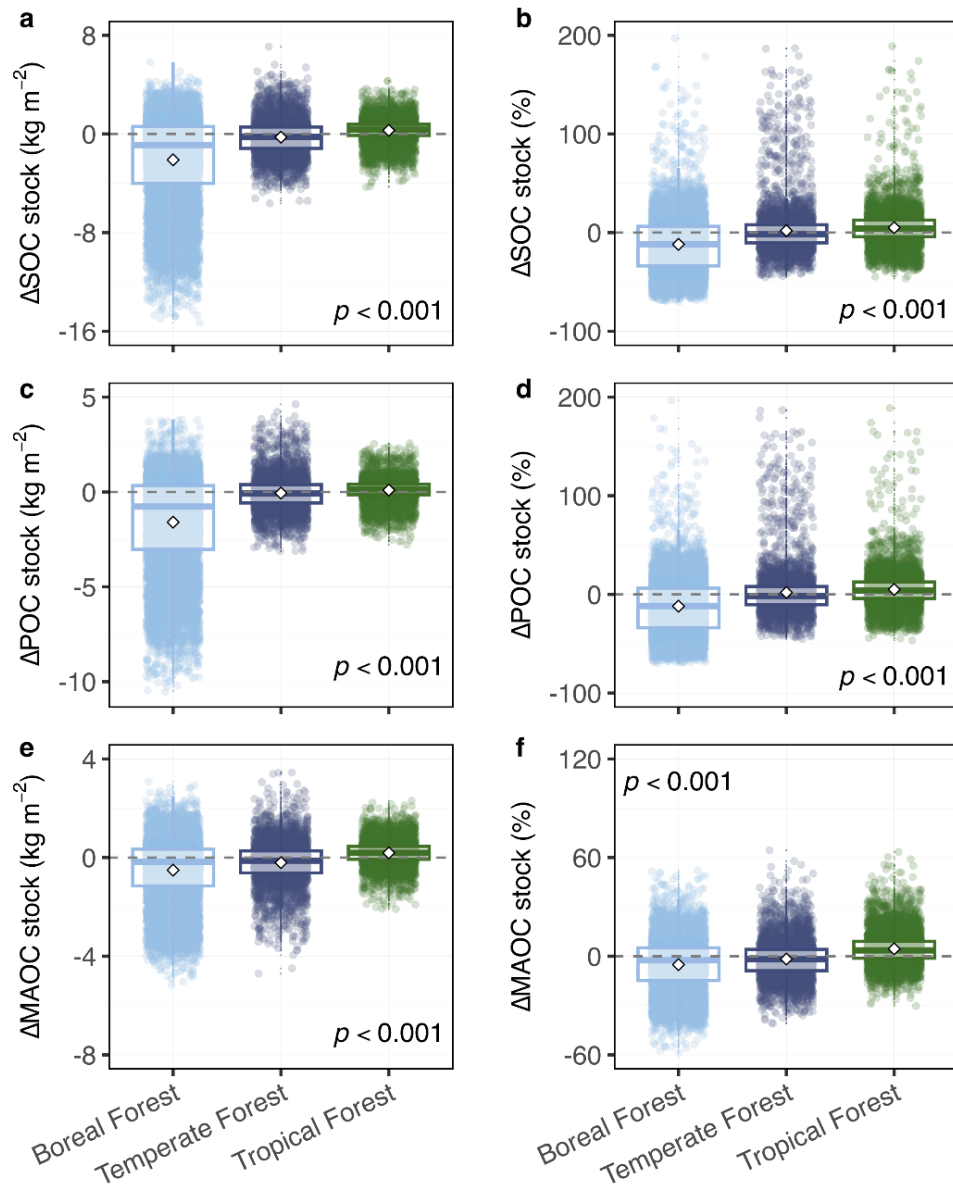




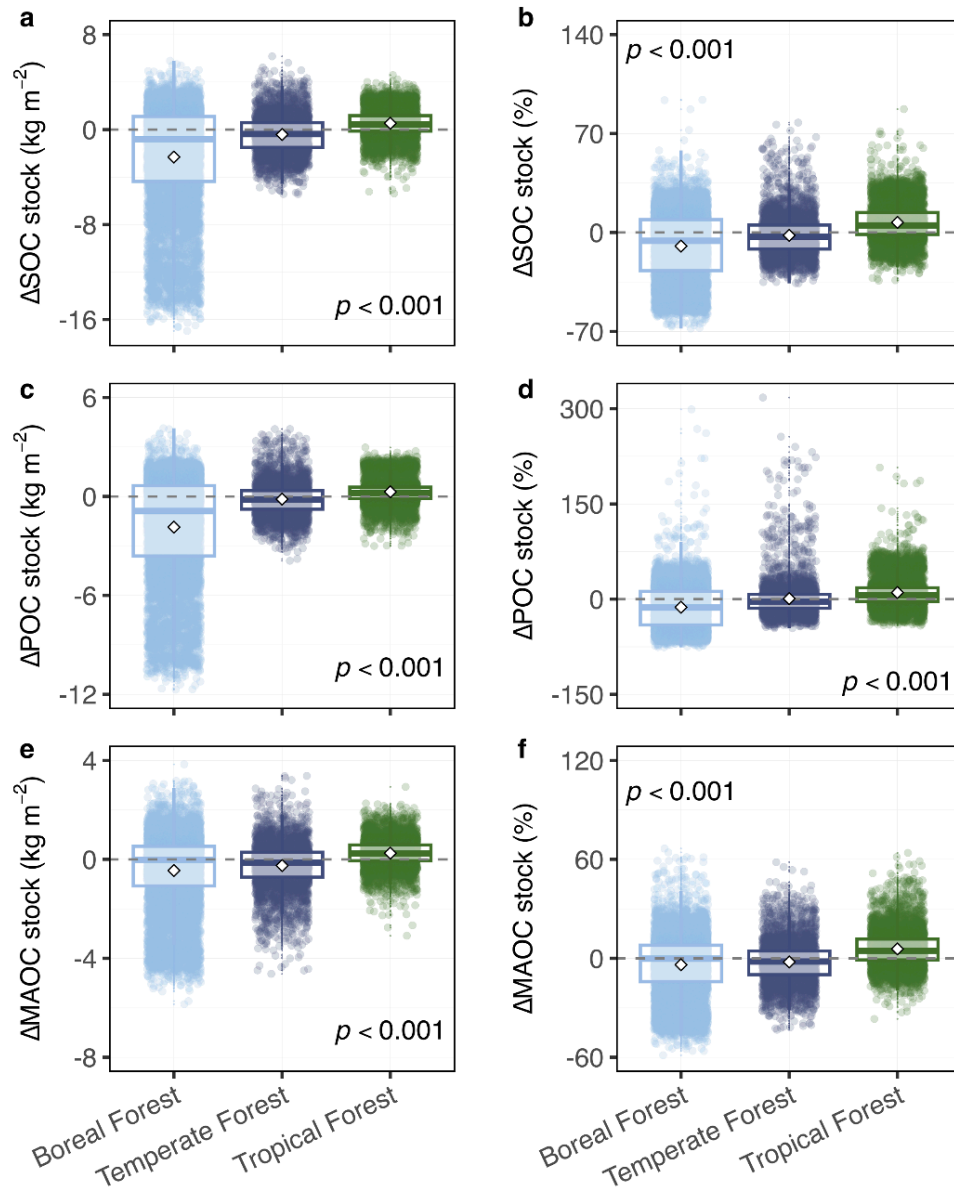
**Supplementary Figure 10** The absolute and relative changes of topsoil (a, b) soil organic carbon (SOC) stock, (c, d) particulate organic carbon (POC) stock, and (e, f) mineral-associated organic carbon (MAOC) stock between different latitude soils under SSP245 scenario from 2081 to 2100. High-latitude: north of 60° N or south of 60° S. Low-latitude: south of 30° N and north of 30° S. Middle-latitude: south of 60° N and north of 30° N; south of 30° S and north of 60° S. Box plots indicate the medians (horizontal lines), 1st and 3rd quartiles (boxes),  $1.5 \times$  interquartile range (whiskers), and means (diamonds). The  $p$ -value indicates the statistical significance between different latitude soils.



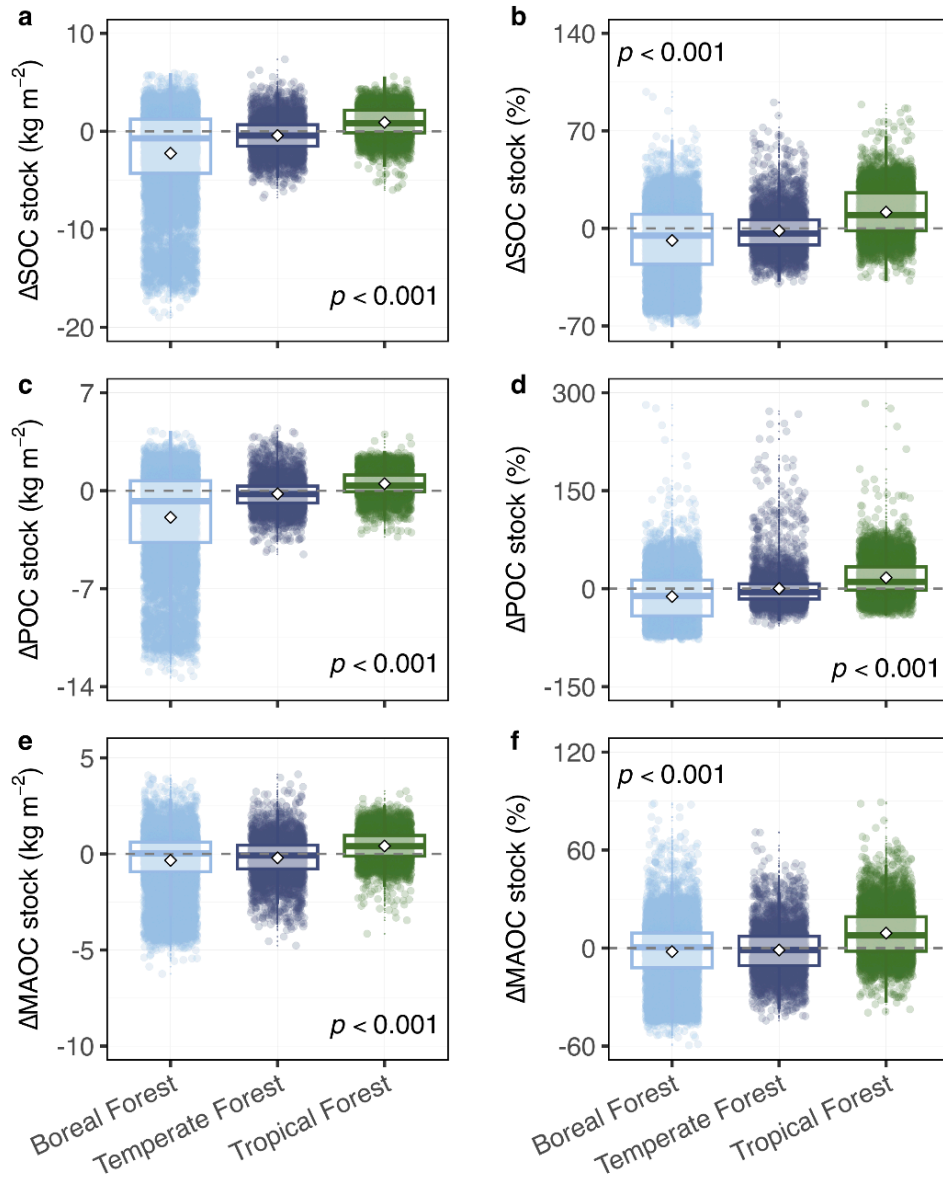
**Supplementary Figure 11** The absolute and relative changes of topsoil (a, b) soil organic carbon (SOC) stock, (c, d) particulate organic carbon (POC) stock, and (e, f) mineral-associated organic carbon (MAOC) stock between different latitude soils under SSP585 scenario from 2081 to 2100. High-latitude: north of 60° N or south of 60° S. Low-latitude: south of 30° N and north of 30° S. Middle-latitude: south of 60° N and north of 30° N; south of 30° S and north of 60° S. Box plots indicate the medians (horizontal lines), 1st and 3rd quartiles (boxes),  $1.5 \times$  interquartile range (whiskers), and means (diamonds). The  $p$ -value indicates the statistical significance between different latitude soils.



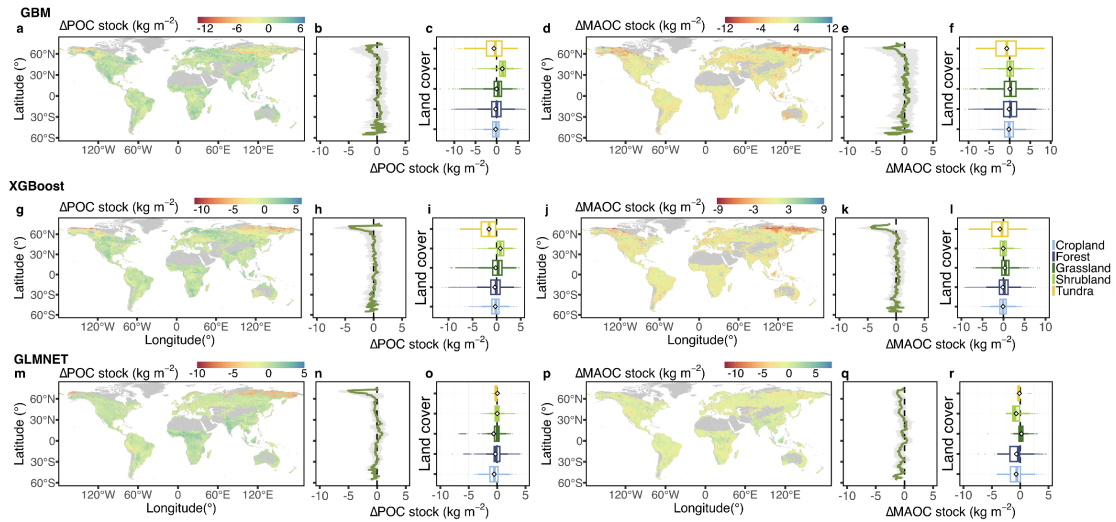
**Supplementary Figure 12** The absolute and relative changes of topsoil (a, b) soil organic carbon (SOC) stock, (c, d) particulate organic carbon (POC) stock, and (e, f) mineral-associated organic carbon (MAOC) stock between different forests under SSP126 scenario from 2081 to 2100. Box plots indicate the medians (horizontal lines), 1st and 3rd quartiles (boxes),  $1.5 \times$  interquartile range (whiskers), and means (diamonds). The  $p$ -value indicates the statistical significance between different forests.



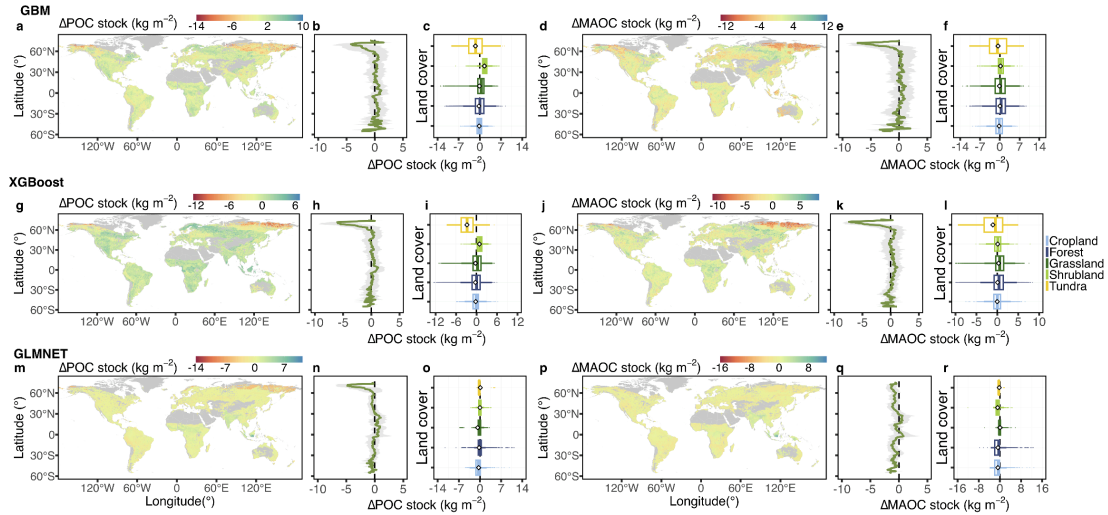
**Supplementary Figure 13** The absolute and relative changes of topsoil (a, b) soil organic carbon (SOC) stock, (c, d) particulate organic carbon (POC) stock, and (e, f) mineral-associated organic carbon (MAOC) stock between different forests under SSP245 scenario from 2081 to 2100. Box plots indicate the medians (horizontal lines), 1st and 3rd quartiles (boxes),  $1.5 \times$  interquartile range (whiskers), and means (diamonds). The  $p$ -value indicates the statistical significance between different forests.



**Supplementary Figure 14** The absolute and relative changes of topsoil (a, b) soil organic carbon (SOC) stock, (c, d) particulate organic carbon (POC) stock, (e, f) mineral-associated organic carbon (MAOC) stock between different forests under SSP585 scenario from 2081 to 2100. Box plots indicate the medians (horizontal lines), 1st and 3rd quartiles (boxes),  $1.5 \times$  interquartile range (whiskers), and means (diamonds). The  $p$ -value indicates the statistical significance between different forests.

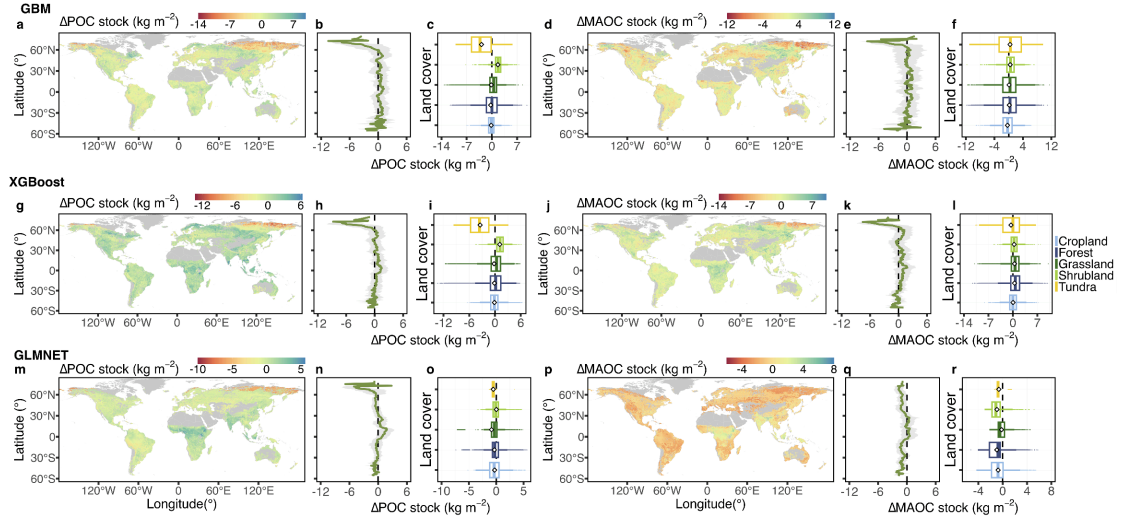


**Supplementary Figure 15 Global distribution of the absolute change of topsoil (a, g, m) particulate organic carbon (POC) stock and (d, j, p) mineral-associated organic carbon (MAOC) stock under SSP126 scenario from 2081 to 2100, as predicted by generalized boosted regression models (GBM), extreme gradient boosting models (XGBoost), and generalized linear models (GLMNET). SSP, shared socioeconomic pathway. Here, SOC stock represents the sum of POC and MAOC stock.  $\Delta\text{POC}$ ,  $\Delta\text{MAOC}$ , and  $\Delta\text{SOC}$  stocks are the differences between the future and present stocks. The POC and MAOC stocks from 2081 to 2100 were calculated using climatic factors of different models under the SSP126 scenario. The future mean annual temperature, mean annual precipitation, temperature seasonality, precipitation seasonality, evapotranspiration, and leaf area index were the means of BCC-CSM2-MR, MPI-ESM1-2-HR, and IPSL-CM6A-LR. The future nitrogen deposition background was the mean of ACCESS-ESM1-5, NorESM2-LM, and NorESM2-MM. The future net primary productivity was the mean of IPSL-CM6A-LR, CMCC-ESM2, and CanESM5-1. All maps were at  $0.5^\circ$  resolution. **b, h, n, e, k, q**, Latitudinal profiles of POC stock and MAOC stock change at  $0.5^\circ$  latitudinal resolution. The green lines represent the absolute or relative change of POC stock and MAOC stock. The grey shading represents the standard deviation. **c, i, o, f, l, r**, The absolute change of POC stock and MAOC stock between land covers.**



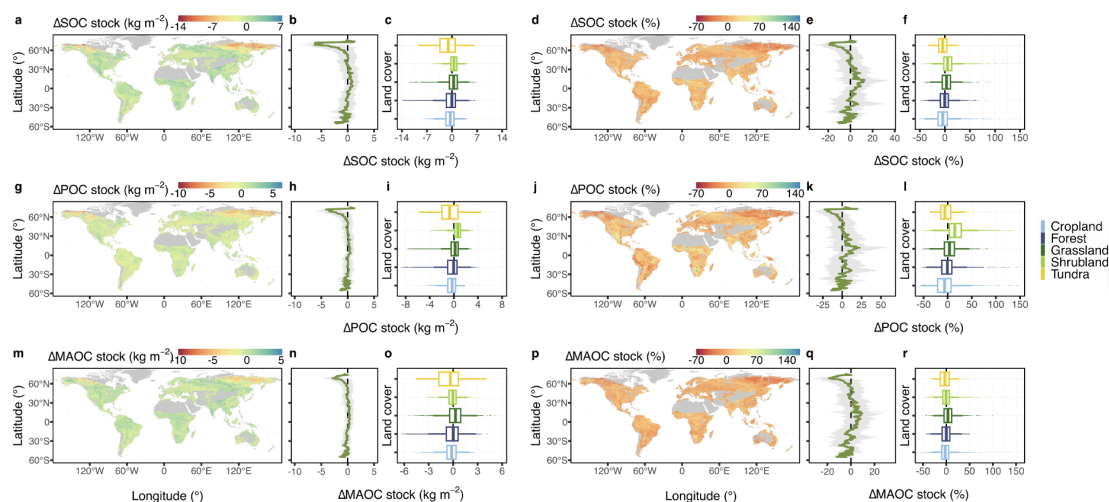
**Supplementary Figure 16 Global distribution of the absolute change of topsoil (a, g, m) particulate organic carbon (POC) stock and (d, j, p) mineral-associated organic carbon (MAOC) stock under SSP245 scenario from 2081 to 2100, as predicted by generalized boosted regression models (GBM), extreme gradient boosting models (XGBoost), and generalized linear models (GLMNET). SSP, shared socioeconomic pathway. Here, SOC stock represents the sum of POC and MAOC stock.  $\Delta$ POC,  $\Delta$ MAOC, and  $\Delta$ SOC stocks are the differences between the future and present stocks. The POC and MAOC stocks from 2081 to 2100 were calculated using climatic factors of different models under the SSP245 scenario. The future mean annual temperature, mean annual precipitation, temperature seasonality, precipitation seasonality, evapotranspiration, and leaf area index were the means of BCC-CSM2-MR, MPI-ESM1-2-HR, and IPSL-CM6A-LR. The future nitrogen deposition background was the mean of ACCESS-ESM1-5, NorESM2-LM, and NorESM2-MM. The future net primary productivity was the mean of IPSL-CM6A-LR, CMCC-ESM2, and CanESM5-1. All maps were at  $0.5^\circ$  resolution. **b, h, n, e, k, q**, Latitudinal profiles of POC stock and MAOC stock change at  $0.5^\circ$  latitudinal resolution. The green lines represent the absolute or relative change of POC stock and MAOC stock. The grey shading represents the standard deviation. **c, i, o, f, l, r**, The absolute change of POC stock and MAOC stock between land covers.**



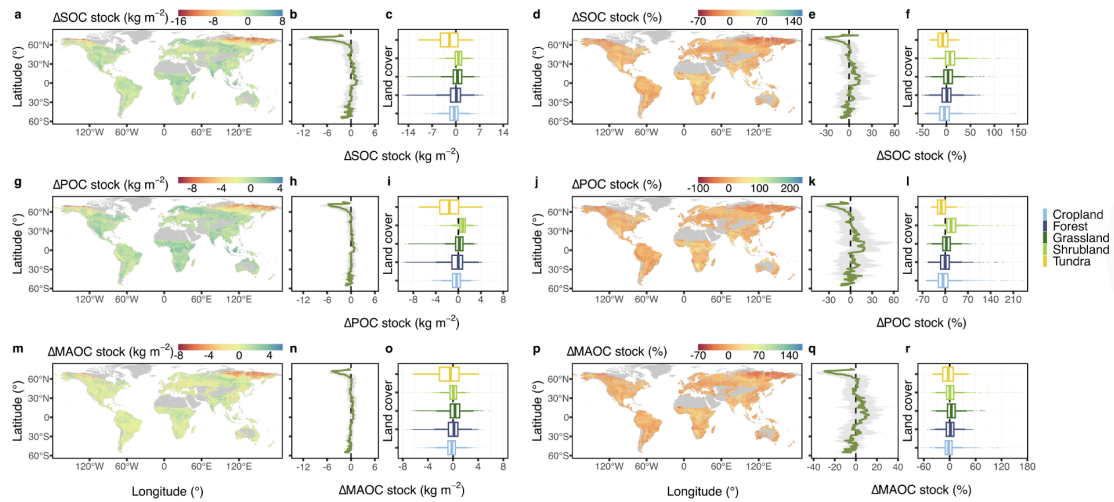


**Supplementary Figure 17 Global distribution of the absolute change of topsoil (a, g, m) particulate organic carbon (POC) stock and (d, j, p) mineral-associated organic carbon (MAOC) stock under SSP585 scenario from 2081 to 2100, as predicted by generalized boosted regression models (GBM), extreme gradient boosting models (XGBoost), and generalized linear models (GLMNET). SSP, shared socioeconomic pathway. Here, SOC stock represents the sum of POC and MAOC stock.  $\Delta\text{POC}$ ,  $\Delta\text{MAOC}$ , and  $\Delta\text{SOC}$  stocks are the differences between the future and present stocks. The POC and MAOC stocks from 2081 to 2100 were calculated using climatic factors of different models under the SSP585 scenario. The future mean annual temperature, mean annual precipitation, temperature seasonality, precipitation seasonality, evapotranspiration, and leaf area index were the means of BCC-CSM2-MR, MPI-ESM1-2-HR, and IPSL-CM6A-LR. The future nitrogen deposition background was the mean of ACCESS-ESM1-5, NorESM2-LM, and NorESM2-MM. The future net primary productivity was the mean of IPSL-CM6A-LR, CMCC-ESM2, and CanESM5-1. All maps were at  $0.5^\circ$  resolution. **b, h, n, e, k, q**, Latitudinal profiles of POC stock and MAOC stock change at  $0.5^\circ$  latitudinal resolution. The green lines represent the absolute or relative change of POC stock and MAOC stock. The grey shading represents the standard deviation. **c, i, o, f, l, r**, The absolute change of POC stock and MAOC stock between land covers.**

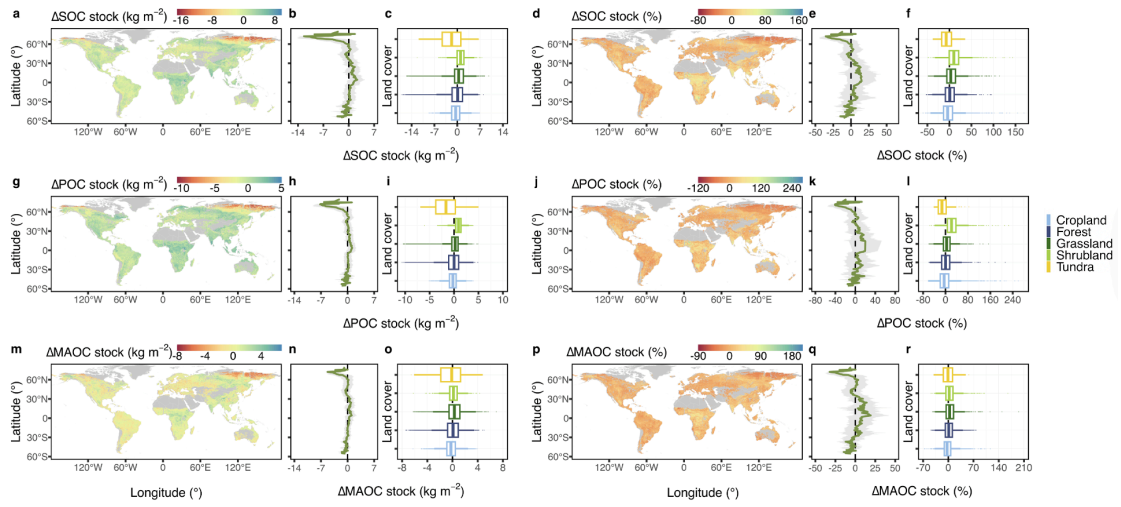




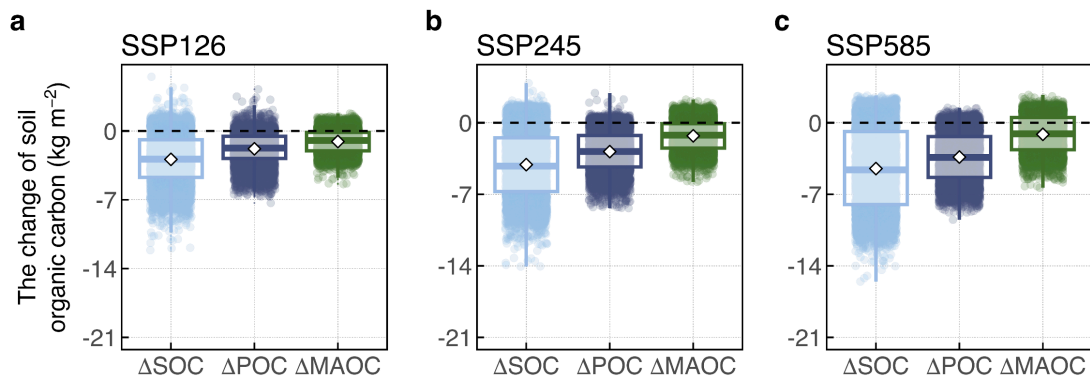
**Supplementary Figure 18 Global distribution of the absolute and relative changes in topsoil (a, d) soil organic carbon (SOC), (g, j) particulate organic carbon (POC), and (m, p) mineral-associated organic carbon (MAOC) stocks under SSP126 scenario for 2081-2100, based on the multi-model mean of four machine learning models (random forest model, generalized boosted regression model, extreme gradient boosting model, and generalized linear model). SSP, shared socioeconomic pathway. Here, SOC stock represents the sum of POC and MAOC stock.  $\Delta$ POC,  $\Delta$ MAOC, and  $\Delta$ SOC stocks are the differences between the future and present stocks. The POC and MAOC stocks from 2081 to 2100 were calculated using climatic factors of different models under SSP126 scenario. The future mean annual temperature, mean annual precipitation, temperature seasonality, precipitation seasonality, evapotranspiration, and leaf area index were the means of BCC-CSM2-MR, MPI-ESM1-2-HR, and IPSL-CM6A-LR. The future nitrogen deposition background was the mean of ACCESS-ESM1-5, NorESM2-LM, and NorESM2-MM. The future net primary productivity was the mean of IPSL-CM6A-LR, CMCC-ESM2, and CanESM5-1. All maps were at  $0.5^\circ$  resolution. **b, e, h, k, n, q**, Latitudinal profiles of SOC stock, POC stock, and MAOC stock change at  $0.5^\circ$  latitudinal resolution. The green lines represent the absolute or relative change of SOC stock, POC stock, and MAOC stock. The grey shading represents the standard deviation. **c, f, i, l, o, r**, The absolute and relative change of SOC stock, POC stock, and MAOC stock between land covers.**



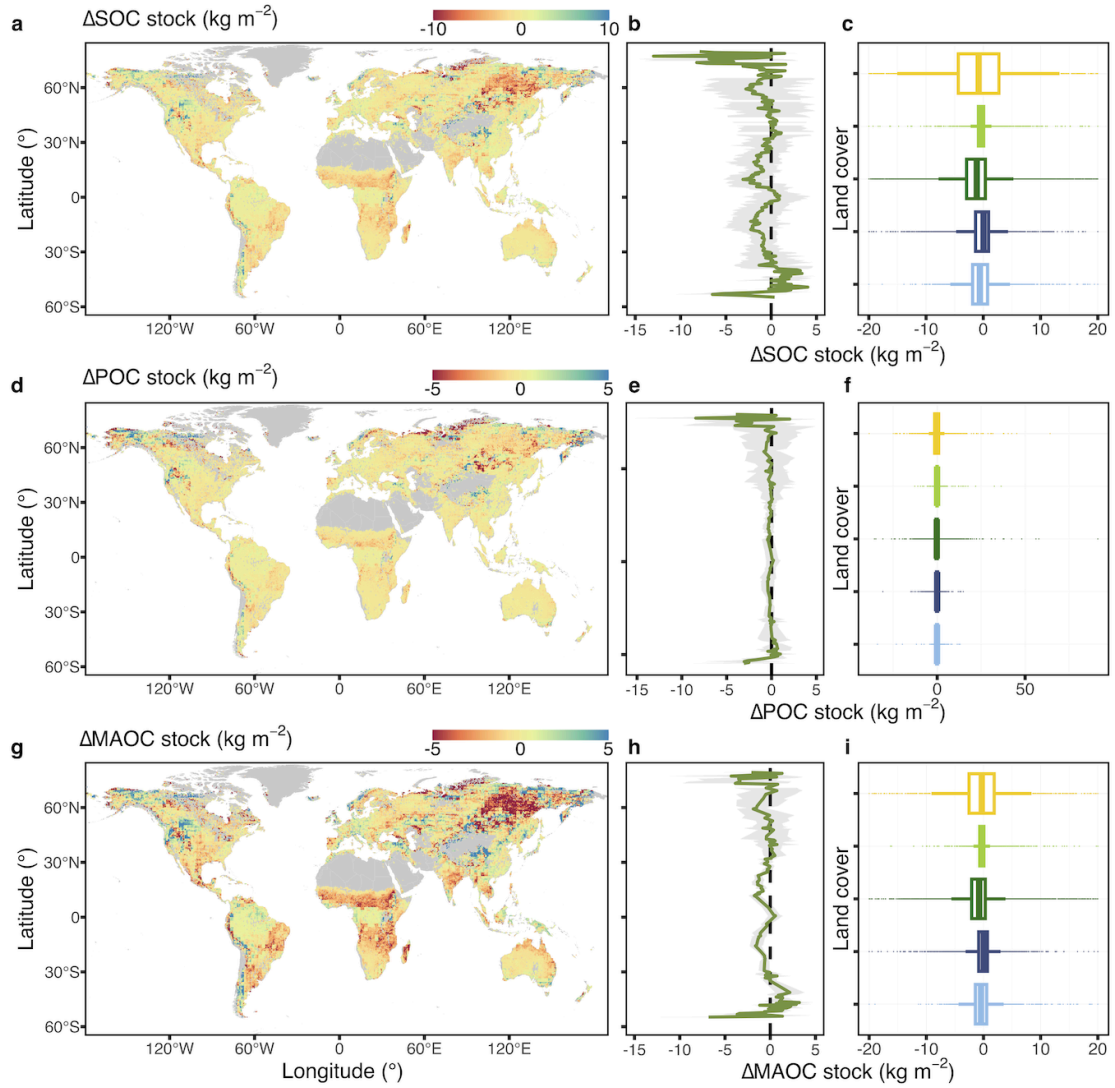
**Supplementary Figure 19 Global distribution of the absolute and relative changes in topsoil (a, d) soil organic carbon (SOC), (g, j) particulate organic carbon (POC), and (m, p) mineral-associated organic carbon (MAOC) stocks under SSP245 scenario for 2081-2100, based on the multi-model mean of four machine learning models (random forest model, generalized boosted regression model, extreme gradient boosting model, and generalized linear model). SSP, shared socioeconomic pathway. Here, SOC stock represents the sum of POC and MAOC stock.  $\Delta$ POC,  $\Delta$ MAOC, and  $\Delta$ SOC stocks are the differences between the future and present stocks. The POC and MAOC stocks from 2081 to 2100 were calculated using climatic factors of different models under SSP245 scenario. The future mean annual temperature, mean annual precipitation, temperature seasonality, precipitation seasonality, evapotranspiration, and leaf area index were the means of BCC-CSM2-MR, MPI-ESM1-2-HR, and IPSL-CM6A-LR. The future nitrogen deposition background was the mean of ACCESS-ESM1-5, NorESM2-LM, and NorESM2-MM. The future net primary productivity was the mean of IPSL-CM6A-LR, CMCC-ESM2, and CanESM5-1. All maps were at  $0.5^\circ$  resolution. **b, e, h, k, n, q**, Latitudinal profiles of SOC stock, POC stock, and MAOC stock change at  $0.5^\circ$  latitudinal resolution. The green lines represent the absolute or relative change of SOC stock, POC stock, and MAOC stock. The grey shading represents the standard deviation. **c, f, i, l, o, r**, The absolute and relative change of SOC stock, POC stock, and MAOC stock between land covers.**



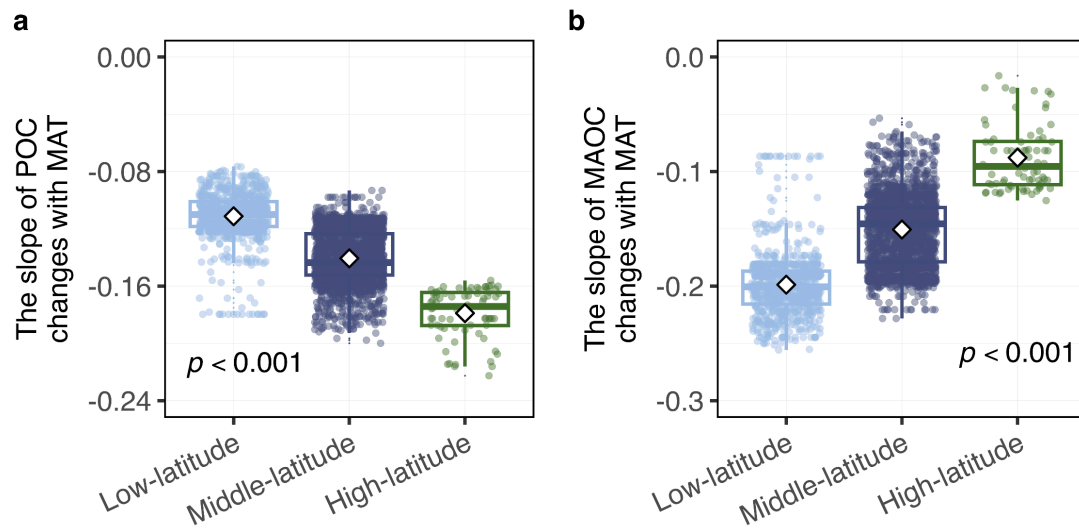
**Supplementary Figure 20 Global distribution of the absolute and relative changes in topsoil (a, d) soil organic carbon (SOC), (g, j) particulate organic carbon (POC), and (m, p) mineral-associated organic carbon (MAOC) stocks under SSP585 scenario for 2081-2100, based on the multi-model mean of four machine learning models (random forest model, generalized boosted regression model, extreme gradient boosting model, and generalized linear model). SSP, shared socioeconomic pathway. Here, SOC stock represents the sum of POC and MAOC stock.  $\Delta$ POC,  $\Delta$ MAOC, and  $\Delta$ SOC stocks are the differences between the future and present stocks. The POC and MAOC stocks from 2081 to 2100 were calculated using climatic factors of different models under SSP585 scenario. The future mean annual temperature, mean annual precipitation, temperature seasonality, precipitation seasonality, evapotranspiration, and leaf area index were the means of BCC-CSM2-MR, MPI-ESM1-2-HR, and IPSL-CM6A-LR. The future nitrogen deposition background was the mean of ACCESS-ESM1-5, NorESM2-LM, and NorESM2-MM. The future net primary productivity was the mean of IPSL-CM6A-LR, CMCC-ESM2, and CanESM5-1. All maps were at  $0.5^\circ$  resolution. **b, e, h, k, n, q**, Latitudinal profiles of SOC stock, POC stock, and MAOC stock change at  $0.5^\circ$  latitudinal resolution. The green lines represent the absolute or relative change of SOC stock, POC stock, and MAOC stock. The grey shading represents the standard deviation. **c, f, i, l, o, r**, The absolute and relative change of SOC stock, POC stock, and MAOC stock between land covers.**



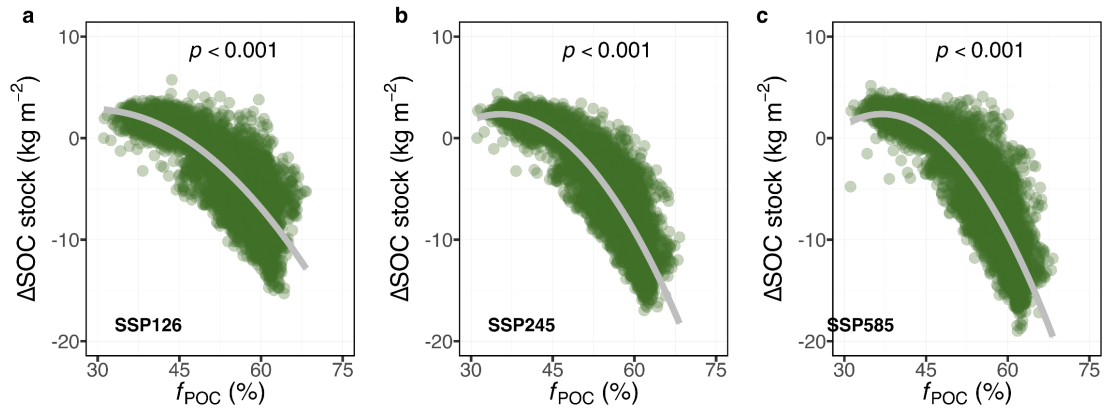
**Supplementary Figure 21** The absolute changes of topsoil soil organic carbon (SOC) stock, particulate organic carbon (POC) stock, and mineral-associated organic carbon (MAOC) stock under (a) SSP126, (b) SSP245, and (c) SSP585 scenarios from 2081 to 2100, based on a model trained exclusively on high-latitude soils. Box plots indicate the medians (horizontal lines), 1st and 3rd quartiles (boxes),  $1.5 \times$  interquartile range (whiskers), and means (diamonds).



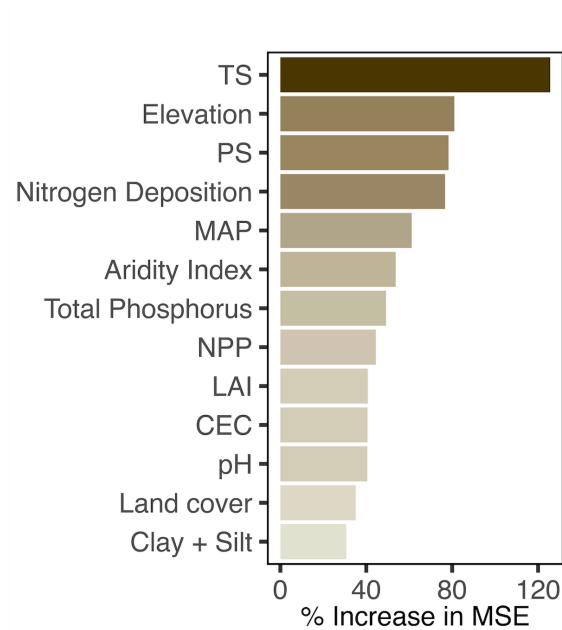
**Supplementary Figure 22 Global distribution of the absolute change of topsoil (a) soil organic carbon (SOC) stock, (d) particulate organic carbon (POC) stock, (g) mineral-associated organic carbon (MAOC) stock under SSP245 scenario from 2081 to 2100 by Biogeochemistry-Informed Neural Network models. SSP, shared socioeconomic pathway. Here, SOC stock represents the sum of POC and MAOC stock.  $\Delta$ POC,  $\Delta$ MAOC, and  $\Delta$ SOC stocks are the differences between the future and present stocks. All maps were at 0.5° resolution. **b, e, h**, Latitudinal profiles of SOC, POC, and MAOC stocks change at 0.5° latitudinal resolution. The green lines represent the absolute change of SOC, POC, and MAOC stocks. The grey shading represents the standard deviation. **c, f, i**, The absolute change of SOC, POC, and MAOC stocks between land covers.**



**Supplementary Figure 23 The slope of (a) particulate organic carbon (POC) and (b) mineral-associated organic carbon (MAOC) among different latitude soils.** MAT, mean annual temperature. Quadratic polynomial models were fitted to capture potential non-linear responses of POC and MAOC to MAT. Point-specific slopes (first derivatives) were calculated from the fitted models, representing the rate of change in POC and MAOC with increasing MAT. Box plots indicate the medians (horizontal lines), 1st and 3rd quartiles (boxes),  $1.5 \times$  interquartile range (whiskers), and means (diamonds). The  $p$ -value indicates the statistical significance between different forests.

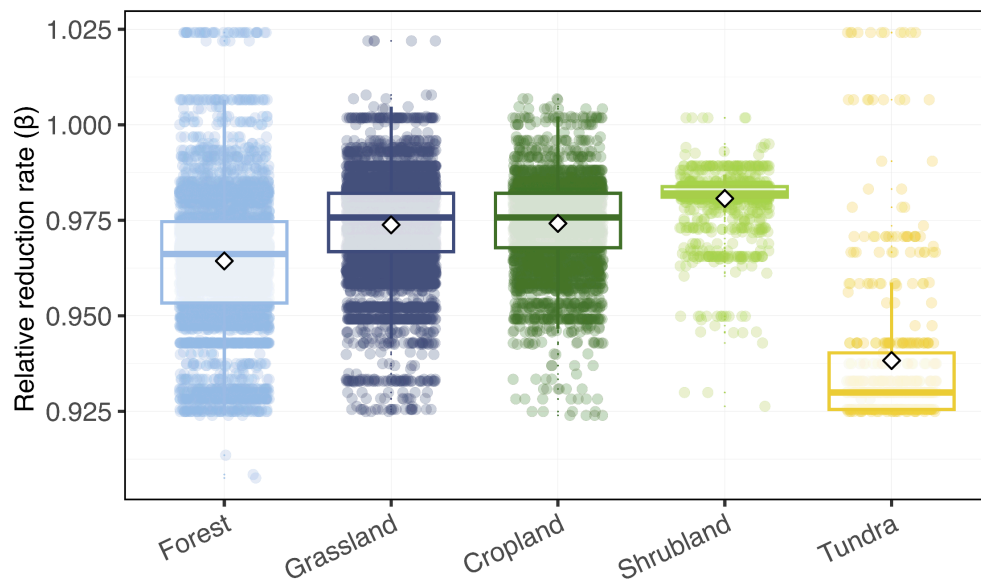


**Supplementary Figure 24 Relationship between the predicted proportion of particulate organic carbon (POC) relative to soil organic carbon ( $f_{\text{POC}}$ ) and the absolute change of (a-c) soil organic carbon (SOC) stock in high-latitude under different climate scenarios from 2081 to 2100. SSP, shared socioeconomic pathway.  $\Delta\text{SOC stock}$  is the difference between the future and present SOC stock. Different colors of points represent the various land covers.**

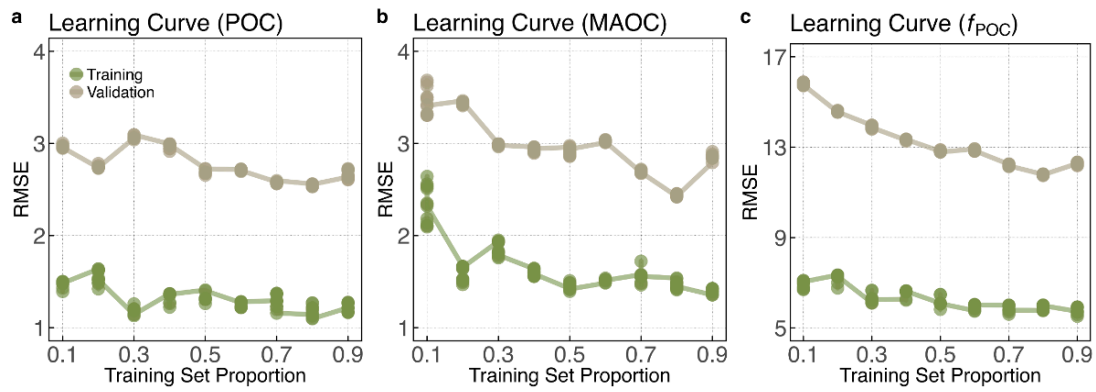


**Supplementary Figure 25 Variable importance of the machine learning random forest model for the slope of particulate organic carbon (POC) stock.** Mean annual precipitation (MAP), temperature seasonality (TS), precipitation seasonality (PS), background nitrogen deposition (Nitrogen deposition), aridity index, cation exchange capacity (CEC), percent of clay and silt (clay + silt), total phosphorus, net primary productivity (NPP), soil pH, and leaf area index (LAI) are continuous variables. Land cover is a categorical variable. Variable importance is ranked by the percent increase in mean square error (MSE).

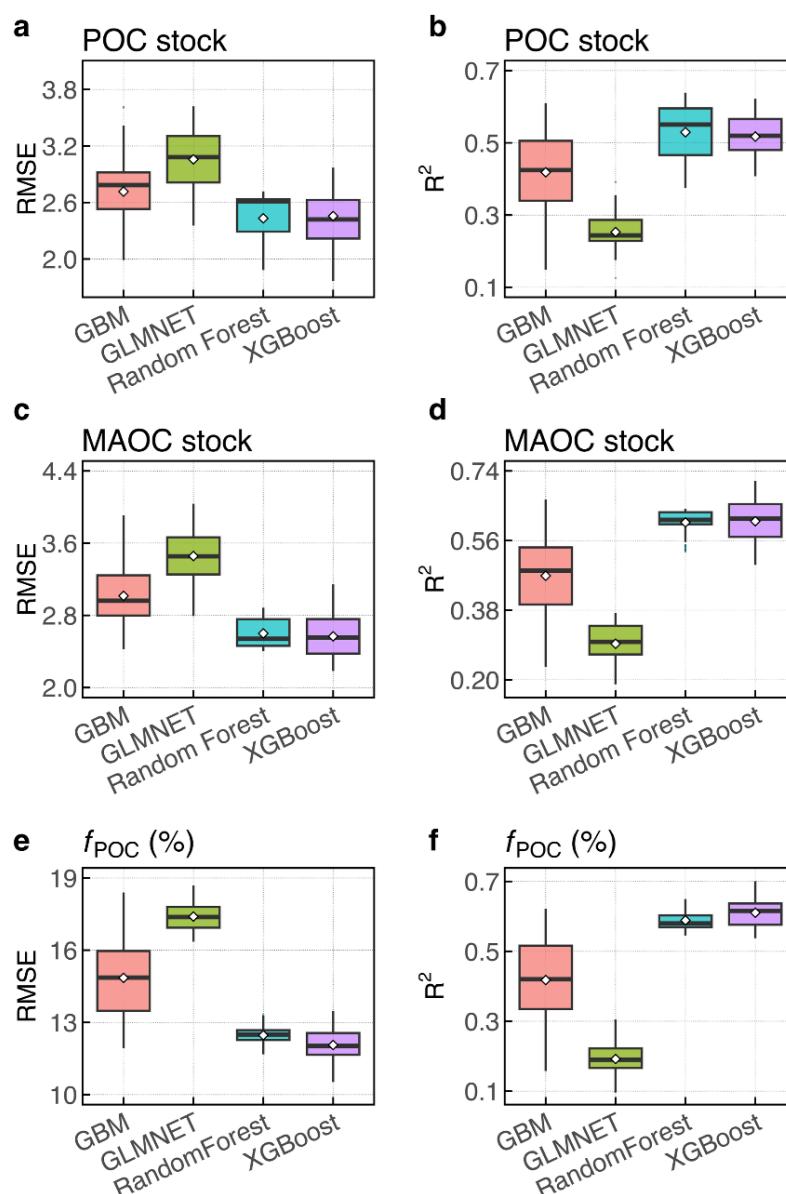




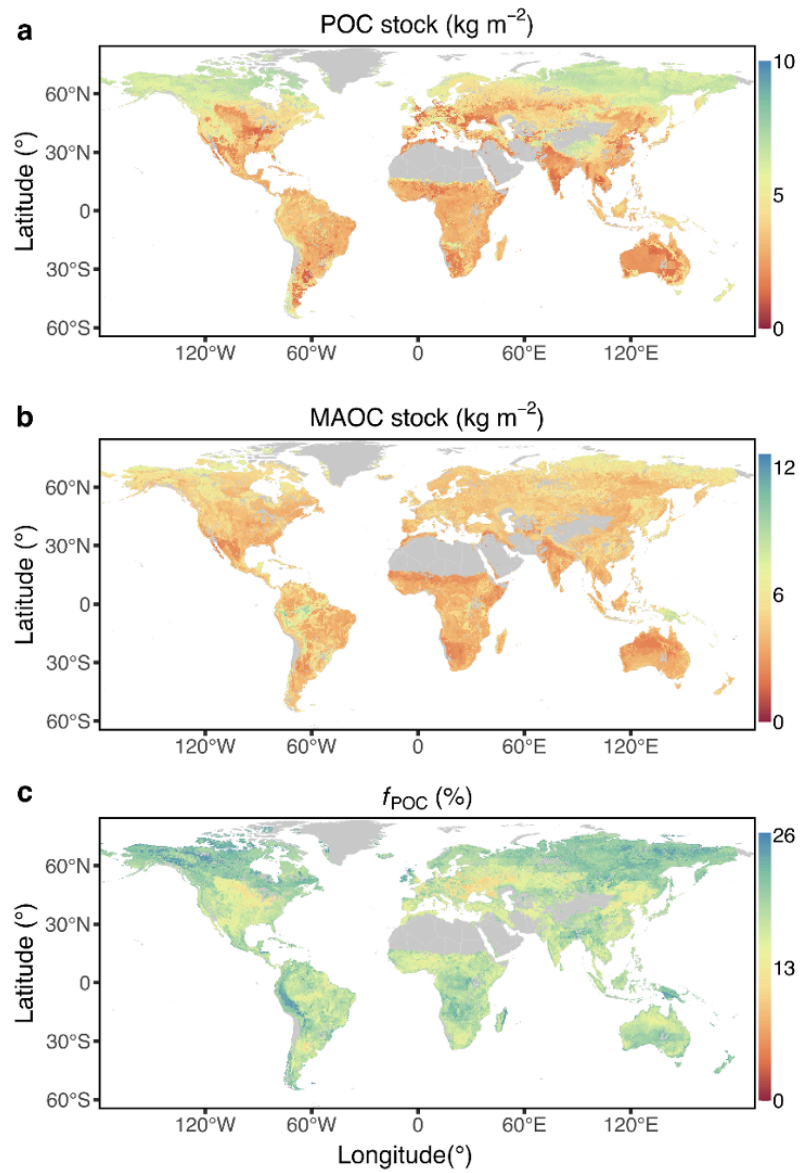
**Supplementary Figure 26** The relative reduction rate ( $\beta$ ) of topsoil soil organic carbon pool with increasing soil depth between different land covers.



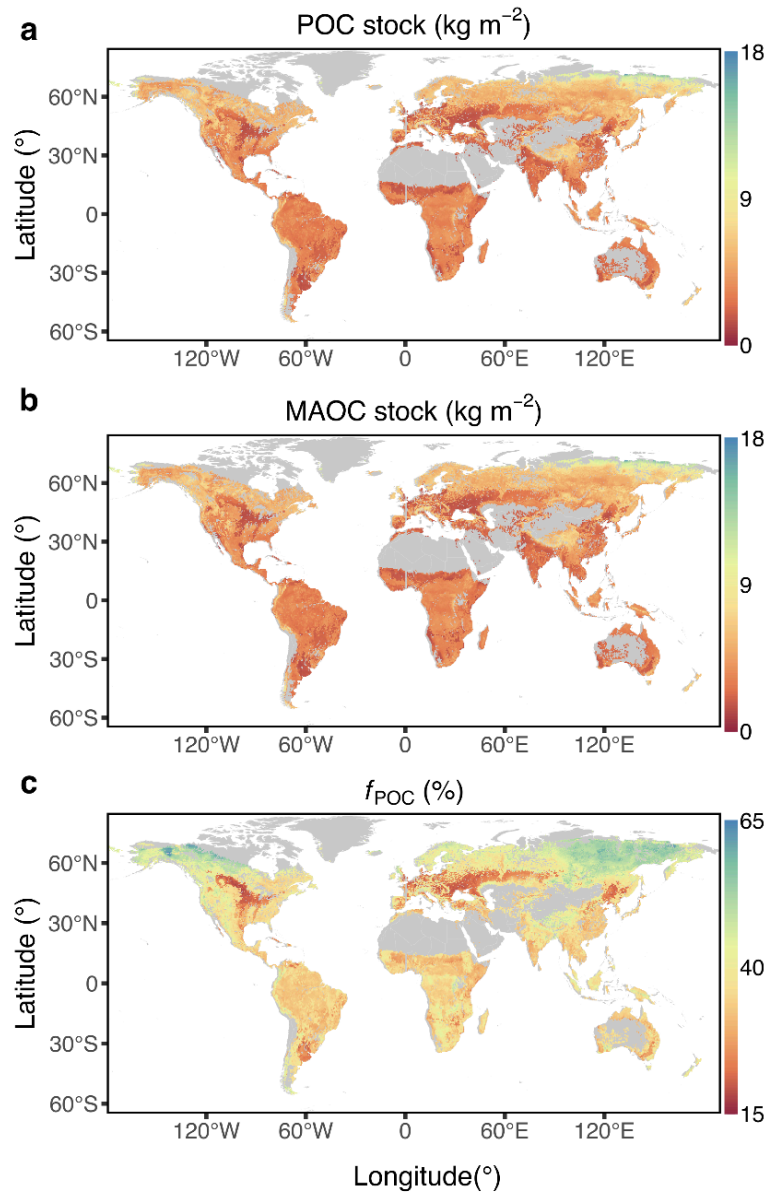
**Supplementary Figure 27** Learning curves of random forest models for (a) particulate organic carbon (POC), (b) mineral-associated organic carbon (MAOC), and (c) the proportion of POC relative to soil organic carbon ( $f_{\text{POC}}$ ) predictions. RMSE, root mean square error.



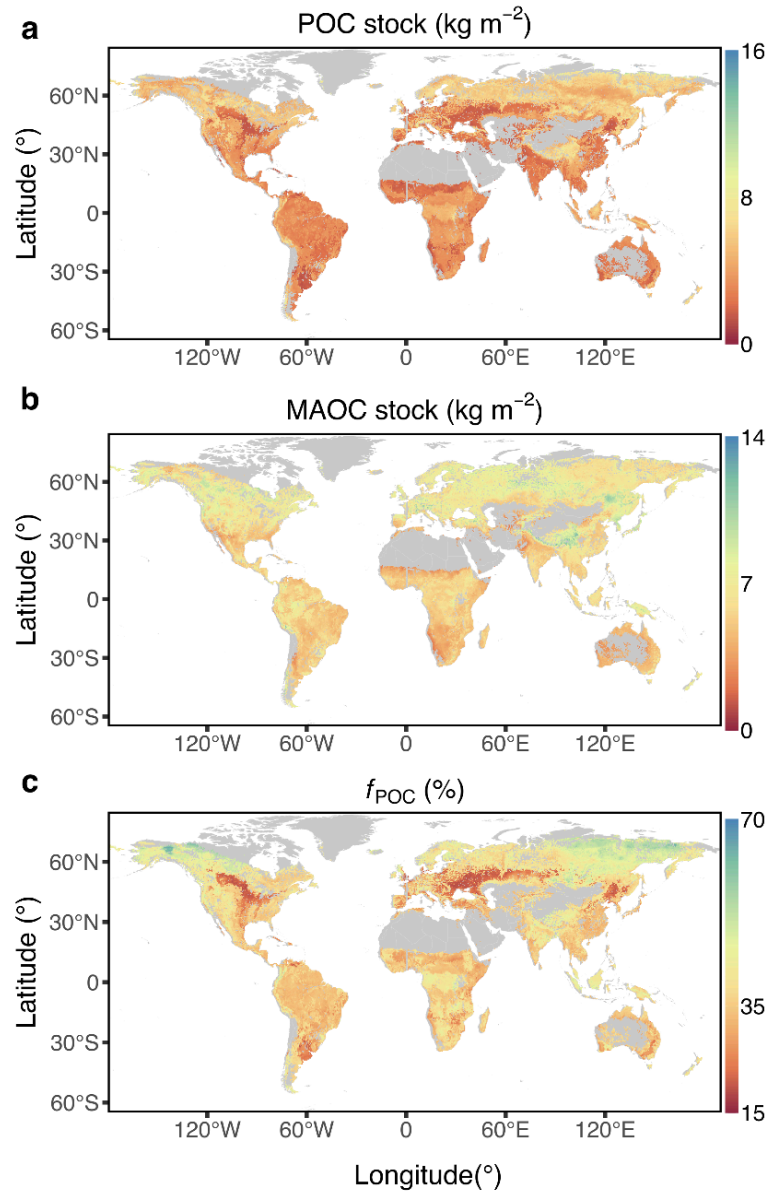
**Supplementary Figure 28** The model performance across random forest models, generalized boosted regression models (GBM), extreme gradient boosting (XGBoost), and generalized linear model (GLMNET). POC, particulate organic carbon. MAOC, mineral-associated organic carbon.  $f_{\text{POC}}$ , the proportion of POC relative to soil organic carbon. **a**, **c**, **e**, Root mean square error (RMSE) and **b**, **d**, **f**, regression coefficients of determination ( $R^2$ ) are two extensively used indicators for validation. Box plots indicate the medians (horizontal lines), 1st and 3rd quartiles (boxes),  $1.5 \times$  interquartile range (whiskers), and means (diamonds).



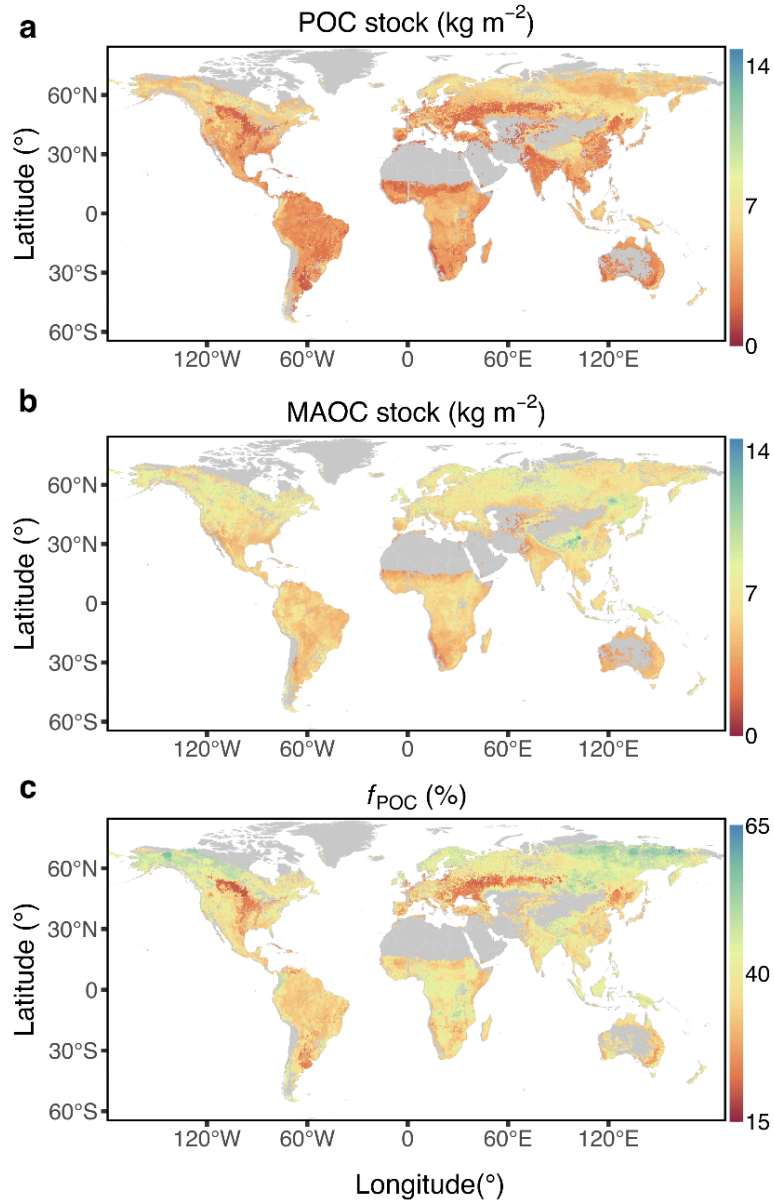
**Supplementary Figure 29** Standard deviation of predicted present (a) particulate organic carbon (POC) stock, (b) mineral-associated organic carbon (MAOC) stock, and (c) the proportion of POC relative to soil organic carbon ( $f_{\text{POC}}$ ) in the topsoil (0-30 cm). All maps were at  $0.5^\circ$  resolution.



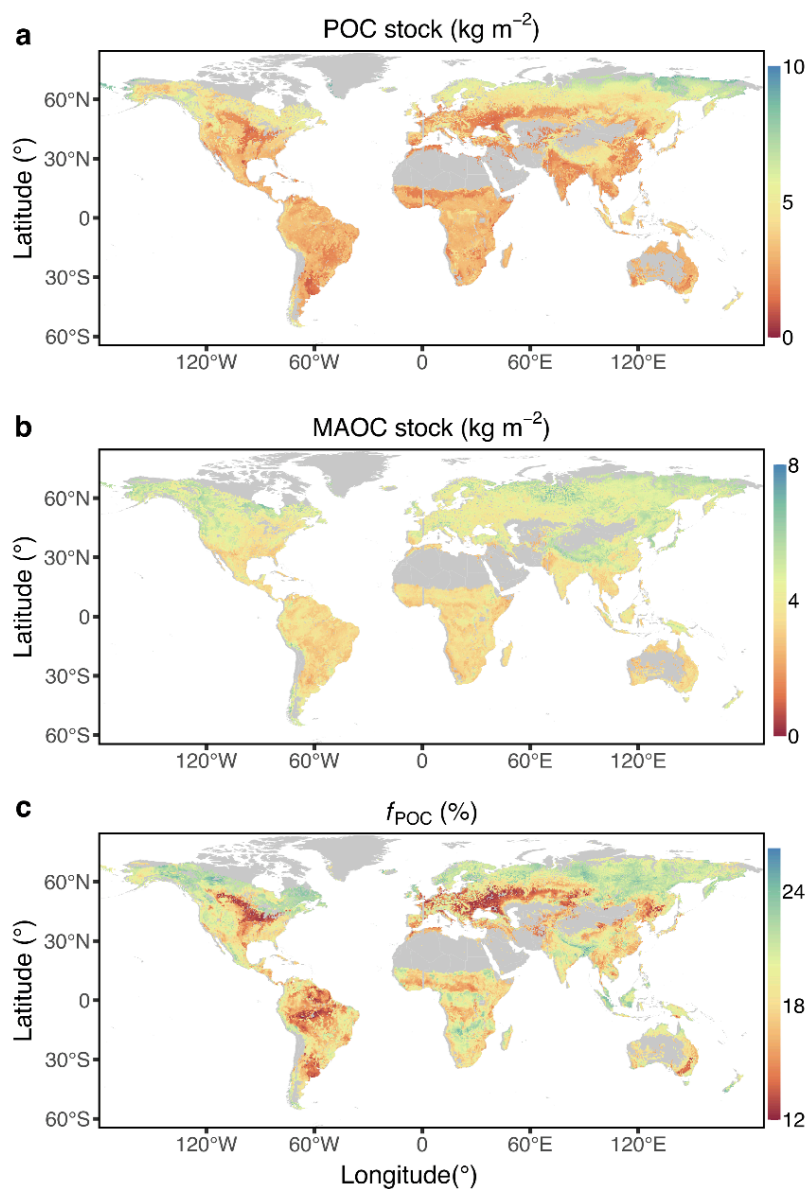
**Supplementary Figure 30** Global distribution of predicted (a) particulate organic carbon (POC) stock, (b) mineral-associated organic carbon (MAOC) stock, and (c) the proportion of POC relative to soil organic carbon ( $f_{\text{POC}}$ ) in the topsoil (0-30 cm) under SSP126 scenario from 2081 to 2100. The POC stock, MAOC stock, and  $f_{\text{POC}}$  were predicted using a random forest model. All maps were at 0.5° resolution.



**Supplementary Figure 31** Global distribution of predicted (a) particulate organic carbon (POC) stock, (b) mineral-associated organic carbon (MAOC) stock, and (c) the proportion of POC relative to soil organic carbon ( $f_{\text{POC}}$ ) in the topsoil (0-30 cm) under SSP245 scenario from 2081 to 2100. The POC stock, MAOC stock, and  $f_{\text{POC}}$  were predicted using a random forest model. All maps were at 0.5° resolution.

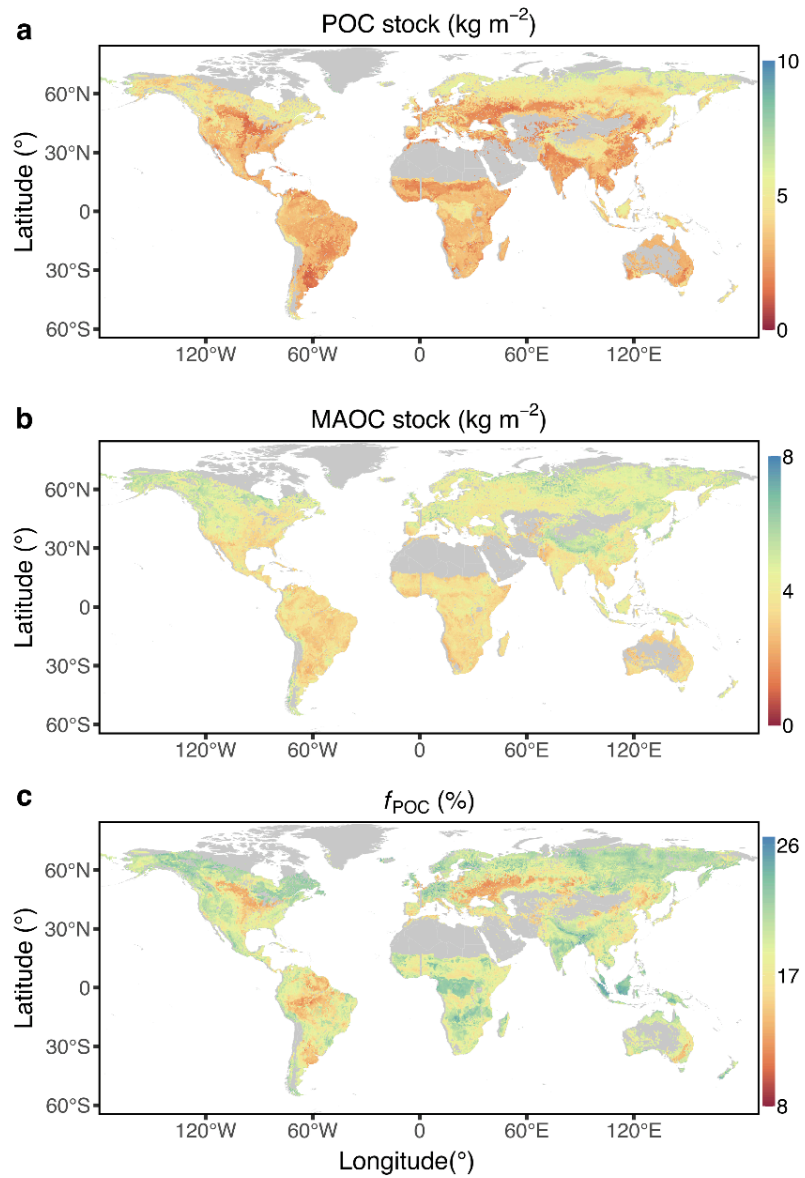


**Supplementary Figure 32** Global distribution of predicted (a) particulate organic carbon (POC) stock, (b) mineral-associated organic carbon (MAOC) stock, and (c) the proportion of POC relative to soil organic carbon ( $f_{\text{POC}}$ ) in the topsoil (0–30 cm) under SSP585 scenario from 2081 to 2100. The POC stock, MAOC stock, and  $f_{\text{POC}}$  were predicted using a random forest model. All maps were at  $0.5^{\circ}$  resolution.

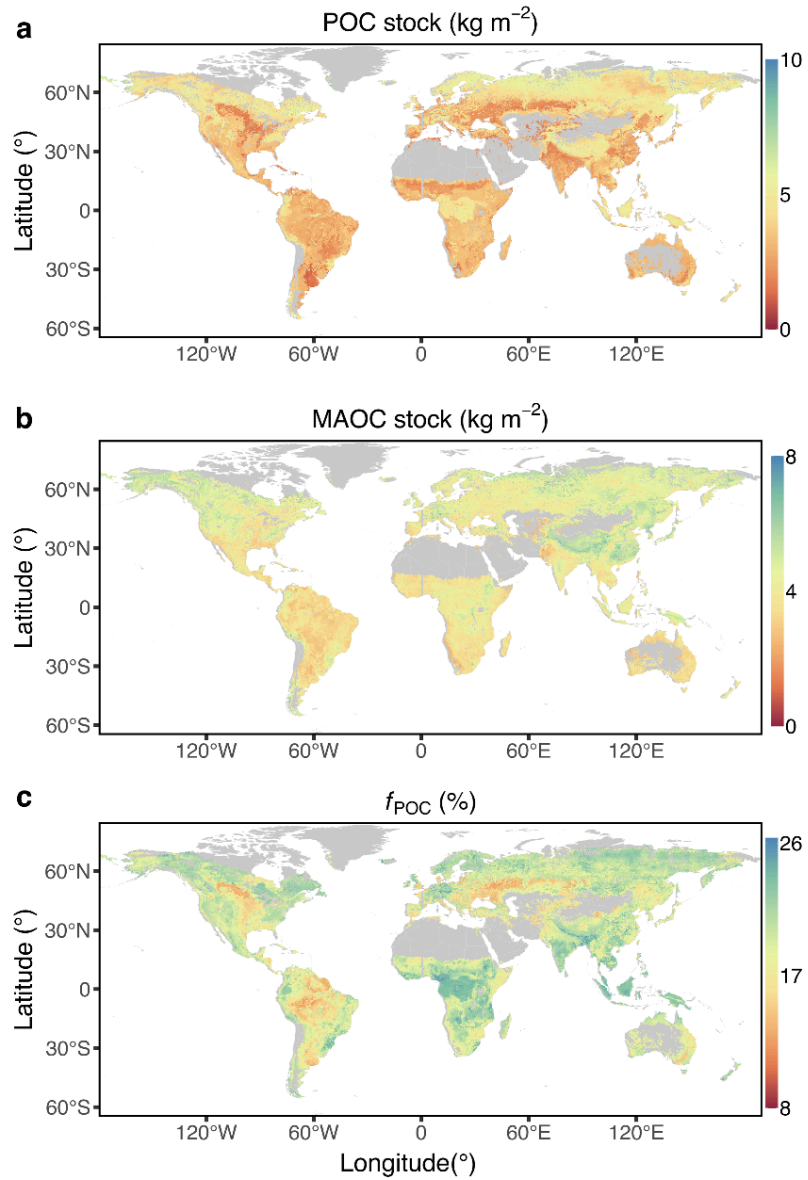


**Supplementary Figure 33** Standard deviation of predicted (a) particulate organic carbon (POC) stock, (b) mineral-associated organic carbon (MAOC) stock, and (c) the proportion of POC relative to soil organic carbon ( $f_{\text{POC}}$ ) in the topsoil (0-30 cm) under SSP126 scenario from 2081 to 2100. All maps were at  $0.5^{\circ}$  resolution.

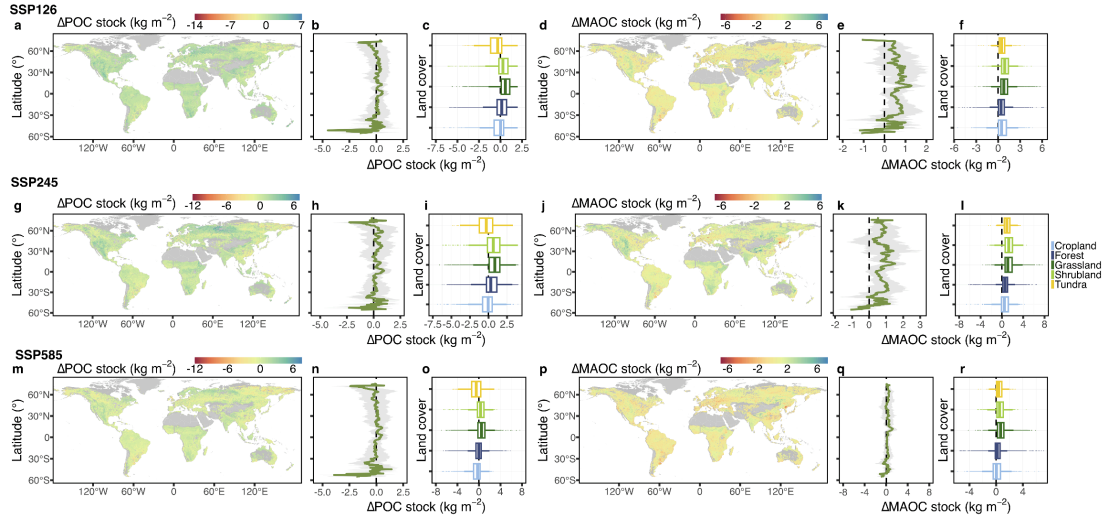




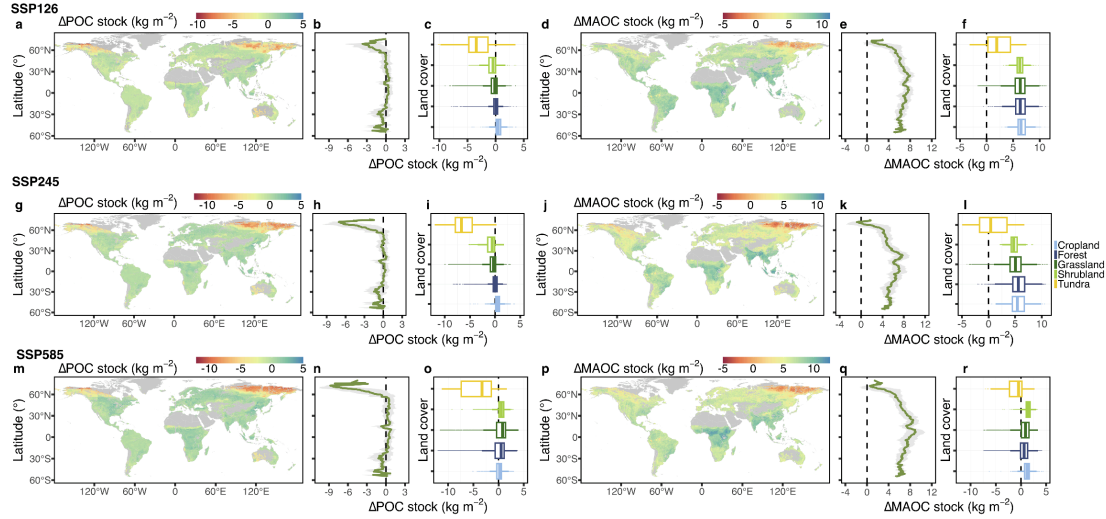
**Supplementary Figure 34 Standard deviation of predicted (a) particulate organic carbon (POC) stock, (b) mineral-associated organic carbon (MAOC) stock, and (c) the proportion of POC relative to soil organic carbon ( $f_{\text{POC}}$ ) in the topsoil (0-30 cm) under SSP245 scenario from 2081 to 2100. All maps were at  $0.5^{\circ}$  resolution.**



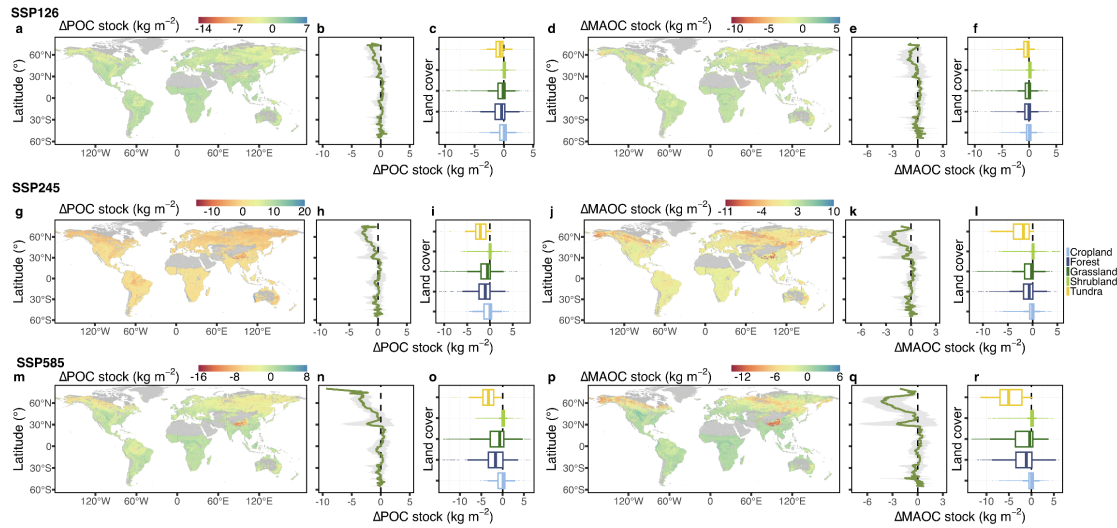
**Supplementary Figure 35** Standard deviation of predicted (a) particulate organic carbon (POC) stock, (b) mineral-associated organic carbon (MAOC) stock, and (c) the proportion of POC relative to soil organic carbon ( $f_{\text{POC}}$ ) in the topsoil (0-30 cm) under SSP585 scenario from 2081 to 2100. All maps were at 0.5° resolution.



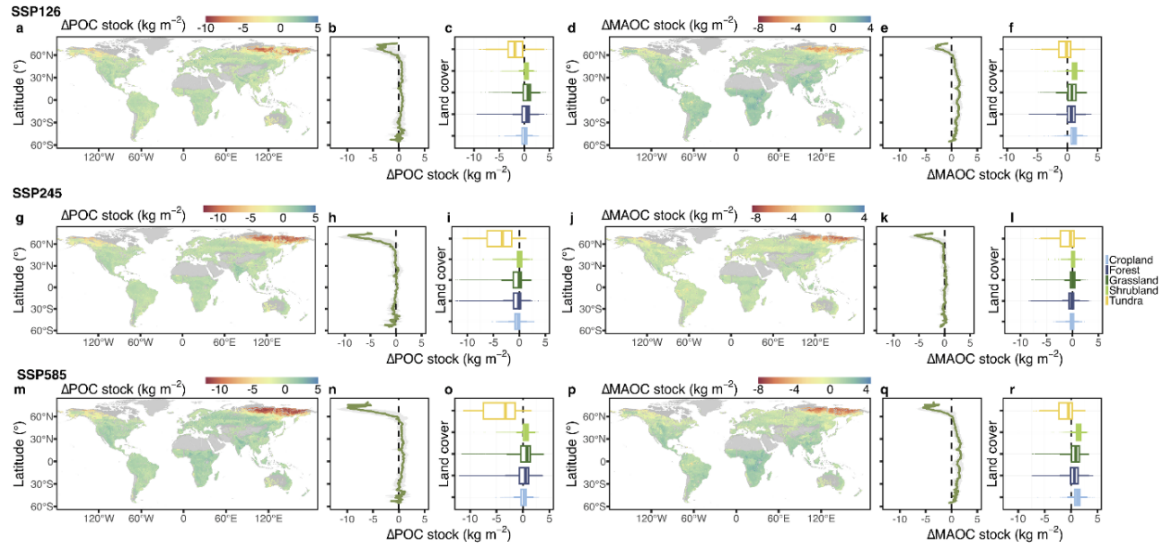
**Supplementary Figure 36 Global distribution of the absolute change of topsoil (a, g, m) particulate organic carbon (POC) stock and (d, j, p) mineral-associated organic carbon (MAOC) stock (0-30 cm) under SSP126, SSP245, and SSP585 scenarios from 2081 to 2100, based on models trained with datasets separated by particle method. SSP, shared socioeconomic pathway.  $\Delta\text{POC}$  and  $\Delta\text{MAOC}$  stocks are the differences between the future and present stocks. b, h, n, e, k, q Latitudinal profiles of POC stock and MAOC stock change at  $0.5^\circ$  latitudinal resolution. The green lines represent the absolute change of POC stock and MAOC stock. The grey shading represents the standard deviation. c, i, o, f, l, r, The absolute change of POC stock and MAOC stock between land covers.**



**Supplementary Figure 37 Global distribution of the absolute change of topsoil (a, g, m) particulate organic carbon (POC) stock and (d, j, p) mineral-associated organic carbon (MAOC) stock under SSP126, SSP245, and SSP585 scenarios from 2081 to 2100, based on models trained with datasets separated by density method. SSP, shared socioeconomic pathway.  $\Delta\text{POC}$  and  $\Delta\text{MAOC}$  stocks are the differences between the future and present stocks. b, h, n, e, k, q Latitudinal profiles of POC stock and MAOC stock change at 0.5° latitudinal resolution. The green lines represent the absolute change of POC stock and MAOC stock. The grey shading represents the standard deviation. c, i, o, f, l, r, The absolute change of POC stock and MAOC stock between land covers.**



**Supplementary Figure 38 Global distribution of the absolute change of topsoil (a, g, m) particulate organic carbon (POC) stock and (d, j, p) mineral-associated organic carbon (MAOC) stock under SSP126, SSP245, and SSP585 scenarios from 2081 to 2100, based on models trained with datasets separated by the combination of particle size and density method. SSP, shared socioeconomic pathway.  $\Delta$ POC and  $\Delta$ MAOC stocks are the differences between the future and present stocks. **b, h, n, e, k, q** Latitudinal profiles of POC stock and MAOC stock change at  $0.5^\circ$  latitudinal resolution. The green lines represent the absolute change of POC stock and MAOC stock. The grey shading represents the standard deviation. **c, i, o, f, l, r** The absolute change of POC stock and MAOC stock between land covers.**



**Supplementary Figure 39** Global distribution of the absolute change of topsoil (a, g, m) particulate organic carbon (POC) stock and (d, j, p) mineral-associated organic carbon (MAOC) stock under SSP126, SSP245, and SSP585 scenarios from 2081 to 2100, based on models trained with the non-standardized dataset. SSP, shared socioeconomic pathway.  $\Delta$ POC and  $\Delta$ MAOC stocks are the differences between the future and present stocks. b, h, n, e, k, q Latitudinal profiles of POC stock and MAOC stock change at  $0.5^\circ$  latitudinal resolution. The green lines represent the absolute change of POC stock and MAOC stock. The grey shading represents the standard deviation. c, i, o, f, l, r, The absolute change of POC stock and MAOC stock between land covers.

## Supplementary References

1. Hassink, J., Whitmore, A. P. & Kubát, J. Size and density fractionation of soil organic matter and the physical capacity of soils to protect organic matter. *Eur. J. Agron.* **7**, 189-199 (1997).
2. Swanston, C. W., et al. Initial characterization of processes of soil carbon stabilization using forest stand-level radiocarbon enrichment. *Geoderma* **128**, 52-62 (2005).
3. Cotrufo, M. F., Ranalli, M. G., Haddix, M. L., Six, J. & Lugato, E. Soil carbon storage informed by particulate and mineral-associated organic matter. *Nat. Geosci.* **12**, 989-994 (2019).
4. Angers, D. A., N'Dayegamiye, A. & Côté, D. Tillage-Induced Differences in Organic Matter of Particle-Size Fractions and Microbial Biomass. *Soil Sci. Soc. Am. J.* **57**, 512-516 (1993).
5. Kögel-Knabner, I., et al. Organo-mineral associations in temperate soils: Integrating biology, mineralogy, and organic matter chemistry. *J. Plant Nutr. Soil Sci.* **171**, 61-82 (2008).
6. Chenu, C. & Plante, A. Clay-sized organo-mineral complexes in a cultivation chronosequence: revisiting the concept of the 'primary organo-mineral complex'. *Eur. J. Soil Sci.* **57**, 596-607 (2006).
7. Tao, F., et al. Deep Learning Optimizes Data-Driven Representation of Soil Organic Carbon in Earth System Model Over the Conterminous United States. *Front. Big Data* **3**, 17 (2020).
8. Lawrence, D. M., et al. The Community Land Model version 5: Description of new features, benchmarking, and impact of forcing uncertainty. *J. Adv. Model. Earth Syst.* **11**, 4245-4287 (2019).
9. Luo, Y., et al. Matrix approach to land carbon cycle modeling. *J. Adv. Model. Earth Syst.* **14**, e2022MS003008 (2022).
10. Huang, Y., et al. Matrix approach to land carbon cycle modeling: A case study with the Community Land Model. *Glob. Change Biol.* **24**, 1394-1404 (2018).
11. Xu, H., et al. Biogeochemistry-Informed Neural Network (BINN) for Improving Accuracy of Model Prediction and Scientific Understanding of Soil Organic Carbon. *arXiv preprint arXiv:2502.00672*, (2025).

12. Luo, Y. & Schuur, E. A. Model parameterization to represent processes at unresolved scales and changing properties of evolving systems. *Glob. Change Biol.* **26**, 1109-1117 (2020).
13. Hansen, P. M., et al. Distinct, direct and climate-mediated environmental controls on global particulate and mineral-associated organic carbon storage. *Glob. Change Biol.* **30**, e17080 (2024).
14. Guo, Z., et al. Dominant edaphic controls on particulate organic carbon in global soils. *Glob. Change Biol.* **30**, e17619 (2024).
15. Zhou, Z., et al. Global turnover of soil mineral-associated and particulate organic carbon. *Nat. Commun.* **15**, 5329 (2024).
16. García-Palacios, P., et al. Dominance of particulate organic carbon in top mineral soils in cold regions. *Nat. Geosci.* **17**, 145-150 (2024).
17. Zhang, Y., et al. Global pattern of organic carbon pools in forest soils. *Glob. Change Biol.* **30**, e17386 (2024).
18. Viscarra Rossel, R. A., et al. Continental-scale soil carbon composition and vulnerability modulated by regional environmental controls. *Nat. Geosci.* **12**, 547-552 (2019).
19. Li, X., et al. A New Global Land-Use and Land-Cover Change Product at a 1-km Resolution for 2010 to 2100 Based on Human–Environment Interactions. *Ann. Am. Assoc. Geogr.* **107**, 1040-1059 (2017).
20. Cao, S., et al. Spatiotemporally consistent global dataset of the GIMMS leaf area index (GIMMS LAI4g) from 1982 to 2020. *Earth Syst. Sci. Data* **15**, 4877-4899 (2023).
21. Ito, A. & Wagai, R. Global distribution of clay-size minerals on land surface for biogeochemical and climatological studies. *Sci. Data* **4**, 170103 (2017).
22. He, X., et al. Global patterns and drivers of soil total phosphorus concentration. *Earth Syst. Sci. Data* **13**, 5831-5846 (2021).
23. Acharya, P., Ghimire, R. & Acosta-Martínez, V. Cover crop-mediated soil carbon storage and soil health in semi-arid irrigated cropping systems. *Agric. Ecosyst. Environ.* **361**, 108813 (2024).
24. Adams, J. L., Tipping, E., Thacker, S. A. & Quinton, J. N. An investigation of the distribution of phosphorus between free and mineral associated soil organic matter,



using density fractionation. *Plant Soil* **427**, 139-148 (2018).

25. Álvaro-Fuentes, J., et al. Stover management modifies soil organic carbon dynamics in the short-term under semiarid continuous maize. *Soil Tillage Res.* **213**, 105143 (2021).
26. An, C., et al. Response of soil microbial organic carbon and particulate organic carbon to different tillage measures in summer soybean. *Xinjiang Agricultural Sciences* **56**, 1012-1021 (2019).
27. Anaya, C. A. & Huber-Sannwald, E. Long-term soil organic carbon and nitrogen dynamics after conversion of tropical forest to traditional sugarcane agriculture in East Mexico. *Soil Tillage Res.* **147**, 20-29 (2015).
28. Aoyama, M. & Kumakura, N. Quantitative and qualitative changes of organic matter in an Ando soil induced by mineral fertilizer and cattle manure applications for 20 years. *Soil Sci. Plant Nutr.* **47**, 241-252 (2001).
29. Assis, C. P., et al. Distribution and quality of the organic matter in light and heavy fractions of a red latosol under different uses and management practices. *Commun. Soil Sci. Plant Anal.* **43**, 835-846 (2012).
30. Atoloye, I. A., Jacobson, A. R., Creech, J. E. & Reeve, J. R. Soil organic carbon pools and soil quality indicators 3 and 24 years after a one-time compost application in organic dryland wheat systems. *Soil Tillage Res.* **224**, 105503 (2022).
31. Bai, Y., et al. Effects of land use change on soil organic carbon and its components in karst rocky desertification of southwest China. *Chinese Journal of Applied Ecology* **31**, 1607-1616 (2020).
32. Bajgai, Y., Kristiansen, P., Hulugalle, N. & McHenry, M. Changes in soil carbon fractions due to incorporating corn residues in organic and conventional vegetable farming systems. *Soil Res.* **52**, 244-252 (2014).
33. Balabane, M. & Plante, A. F. Aggregation and carbon storage in silty soil using physical fractionation techniques. *Eur. J. Soil Sci.* **55**, 415-427 (2004).
34. Balesdent, J., Besnard, E., Arrouays, D. & Chenu, C. The dynamics of carbon in particle-size fractions of soil in a forest-cultivation sequence. *Plant Soil* **201**, 49-57 (1998).
35. Bandyopadhyay, K. K., and R. Lal. Effect of long-term land use management practices on distribution of C and N pools in water stable aggregates in Alfisols. *J. Indian Soc. Soil Sci.* **63**, 53-63 (2015).

36. Begill, N., Don, A. & Poeplau, C. No detectable upper limit of mineral-associated organic carbon in temperate agricultural soils. *Glob. Change Biol.* **29**, 4662-4669 (2023).
37. Beheshti, A., Raiesi, F. & Golchin, A. Soil properties, C fractions and their dynamics in land use conversion from native forests to croplands in northern Iran. *Agric. Ecosyst. Environ.* **148**, 121-133 (2012).
38. Benbi, D. K., Boparai, A. K. & Brar, K. Decomposition of particulate organic matter is more sensitive to temperature than the mineral associated organic matter. *Soil Biol. Biochem.* **70**, 183-192 (2014).
39. Benbi, D. K., Toor, A. S. & Kumar, S. Management of organic amendments in rice-wheat cropping system determines the pool where carbon is sequestered. *Plant Soil* **360**, 145-162 (2012).
40. Berhe, A. A., et al. Persistence of soil organic matter in eroding versus depositional landform positions. *J. Geophys. Res.: Biogeosci.* **117**, G02019 (2012).
41. Bieluczyk, W., et al. Granulometric and oxidizable carbon fractions of soil organic matter in crop-livestock integration systems. *Semina Cienc. Agrar.* **38**, 607-621 (2017).
42. Blanco-Moure, N., Gracia, R., Bielsa, A. C. & López, M. V. Long-term no-tillage effects on particulate and mineral-associated soil organic matter under rainfed Mediterranean conditions. *Soil Use Manage.* **29**, 250-259 (2013).
43. Błońska, E., Lasota, J., Tullus, A., Lutter, R. & Ostonen, I. Impact of deadwood decomposition on soil organic carbon sequestration in Estonian and Polish forests. *Ann. For. Sci.* **76**, 102 (2019).
44. Boeni, M., et al. Organic matter composition in density fractions of Cerrado Ferralsols as revealed by CPMAS <sup>13</sup>C NMR: Influence of pastureland, cropland and integrated crop-livestock. *Agric. Ecosyst. Environ.* **190**, 80-86 (2014).
45. Boone, R. D. Light-fraction soil organic matter: origin and contribution to net nitrogen mineralization. *Soil Biol. Biochem.* **26**, 1459-1468 (1994).
46. Borges, B. M. M. N., Bordonal, R. d. O., Silveira, M. L. & Coutinho, E. L. M. Short-term impacts of high levels of nitrogen fertilization on soil carbon dynamics in a tropical pasture. *CATENA* **174**, 413-416 (2019).
47. Bornemann, L., Herbst, M., Welp, G., Vereecken, H. & Amelung, W. Rock

fragments control size and saturation of organic carbon pools in agricultural topsoil. *Soil Sci. Soc. Am. J.* **75**, 1898-1907 (2011).

48. Bremer, E., Ellert, B. H. & Janzen, H. H. Total and light-fraction carbon dynamics during four decades after cropping changes. *Soil Sci. Soc. Am. J.* **59**, 1398-1403 (1995).
49. Cambardella, C. A. & Elliott, E. T. Particulate soil organic-matter changes across a grassland cultivation sequence. *Soil Sci. Soc. Am. J.* **56**, 777-783 (1992).
50. Campos, B.-H. C. d., Amado, T. J. C., Bayer, C., Nicoloso, R. d. S. & Fiorin, J. E. Carbon stock and its compartments in a subtropical oxisol under long-term tillage and crop rotation systems. *Revista Brasileira de Ciência do Solo* **35**, 805-817 (2011).
51. Cao, Y., Ding, S., Qin, Y., He, X. & Ma, J. Effects of bamboo-tea mixed model on surface soil organic carbon storage and components. *Guihaia* **43**, 1668-1677 (2022).
52. Carter, M. R. & Gregorich, E. G. Carbon and nitrogen storage by deep-rooted tall fescue (*Lolium arundinaceum*) in the surface and subsurface soil of a fine sandy loam in eastern Canada. *Agric. Ecosyst. Environ.* **136**, 125-132 (2010).
53. Castro, G. S. A., Crusciol, C. A. C., Calonego, J. C. & Rosolem, C. A. Management Impacts on soil organic matter of tropical soils. *Vadose Zone J.* **14**, 1-8 (2015).
54. Catroux, G. & Schnitzer, M. Chemical, spectroscopic, and biological characteristics of the organic matter in particle size fractions separated from an Aquoll. *Soil Sci. Soc. Am. J.* **51**, 1200-1207 (1987).
55. Cavalieri-Polizeli, K. M. V., et al. Conservative farming systems and their effects on soil organic carbon and structural quality. *Soil Tillage Res.* **242**, 106143 (2024).
56. Centurión, N., et al. Increasing legume Input through Interseeding cover crops: soil and crop response as affected by tillage system. *Agronomy* **13**, 1388 (2023).
57. Chacón, P., Lorenz, K., Lal, R., Calhoun, F. G. & Fausey, N. R. Association of soil organic carbon with physically separated soil fractions in different land uses of Costa Rica. *Acta Agriculturae Scandinavica, Section B — Soil & Plant Science* **65**, 448-459 (2015).
58. Chan, K. Y. Soil particulate organic carbon under different land use and management. *Soil Use Manage.* **17**, 217-221 (2001).

59. Chatterjee, A. & Lal, R. On farm assessment of tillage impact on soil carbon and associated soil quality parameters. *Soil Tillage Res.* **104**, 270-277 (2009).
60. Chen, G., et al. Effects of land use types on soil organic carbon and its fractions in karst area. *J. Soil Water Conserv.* **29**, 123-129 (2015).
61. Chen, G., Tu, L., Chen, G., Hu, J. & Han, Z. Effect of six years of nitrogen additions on soil chemistry in a subtropical *Pleioblastus amarus* forest, Southwest China. *J. For. Res.* **29**, 1657-1664 (2018).
62. Chen, J., Ji, C., Fang, J., He, H. & Zhu, B. Dynamics of microbial residues control the responses of mineral-associated soil organic carbon to N addition in two temperate forests. *Sci. Total Environ.* **748**, 141318 (2020).
63. Chen, J., Xiao, W., Zheng, C. & Zhu, B. Nitrogen addition has contrasting effects on particulate and mineral-associated soil organic carbon in a subtropical forest. *Soil Biol. Biochem.* **142**, 107708 (2020).
64. Chen, J., et al. Nitrogen addition promotes the accumulation of soil particulate organic carbon in a subtropical forest. *Forests* **15**, 619 (2024).
65. Chen, M., et al. Response of soil organic carbon stability and sequestration to long-term phosphorus application: insight from a 9-year field experiment in saline alkaline paddy soil. *Plant Soil* **496**, 415-429 (2023).
66. Chen, R., et al. Mineral-associated organic carbon predicts the variations in microbial biomass and specific enzyme activities in a subtropical forest. *Geoderma* **439**, 116671 (2023).
67. Chen, S., et al. The influence of the type of crop residue on soil organic carbon fractions: an 11-year field study of rice-based cropping systems in southeast China. *Agric. Ecosyst. Environ.* **223**, 261-269 (2016).
68. Chen, X., Hu, M., Zheng, G. & Chen, H. Y. H. Persistent soil organic carbon deficits from converting primary forests to plantations and secondary forests in subtropical China. *Global Ecol. Conserv.* **45**, e02530 (2023).
69. Chen, X., et al. Effects of nitrogen deposition on soil organic carbon fractions in the subtropical forest ecosystems of S China. *J. Plant Nutr. Soil Sci.* **175**, 947-953 (2012).
70. Chen, X., et al. Effects of precipitation intensity on soil organic carbon fractions and their distribution under subtropical forests of South China. *Chinese Journal of Applied Ecology* **21**, 1210-1216 (2010).

71. Chen, X., Liu, J., Deng, Q., Yan, J. & Zhang, D. Effects of elevated CO<sub>2</sub> and nitrogen addition on soil organic carbon fractions in a subtropical forest. *Plant Soil* **357**, 25-34 (2012).
72. Chen, X., et al. Soil microbial communities under wheat and maize straw incorporation are closely associated with soil organic carbon fractions and chemical structure. *Appl. Soil Ecol.* **182**, 104724 (2023).
73. Chen, Y., et al. Long-term warming reduces surface soil organic carbon by reducing mineral-associated carbon rather than “free” particulate carbon. *Soil Biol. Biochem.* **177**, 108905 (2023).
74. Chen, Y., et al. Biochemical composition of soil organic matter physical fractions under 32-year fertilization in Ferralic Cambisol. *Carbon Res.* **2**, 1-14 (2023).
75. Chen, Y., Liu, X., Hou, Y., Zhou, S. & Zhu, B. Particulate organic carbon is more vulnerable to nitrogen addition than mineral-associated organic carbon in soil of an alpine meadow. *Plant Soil* **458**, 93-103 (2021).
76. Cheng, S., Fang, H. & Yu, G. Threshold responses of soil organic carbon concentration and composition to multi-level nitrogen addition in a temperate needle-broadleaved forest. *Biogeochemistry* **137**, 219-233 (2018).
77. Cheng, X., Yu, M. & Wang, G. G. Effects of thinning on soil organic carbon fractions and soil properties in *cunninghamia lanceolata* stands in Eastern China. *Forests* **8**, 198 (2017).
78. Ci, E., et al. Active fractions and  $\delta^{13}\text{C}$  value of soil organic carbon in paddy fields under ridge-cultivation and no tillage system. *Scientia Agricultura Sinica* **46**, 978-986 (2013).
79. Conceição, P. C., Dieckow, J. & Bayer, C. Combined role of no-tillage and cropping systems in soil carbon stocks and stabilization. *Soil Tillage Res.* **129**, 40-47 (2013).
80. Cordeiro, C. F. d. S., Rodrigues, D. R., Silva, G. F. d., Echer, F. R. & Calonego, J. C. Soil organic carbon stock is improved by cover crops in a tropical sandy soil. *Agron. J.* **114**, 1546-1556 (2022).
81. Coulter, J. A., Nafziger, E. D. & Wander, M. M. Soil organic matter response to Cropping system and nitrogen fertilization. *Agron. J.* **101**, 592-599 (2009).
82. Cusack, D. F., et al. Decadal-scale litter manipulation alters the biochemical and

- physical character of tropical forest soil carbon. *Soil Biol. Biochem.* **124**, 199-209 (2018).
83. Cusack, D. F., Silver, W. L., Torn, M. S. & McDowell, W. H. Effects of nitrogen additions on above- and belowground carbon dynamics in two tropical forests. *Biogeochemistry* **104**, 203-225 (2011).
  84. da Rocha Junior, P. R., et al. Can soil organic carbon pools indicate the degradation levels of pastures in the Atlantic forest biome? *J. Agric. Sci.* **6**, 84 (2014).
  85. da Silva, F. D. d., et al. Soil carbon indices as affected by 10 years of integrated crop–livestock production with different pasture grazing intensities in Southern Brazil. *Agric. Ecosyst. Environ.* **190**, 60-69 (2014).
  86. da Silva Rodrigues Pinto, L. A., et al. Temporal evaluation of soil attributes in no-tillage areas after burning in the Cerrado Biome, Brazil. *J. Soil Sci. Plant Nutr.* **23**, 5552-5566 (2023).
  87. Dai, W., Fan, Y., Cao, L., Cao, L. & Sha, Z. Soil organic carbon dynamics shift by incorporating wheat straw in paddy soil in China. *J. Environ. Qual.* **52**, 960-971 (2023).
  88. de Carvalho, A. M., et al. Chemical composition of cover crops and soil organic matter pools in no-tillage systems in the Cerrado. *Soil Use Manage.* **38**, 940-952 (2022).
  89. de Moraes Sá, J. C., et al. Soil carbon fractions and biological activity based indices can be used to study the impact of land management and ecological successions. *Ecol. Indic.* **84**, 96-105 (2018).
  90. de Moraes, J. R., Castilhos, R. M. V., Lacerda, C. L., Pinto, L. F. S. & Carlos, F. S. Carbon and nitrogen stocks and microbiological attributes of soil under eucalyptus cultivation in the Pampa biome of southern Brazil. *Geoderma Regional* **25**, e00392 (2021).
  91. de Oliveira, H. M. R., et al. Repercussion of pastoral systems in C and N fractions stock in northeast Amazonia. *CATENA* **208**, 105742 (2022).
  92. de Souza, G. P., de Figueiredo, C. C. & de Sousa, D. M. G. Relationships between labile soil organic carbon fractions under different soil management systems. *Sci. Agric.* **73**, 535-542 (2016).
  93. Delgado-Baquerizo, M., et al. Biogenic factors explain soil carbon in paired urban and natural ecosystems worldwide. *Nat. Clim. Change* **13**, 450-455 (2023).

94. Deng, X., et al. Effects of warming and fertilization on soil organic carbon and its labile components in rice-wheat rotation. *Environmental Science* **44**, 1553-1561 (2023).
95. Díaz-Martínez, P., et al. Vulnerability of mineral-associated soil organic carbon to climate across global drylands. *Nat. Clim. Change* **14**, 976-982 (2024).
96. Díaz-Pinés, E., Rubio, A., Van Miegroet, H., Montes, F. & Benito, M. Does tree species composition control soil organic carbon pools in Mediterranean mountain forests? *For. Ecol. Manage.* **262**, 1895-1904 (2011).
97. Dietterich, L. H., Karpman, J., Neupane, A., Ciochina, M. & Cusack, D. F. Carbon content of soil fractions varies with season, rainfall, and soil fertility across a lowland tropical moist forest gradient. *Biogeochemistry* **155**, 431-452 (2021).
98. Dikgwatlhe, S. B., et al. Tillage and residue management effects on temporal changes in soil organic carbon and fractions of a silty loam soil in the North China Plain. *Soil Use Manage.* **30**, 496-506 (2014).
99. Ding, T., et al. Effects of straw return methods on the soil organic carbon fractions and pore structure characteristics of Shajiang black soil (Vertisol). *Transactions of the Chinese Society of Agricultural Engineering* **39**, 71-78 (2023).
100. Diochon, A., Gregorich, E. G. & Tarnocai, C. Evaluating the quantity and biodegradability of soil organic matter in some Canadian Turbic Cryosols. *Geoderma* **202-203**, 82-87 (2013).
101. Doetterl, S., et al. Organic matter cycling along geochemical, geomorphic, and disturbance gradients in forest and cropland of the African Tropics – project TropSOC database version 1.0. *Earth Syst. Sci. Data* **13**, 4133-4153 (2021).
102. Doetterl, S., et al. Soil carbon storage controlled by interactions between geochemistry and climate. *Nat. Geosci.* **8**, 780-783 (2015).
103. Domínguez, G. F., Diovisalvi, N. V., Studdert, G. A. & Monterubbianesi, M. G. Soil organic C and N fractions under continuous cropping with contrasting tillage systems on mollisols of the southeastern Pampas. *Soil Tillage Res.* **102**, 93-100 (2009).
104. Dong, X., et al. Effects of forest types on soil carbon content in aggregate fraction under climate transition zone. *Front. Environ. Sci.* **10**, 1052175 (2023).
105. Dong, Y., An, S., Sun, Z., Yang, H. & Yang, J. Effects of grazing exclusion on soil

active organic carbon fractions in moderately degraded desert of *Seriphidium transiliense*. *Chinses Journal of Soil Science* **47**, 364-370 (2016).

106. Dong, Y., et al. Fraction and content of soil organic carbon at different elevations in Maoer Mountain. *Chinses Journal of Soil Science* **51**, 1142-1151 (2020).
107. Dörfer, C., Kühn, P., Baumann, F., He, J.-S. & Scholten, T. Soil organic carbon pools and stocks in permafrost-affected soils on the Tibetan plateau. *PLoS One* **8**, e57024 (2013).
108. Dorodnikov, M., Kuzyakov, Y., Fangmeier, A. & Wiesenberger, G. L. B. C and N in soil organic matter density fractions under elevated atmospheric CO<sub>2</sub>: turnover vs. stabilization. *Soil Biol. Biochem.* **43**, 579-589 (2011).
109. dos Reis, C. E. S., Dick, D. P., Caldas, J. d. S. & Bayer, C. Carbon sequestration in clay and silt fractions of Brazilian soils under conventional and no-tillage systems. *Sci. Agric.* **71**, 292-301 (2014).
110. Dou, F. & Hons, F. M. Tillage and nitrogen effects on soil organic matter fractions in wheat-based systems. *Soil Sci. Soc. Am. J.* **70**, 1896-1905 (2006).
111. Duan, P., Wang, K. & Li, D. Nitrogen addition effects on soil mineral-associated carbon differ between the valley and slope in a subtropical karst forest. *Geoderma* **430**, 116357 (2023).
112. Duval, M. E., Galantini, J. A., Capurro, J. E. & Martinez, J. M. Winter cover crops in soybean monoculture: effects on soil organic carbon and its fractions. *Soil Tillage Res.* **161**, 95-105 (2016).
113. Dymov, A. A., Milanovskii, E. Y. & Kholodov, V. A. Composition and hydrophobic properties of organic matter in the densimetric fractions of soils from the Subpolar Urals. *Eurasian Soil Sci.* **48**, 1212-1221 (2015).
114. Elias, D. M. O., et al. The potential to increase grassland soil C stocks by extending reseeding intervals is dependent on soil texture and depth. *J. Environ. Manage.* **334**, 117465 (2023).
115. F., P. A., E., S. C., T., C. R., K., P. & J., S. Soil management effects on organic carbon in isolated fractions of a Gray Luvisol. *Can. J. Soil Sci.* **86**, 141-151 (2006).
116. Fabrizzi, K. P., Morón, A. & García, F. O. Soil carbon and nitrogen organic fractions in degraded vs. non-degraded Mollisols in Argentina. *Soil Sci. Soc. Am. J.* **67**, 1831-1841 (2003).



117. Fang, H., Yang, X., Zhang, X., Liang, A. & Shen, Y. Spatial distribution of particulate organic carbon and aggregate associated carbon in topsoil of a sloping farmland in the Black Soil region, Northeast China. *Acta Ecol. Sin.*, 2847-2854 (2006).
118. Fang, H., Yang, X., Zhang, X., Liang, A. & Shen, Y. Effects of soil erosion and deposition on loss and accumulation of soil organic carbon in physical fractions. *Acta Pedologica Sinica*, 467-474 (2007).
119. Fang, H. J., et al. Nitrogen deposition impacts on the amount and stability of soil organic matter in an alpine meadow ecosystem depend on the form and rate of applied nitrogen. *Eur. J. Soil Sci.* **65**, 510-519 (2014).
120. Fang, X., et al. Litter addition and understory removal influenced soil organic carbon quality and mineral nitrogen supply in a subtropical plantation forest. *Plant Soil* **460**, 527-540 (2021).
121. Fang, X., et al. Phosphorus addition alters the response of soil organic carbon decomposition to nitrogen deposition in a subtropical forest. *Soil Biol. Biochem.* **133**, 119-128 (2019).
122. Feng, W., et al. Testing for soil carbon saturation behavior in agricultural soils receiving long-term manure amendments. *Can. J. Soil Sci.* **94**, 281-294 (2013).
123. Feng, X., et al. Nitrogen input enhances microbial carbon use efficiency by altering plant-microbe-mineral interactions. *Glob. Change Biol.* **28**, 4845-4860 (2022).
124. Figueiredo, C. C., Resck, D. V. S., Carneiro, M. A. C., Ramos, M. L. G. & Sá, J. C. M. Stratification ratio of organic matter pools influenced by management systems in a weathered Oxisol from a tropical agro-ecoregion in Brazil. *Soil Res.* **51**, 133-141 (2013).
125. Fontana, M. B., et al. Long-term fertilizer application and cover crops improve soil quality and soybean yield in the Northeastern Pampas region of Argentina. *Geoderma* **385**, 114902 (2021).
126. Frasier, I., et al. High quality residues from cover crops favor changes in microbial community and enhance C and N sequestration. *Global Ecol. Conserv.* **6**, 242-256 (2016).
127. Fraterrigo, J. M. & Rembelski, M. K. Frequent fire reduces the magnitude of positive interactions between an Invasive grass and soil Microbes in Temperate Forests. *Ecosystems* **24**, 1738-1755 (2021).

128. Freixo, A. A., Machado, P. L. O. d. A., dos Santos, H. P., Silva, C. A. & Fadigas, F. d. S. Soil organic carbon and fractions of a Rhodic Ferralsol under the influence of tillage and crop rotation systems in southern Brazil. *Soil Tillage Res.* **64**, 221-230 (2002).
129. Frey, S. D., Elliott, E. T. & Paustian, K. Bacterial and fungal abundance and biomass in conventional and no-tillage agroecosystems along two climatic gradients. *Soil Biol. Biochem.* **31**, 573-585 (1999).
130. Fu, X., Wang, J., Sainju, U. M. & Liu, W. Soil carbon fractions in response to long-term crop rotations in the Loess Plateau of China. *Soil Sci. Soc. Am. J.* **81**, 503-513 (2017).
131. G., G. E., R., C. M., A., A. D. & F., D. C. Using a sequential density and particle-size fractionation to evaluate carbon and nitrogen storage in the profile of tilled and no-till soils in eastern Canada. *Can. J. Soil Sci.* **89**, 255-267 (2009).
132. Gao, F., Cui, X., Chen, M. & Sang, Y. Forest conversion changes soil particulate organic carbon and mineral-associated organic carbon via plant inputs and microbial processes. *Forests* **14**, 1234 (2023).
133. Gao, L., et al. Effects of different long-term tillage systems on the composition of organic matter by  $^{13}\text{C}$  CP/TOSS NMR in physical fractions in the Loess Plateau of China. *Soil Tillage Res.* **194**, 104321 (2019).
134. Gao, X., He, P., Dend, I., Zhang, S. & Huang, C. Distribution characteristics of soil total organic carbon and particle organic carbon on the purple hilly region slopes. *Ecology and Environment* **18**, 337-342 (2009).
135. Gao, Y., et al. Precipitation increment reinforced warming-induced increases in soil mineral-associated and particulate organic matter under agricultural ecosystem. *Appl. Soil Ecol.* **196**, 105301 (2024).
136. García, G. V., et al. Soil survey reveals a positive relationship between aggregate stability and anaerobically mineralizable nitrogen. *Ecol. Indic.* **117**, 106640 (2020).
137. Geng, H., Wang, X., Shi, S., Ye, Z. & Zhou, W. Fertilization makes strong associations between organic carbon composition and microbial properties in paddy soil. *J. Environ. Manage.* **325**, 116605 (2023).
138. Geng, J., et al. Nitrogen fertilization changes the molecular composition of soil organic matter in a subtropical plantation forest. *Soil Sci. Soc. Am. J.* **84**, 68-81 (2020).

139. Gentsch, N., et al. Properties and bioavailability of particulate and mineral-associated organic matter in Arctic permafrost soils, Lower Kolyma Region, Russia. *Eur. J. Soil Sci.* **66**, 722-734 (2015).
140. Gentsch, N., et al. Temperature response of permafrost soil carbon is attenuated by mineral protection. *Glob. Change Biol.* **24**, 3401-3415 (2018).
141. Ghafoor, A., Poeplau, C. & Kätterer, T. Fate of straw- and root-derived carbon in a Swedish agricultural soil. *Biol. Fertil. Soils* **53**, 257-267 (2017).
142. Gómez-Paccard, C., et al. Ca-amendment and tillage: medium term synergies for improving key soil properties of acid soils. *Soil Tillage Res.* **134**, 195-206 (2013).
143. Gong, W., et al. Effects of long-term fertilization on soil particulate organic carbon and nitrogen in a wheat-maize cropping system. *Chinese Journal of Applied Ecology* **19**, 2375-2381 (2008).
144. Gong, W., Yan, X., Wang, J., Hu, T. & Gong, Y. Long-term manure and fertilizer effects on soil organic matter fractions and microbes under a wheat–maize cropping system in northern China. *Geoderma* **149**, 318-324 (2009).
145. Griffin, T. S. & Porter, G. A. Altering soil carbon and nitrogen stocks in intensively tilled two-year rotations. *Biol. Fertil. Soils* **39**, 366-374 (2004).
146. Guo, X., Luo, Z. & Sun, O. J. Long-term litter type treatments alter soil carbon composition but not microbial carbon utilization in a mixed pine-oak forest. *Biogeochemistry* **152**, 327-343 (2021).
147. Gutiérrez del Arroyo, O. & Silver, W. L. Disentangling the long-term effects of disturbance on soil biogeochemistry in a wet tropical forest ecosystem. *Glob. Change Biol.* **24**, 1673-1684 (2018).
148. Haile-Mariam, S., Collins, H. P., Wright, S. & Paul, E. A. Fractionation and long-term laboratory Incubation to measure soil organic matter dynamics. *Soil Sci. Soc. Am. J.* **72**, 370-378 (2008).
149. Han, Y., et al. Characterization of organic carbon pool and the source of paddy soil from typical rice terraces across southern China. *Journal of Agricultural Resources and Environment* **42**, 139-148 (2025).
150. Hao, M., et al. The soil microbial necromass carbon and the carbon pool stability drive a strong priming effect following vegetation restoration. *J. Environ. Manage.* **351**, 119859 (2024).

151. He, N., Chen, Q., Han, X., Yu, G. & Li, L. Warming and increased precipitation individually influence soil carbon sequestration of Inner Mongolian grasslands, China. *Agric. Ecosyst. Environ.* **158**, 184-191 (2012).
152. He, W., et al. Effect of long-term application of organic manure expanding organic carbon fractions in fluvo-aquic soil. *Acta Pedologica Sinica* **57**, 425-434 (2020).
153. He, Y., Zhang, F. & Yang, M. Effects of soil erosion on organic carbon fractions in black soils in sloping farmland of Northeast China by using  $^{137}\text{Cs}$  tracer measurements. *Transactions of the Chinese Society of Agricultural Engineering* **37**, 60-68 (2021).
154. Heckman, K., et al. Beyond bulk: density fractions explain heterogeneity in global soil carbon abundance and persistence. *Glob. Change Biol.* **28**, 1178-1196 (2022).
155. Heckman, K., Lawrence, C. R. & Harden, J. W. A sequential selective dissolution method to quantify storage and stability of organic carbon associated with Al and Fe hydroxide phases. *Geoderma* **312**, 24-35 (2018).
156. Hernandez-Ramirez, G., Brouder, S. M., Smith, D. R. & Van Scoyoc, G. E. Carbon and nitrogen dynamics in an eastern corn belt soil: nitrogen source and rotation. *Soil Sci. Soc. Am. J.* **73**, 128-137 (2009).
157. Herold, N., Schöning, I., Michalzik, B., Trumbore, S. & Schrumpf, M. Controls on soil carbon storage and turnover in German landscapes. *Biogeochemistry* **119**, 435-451 (2014).
158. Hok, L., et al. Short-term conservation agriculture and biomass-C input impacts on soil C dynamics in a savanna ecosystem in Cambodia. *Agric. Ecosyst. Environ.* **214**, 54-67 (2015).
159. Hontoria, C., et al. Aggregate size distribution and associated organic C and N under different tillage systems and Ca-amendment in a degraded Ultisol. *Soil Tillage Res.* **160**, 42-52 (2016).
160. Hook, P. B. & Burke, I. C. Biogeochemistry I in A shortgrass landscape: control by topography, soil texture, and microclimate. *Ecology* **81**, 2686-2703 (2000).
161. Hounkpatin, K. O. L., Welp, G., Akponikpè, P. B. I., Rosendahl, I. & Amelung, W. Carbon losses from prolonged arable cropping of Plinthosols in southwest Burkina Faso. *Soil Tillage Res.* **175**, 51-61 (2018).
162. Hu, D.-Y., et al. Soil carbon pool allocation dynamics during soil development in

the Lower Yangtze River Alluvial Plain. *Environmental Science* **45**, 314-322 (2024).

163. Huang, Q., et al. Shifts in C-degradation genes and microbial metabolic activity with vegetation types affected the surface soil organic carbon pool. *Soil Biol. Biochem.* **192**, 109371 (2024).
164. Huang, Z., Clinton, P. W., Baisden, W. T. & Davis, M. R. Long-term nitrogen additions increased surface soil carbon concentration in a forest plantation despite elevated decomposition. *Soil Biol. Biochem.* **43**, 302-307 (2011).
165. Hussain, I., Olson, K. R. & Ebelhar, S. A. Long-term tillage effects on soil chemical properties and organic matter fractions. *Soil Sci. Soc. Am. J.* **63**, 1335-1341 (1999).
166. Jakab, G., et al. Soil organic matter gain by reduced tillage intensity: storage, pools, and chemical composition. *Soil Tillage Res.* **226**, 105584 (2023).
167. Jandl, G., Leinweber, P., Schulten, H. R. & Eusterhues, K. The concentrations of fatty acids in organo-mineral particle-size fractions of a Chernozem. *Eur. J. Soil Sci.* **55**, 459-470 (2004).
168. Jantalia, C. P. & Halvorson, A. D. Nitrogen fertilizer effects on irrigated conventional tillage corn yields and soil carbon and nitrogen pools. *Agron. J.* **103**, 871-878 (2011).
169. Ji, Q., Sun, H., Wang, Y., Liu, S. & Wang, X. Responses of soil particulate organic carbon and mineral-bound organic carbon to four kinds of tillage practices. *J. Soil Water Conserv.* **26**, 132-137 (2012).
170. Jia, Y., et al. Plant and microbial pathways driving plant diversity effects on soil carbon accumulation in subtropical forest. *Soil Biol. Biochem.* **161**, 108375 (2021).
171. Jia, Z., et al. Effects of long-term phosphorus fertilization on maize and soil C:N:P and organic matter stability. *Journal of Hunan Ecological Science* **9**, 10-18 (2022).
172. Jiang, M., Lyu, M., Lin, W., Xie, J. & Yang, Y. Effects of ecological restoration on soil organic carbon components and stability in a red soil erosion area. *Acta Ecol. Sin.* **38**, 4861-4868 (2018).
173. Jiang, S., et al. Profile and nano-scale distribution of soil organic carbon for upland and paddy soils from an alluvial plain in South China. *Chem. Geol.* **640**, 121740 (2023).

174. Jung, J. Y., et al. Responses of surface SOC to long-term experimental warming vary between different heath types in the high Arctic tundra. *Eur. J. Soil Sci.* **71**, 752-767 (2020).
175. Júnior, A. M. F., et al. Edaphic properties in a eucalyptus forest ecotone in the Nova Baden State Park, Southeastern Brazil. *Revista Brasileira de Ciencia do Solo* **47**, e0230074 (2023).
176. Kahle, M., Kleber, M. & Jahn, R. Carbon storage in loess derived surface soils from central Germany: Influence of mineral phase variables. *J. Plant Nutr. Soil Sci.* **165**, 141-149 (2002).
177. Kane, E. S., Valentine, D. W., Schuur, E. A. G. & Dutta, K. Soil carbon stabilization along climate and stand productivity gradients in black spruce forests of interior Alaska. *Can. J. For. Res.* **35**, 2118-2129 (2005).
178. Kang, L., Wu, J., Zhang, C., Zhu, B. & Chu, G. The alterations of soil aggregates and intra-aggregate organic carbon fractions after soil conversion from paddy to upland soil: distribution, mineralization and driving mechanism. *Pedosphere* **34**, 121-135 (2024).
179. Karhu, K., et al. Temperature sensitivity of soil carbon fractions in boreal forest soil. *Ecology* **91**, 370-376 (2010).
180. Kauer, K., Pärnpuu, S., Talgre, L., Eremeev, V. & Luik, A. Soil particulate and mineral-associated organic matter increases in organic farming under cover cropping and manure addition. *Agriculture* **11**, 903 (2021).
181. Keller, A. B., et al. Soil carbon stocks in temperate grasslands differ strongly across sites but are insensitive to decade-long fertilization. *Glob. Change Biol.* **28**, 1659-1677 (2022).
182. Kim, K., Daly, E. J., Gorzelak, M. & Hernandez-Ramirez, G. Soil organic matter pools response to perennial grain cropping and nitrogen fertilizer. *Soil Tillage Res.* **220**, 105376 (2022).
183. King, A. E., et al. A soil matrix capacity index to predict mineral-associated but not particulate organic carbon across a range of climate and soil pH. *Biogeochemistry* **165**, 1-14 (2023).
184. Kooch, Y. & Bayranvand, M. Labile soil organic matter changes related to forest floor quality of tree species mixtures in Oriental beech forests. *Ecol. Indic.* **107**, 105598 (2019).

185. Kooch, Y., Ghorbanzadeh, N., Hajimirzaaghaee, S. & Francaviglia, R. Soil biological quality as affected by vegetation types in shrublands of a semi-arid montane environment. *Appl. Soil Ecol.* **189**, 104980 (2023).
186. Kuneski, A. C., et al. Effects of tillage and cover crops on total carbon and nitrogen stocks and particle-size fractions of soil organic matter under onion crop. *Horticulturae* **9**, 822 (2023).
187. L., M. H., G., Z. J., B., X. Z., G., L. & Q., Z. Effects of increased residue biomass under elevated CO<sub>2</sub> on carbon and nitrogen in soil aggregate size classes (rice-wheat rotation system, China). *Can. J. Soil Sci.* **89**, 567-577 (2009).
188. Lammerding, D. M., Hontoria, C., Tenorio, J. L. & Walter, I. Mediterranean dryland farming: effect of tillage practices on selected soil properties. *Agron. J.* **103**, 382-389 (2011).
189. Lan, J., Wang, J., Wang, S., Qli, X. & Long, Q. Impact of controlling karst rocky desertification on soil particulate organic carbon and aggregate-associated organic carbon. *Carsologica Sinica* **41**, 773-783 (2022).
190. Lan, X., et al. Effects of long-term manure substitution regimes on soil organic carbon composition in a red paddy soil of southern China. *Soil Tillage Res.* **221**, 105395 (2022).
191. Landriscini, M., Duval, M. E., Galantini, J. A., Iglesias, J. O. & Cazorla, C. R. Changes in soil organic carbon fractions in a sequence with cover crops. *Spanish Journal of Soil Science: SJSS* **10**, 137-153 (2020).
192. Lei, L., Thompson, J. A. & McDonald, L. M. Soil organic carbon pools and Indices in surface soil: comparing a cropland, pasture, and forest soil in the central Appalachian region, west Virginia, U.S.A. *Commun. Soil Sci. Plant Anal.* **53**, 17-29 (2022).
193. Li, J., et al. Responses of particulate and mineral-associated organic carbon to temperature changes and their mineral protection mechanisms: A soil translocation experiment. *Sci. Total Environ.* **948**, 174689 (2024).
194. Li, J., et al. Soil organic matter dynamics in long-term temperate agroecosystems: rotation and nutrient addition effects. *Can. J. Soil Sci.* **98**, 232-245 (2018).
195. Li, J., et al. Mycorrhizal mediation of soil carbon in permafrost regions depends on soil nutrient stoichiometry and physical protection. *Sci. Total Environ.* **920**, 170907 (2024).

196. Li, L., et al. Effects of nitrogen enrichment on transfer and accumulation of soil organic carbon in alpine meadows on the Qinghai-Tibetan Plateau. *Acta Pedologica Sinica* **52**, 183-193 (2015).
197. Li, L., et al. Association of soil aggregation with the distribution and quality of organic carbon in soil along an elevation gradient on Wuyi Mountain in China. *PLoS One* **11**, e0150898 (2016).
198. Li, P., et al. Wind erosion enhanced by land use changes significantly reduces ecosystem carbon storage and carbon sequestration potentials in semiarid grasslands. *Land Degradation & Development* **29**, 3469-3478 (2018).
199. Li, R., Wang, J., Mao, H. & Fu, X. Effects of straw mulching on soil organic carbon and fractions of soil carbon in a winter wheat field. *J. Soil Water Conserv.* **31**, 187-192 (2017).
200. Li, T., et al. Divergent accumulation of amino sugars and lignins mediated by soil functional carbon pools under tropical forest conversion. *Sci. Total Environ.* **881**, 163204 (2023).
201. Li, T., Wang, J., Huang, L. & Wang, H. Effects of straw returning and replacing chemical fertilizer on soil organic carbon fractions and winter wheat. *Journal of Shanxi Agricultural Sciences* **50**, 771-780 (2022).
202. Li, X., et al. Changes in soil organic carbon, nutrients and aggregation after conversion of native desert soil into irrigated arable land. *Soil Tillage Res.* **104**, 263-269 (2009).
203. Li, X., Liu, F. & Fan, W. Distribution characteristics of organic carbon in soil water-stable aggregates of Wutai Mountain. *J. Soil Water Conserv.* **31**, 159-165+197 (2017).
204. Li, X., Zhang, Q., Feng, J., Jiang, D. & Zhu, B. Forest management causes soil carbon loss by reducing particulate organic carbon in Guangxi, southern China. *For. Ecosyst.* **10**, 100092 (2023).
205. Li, Y., et al. Content and distribution of unprotected soil organic carbon in Karst ecosystem. *Journal of Agro-Environment Science* **25**, 402-406 (2006).
206. Li, Y., et al. Revegetation promotes soil mineral-associated organic carbon sequestration and soil carbon stability in the Tengger Desert, northern China. *Soil Biol. Biochem.* **185**, 109155 (2023).
207. Li, Z., et al. Effects of straw management and nitrogen application rate on soil



- organic matter fractions and microbial properties in North China Plain. *J. Soils Sediments* **19**, 618-628 (2019).
208. Liang, Y., Han, X., Wang, F. & Wang, F. Characteristics of soil labile organic carbon fractions in black soil under grassland and farmland ecosystem. *Chinses Journal of Soil Science* **42**, 864-871 (2011).
209. Liang, Z., Rasmussen, J., Poeplau, C. & Elsgaard, L. Priming effects decrease with the quantity of cover crop residues – Potential implications for soil carbon sequestration. *Soil Biol. Biochem.* **184**, 109110 (2023).
210. Liebig, M. A., Tanaka, D. L. & Wienhold, B. J. Tillage and cropping effects on soil quality indicators in the northern Great Plains. *Soil Tillage Res.* **78**, 131-141 (2004).
211. Liu, B., et al. 14 year applications of chemical fertilizers and crop straw effects on soil labile organic carbon fractions, enzyme activities and microbial community in rice-wheat rotation of middle China. *Sci. Total Environ.* **841**, 156608 (2022).
212. Liu, C., et al. Effects of diferent crops on the content of soil total organic carbon and particulate organic carbon in continuous cropping corn fields. *Journal of Shanxi Agricultural University(Nature Science Edition)* **38**, 1-7 (2018).
213. Liu, D., et al. Storage and stability of soil organic carbon in two temperate forests in northeastern China. *Land* **12**, 1019 (2023).
214. Liu, E., Yan, C., Mei, X., Zhang, Y. & Fan, T. Long-term effect of manure and fertilizer on soil organic carbon pools in dryland farming in northwest China. *PLoS One* **8**, e56536 (2013).
215. Liu, F., et al. Divergent changes in particulate and mineral-associated organic carbon upon permafrost thaw. *Nat. Commun.* **13**, 5073 (2022).
216. Liu, F., Zhang, Y. & Luo, J. The effects of experimental warming and CO<sub>2</sub> concentration doubling on soil organic carbon fractions of a montane coniferous forest on the eastern Qinghai-Tibetan plateau. *European Journal of Forest Research* **137**, 211-221 (2018).
217. Liu, J., et al. Effects of fire on soil enzyme activities and organic carbon fractions in *Pinus massoniana* forest. *Acta Ecol. Sin.* **38**, 5374-5382 (2018).
218. Liu, J., Xu, S. & Liu, L. Effect of different reafforestation patterns on soil particulate organic carbon content in Loess Hilly region of western Henan. *Journal of Henan Agricultural Sciences* **44**, 72-76 (2015).

219. Liu, J., et al. Nitrogen addition increases topsoil carbon stock in an alpine meadow of the Qinghai-Tibet Plateau. *Sci. Total Environ.* **888**, 164071 (2023).
220. Liu, M., Chang, Q., Qi, Y. & Sun, N. Soil organic carbon and Particulate organic carbon under different land use types on the Loess Plateau. *Journal of Natural Resources* **25**, 218-226 (2010).
221. Liu, W., et al. Distribution and stabilization of photosynthetic carbon in rice-soil system under long-term multiple cropping of green manure. *Acta Pedologica Sinica* **60**, 1067-1076 (2023).
222. Locatelli, J. L., Santos, R. S., Cherubin, M. R. & Cerri, C. E. P. Changes in soil organic matter fractions induced by cropland and pasture expansion in Brazil's new agricultural frontier. *Geoderma Regional* **28**, e00474 (2022).
223. Logah, V., et al. Soil carbon, nutrient, and vegetation dynamics of an old Anogeissus grove in Mole National Park, Ghana. *Biotropica* **56**, e13299 (2024).
224. Long, Q., Lan, J. & Jiang, Y. Effects of soil organic carbon fractions on aggregates under ecological restoration in rocky desertification region. *Acta Ecol. Sin.* **42**, 7390-7402 (2022).
225. Loss, A., Pereira, M. G., Perin, A., Coutinho, F. S. & Cunha dos Anjos, L. H. Particulate organic matter in soil under different management systems in the Brazilian Cerrado. *Soil Res.* **50**, 685-693 (2012).
226. Lu, C., Xu, C., Huang, R., Tian, D. & Gao, M. Effect of straw and biochar on soil organic carbon and carbon pool management index in purple soil under rape-maize rotation. *Pratacultural Science* **35**, 482-490 (2018).
227. Lu, G., Haixia, H., Zhou, X., Xueping, C. & Zhao, A. Characteristics of soil organic carbon and changes of enzyme activities in burned area of spruce-fir forests in Diebu Forest region. *Acta Agrestia Sinica* **30**, 943-949 (2022).
228. Lu, J., et al. Effects of reduced tillage with stubble remaining and nitrogen application on soil aggregation, soil organic carbon and grain yield in maize-wheat rotation system. *Eur. J. Agron.* **149**, 126920 (2023).
229. Luan, J., et al. Assessments of the impacts of Chinese fir plantation and natural regenerated forest on soil organic matter quality at Longmen mountain, Sichuan, China. *Geoderma* **156**, 228-236 (2010).
230. Luce, M. S., Ziadi, N., Chantigny, M. H. & Braun, J. Long-term effects of tillage and nitrogen fertilization on soil C and N fractions in a corn-soybean rotation.

*Can. J. Soil Sci.* **102**, 277-292 (2022).

231. Luo, M., et al. Characteristics of Particulate Organic Carbon and Nitrogen in Soil of *Leucaena leucocephala* Plantation in the Dry-hot Valley. *Forest Research* **35**, 40-47 (2022).
232. Luo, X., Hou, E., Zhang, L. & Wen, D. Soil carbon dynamics in different types of subtropical forests as determined by density fractionation and stable isotope analysis. *For. Ecol. Manage.* **475**, 118401 (2020).
233. Luo, Z., Viscarra Rossel, R. A. & Shi, Z. Distinct controls over the temporal dynamics of soil carbon fractions after land use change. *Glob. Change Biol.* **26**, 4614-4625 (2020).
234. Lv, J., Shi, J., Wang, Z., Peng, Y. & Wang, X. Effects of erosion and deposition on the extent and characteristics of organic carbon associated with soil minerals in Mollisol landscape. *CATENA* **228**, 107190 (2023).
235. Lyu, M., et al. Dynamics of unprotected soil organic carbon with the restoration process of *Pinus massoniana* plantation in red soil erosion area. *Chinese Journal of Applied Ecology* **25**, 37-44 (2014).
236. M., S. U., F., W. W. & P., S. B. Cover crops and nitrogen fertilization effects on soil aggregation and carbon and nitrogen pools. *Can. J. Soil Sci.* **83**, 155-165 (2003).
237. M., Y. X. & D., K. B. Impacts of tillage practices on total, loose- and occluded-particulate, and humified organic carbon fractions in soils within a field in southern Ontario. *Can. J. Soil Sci.* **81**, 149-156 (2001).
238. Ma, H. & Dong, Z. Vertical distribution characteristics of surface soil organic carbon on the north slope of Sygera Mountains, Tibet. *Journal of Plateau Agriculture* **4**, 115-122 (2020).
239. Ma, H., Guo, Q., Liu, H. & Qian, D. Changes of soil organic carbon and total nitrogen at different altitudes in west slope of Sejila Mountain of Tibet. *Forest Research* **26**, 240-246 (2013).
240. Ma, H., Guo, Q., Liu, H. & Qian, D. Soil organic carbon pool at the western side of the sygera Mountains, southeast Tibet, China. *Acta Ecol. Sin.* **33**, 3122-3128 (2013).
241. Maillard, É., et al. Carbon accumulates in organo-mineral complexes after long-term liquid dairy manure application. *Agric. Ecosyst. Environ.* **202**, 108-119

(2015).

242. Mandiola, M., Studdert, G. A., Domínguez, G. F. & Videla, C. C. Organic matter distribution in aggregate sizes of a mollisol under contrasting management. *J. Soil Sci. Plant Nutr.* **11**, 41-57 (2011).
243. Manna, M. C., Swarup, A., Wanjari, R. H., Mishra, B. & Shahi, D. K. Long-term fertilization, manure and liming effects on soil organic matter and crop yields. *Soil Tillage Res.* **94**, 397-409 (2007).
244. Mao, X., et al. Microbial adaption to stoichiometric imbalances regulated the size of soil mineral-associated organic carbon pool under continuous organic amendments. *Geoderma* **445**, 116883 (2024).
245. Marín-Spiotta, E., Swanston, C. W., Torn, M. S., Silver, W. L. & Burton, S. D. Chemical and mineral control of soil carbon turnover in abandoned tropical pastures. *Geoderma* **143**, 49-62 (2008).
246. Martínez, J. M., Galantini, J. A., Duval, M. E. & López, F. M. Soil quality assessment based on soil organic matter pools under long-term tillage systems and following tillage conversion in a semi-humid region. *Soil Use Manage.* **36**, 400-409 (2020).
247. Martinez, J. P., et al. Soil organic carbon in cropping sequences with predominance of soya bean in the argentinean humid Pampas. *Soil Use Manage.* **36**, 173-183 (2020).
248. Martins, A. P., et al. Short-term Impacts on soil-quality assessment in alternative land uses of traditional paddy fields in southern Brazil. *Land Degradation & Development* **28**, 534-542 (2017).
249. Martins, M. R., Angers, D. A. & Corá, J. E. Co-accumulation of microbial residues and particulate organic matter in the surface layer of a no-till Oxisol under different crops. *Soil Biol. Biochem.* **50**, 208-213 (2012).
250. Matos, E. S., et al. Organic-carbon and nitrogen stocks and organic-carbon fractions in soil under mixed pine and oak forest stands of different ages in NE Germany. *J. Plant Nutr. Soil Sci.* **173**, 654-661 (2010).
251. Matos, P. S., et al. Soil organic carbon fractions in agroforestry system in Brazil: seasonality and short-term dynamic assessment. *Revista Brasileira de Ciência do Solo* **47**, e0220095 (2023).
252. McFarlane, K. J., et al. Comparison of soil organic matter dynamics at five

- temperate deciduous forests with physical fractionation and radiocarbon measurements. *Biogeochemistry* **112**, 457-476 (2013).
253. Medeiros, A. D. S., Soares, A. A. S. & Maia, S. M. F. Soil carbon stocks and compartments of organic matter under conventional systems in Brazilian semi-arid region. *Revista Caatinga* **35**, 697–710 (2022).
  254. Meng, F., Lal, R., Kuang, X., Ding, G. & Wu, W. Soil organic carbon dynamics within density and particle-size fractions of Aquic Cambisols under different land use in northern China. *Geoderma Regional* **1**, 1-9 (2014).
  255. Meyer, N., et al. Carbon saturation drives spatial patterns of soil organic matter losses under long-term bare fallow. *Geoderma* **306**, 89-98 (2017).
  256. Mikha, M. M., Hergert, G. W., Benjamin, J. G., Jabro, J. D. & Nielsen, R. A. Soil organic carbon and nitrogen in long-term manure management system. *Soil Sci. Soc. Am. J.* **81**, 153-165 (2017).
  257. Mikha, M. M. & Marake, M. V. Soil organic matter fractions and carbon distribution under different management in Lesotho, southern Africa. *Soil Sci. Soc. Am. J.* **87**, 140-155 (2023).
  258. Mikha, M. M., Vigil, M. F. & Benjamin, J. G. Long-term tillage impacts on soil aggregation and carbon dynamics under wheat-fallow in the Central Great Plains. *Soil Sci. Soc. Am. J.* **77**, 594-605 (2013).
  259. Mosier, S., et al. Adaptive multi-paddock grazing enhances soil carbon and nitrogen stocks and stabilization through mineral association in southeastern U.S. grazing lands. *J. Environ. Manage.* **288**, 112409 (2021).
  260. Mosier, S., Paustian, K., Davies, C., Kane, M. & Cotrufo, M. F. Soil organic matter pools under management intensification of loblolly pine plantations. *For. Ecol. Manage.* **447**, 60-66 (2019).
  261. Motta, A. C. V., Wayne Reeves, D., Burmester, C. & Feng, Y. Conservation tillage, rotations, and cover crop affecting soil quality in the Tennessee valley: particulate organic matter, organic matter, and microbial Biomass. *Commun. Soil Sci. Plant Anal.* **38**, 2831-2847 (2007).
  262. Mou, L., Zhang, L., Chen, Z., Tan, B. & Xu, Z. Characteristics of soil organic carbon component of four plantations on the western edge of Sichuan Basin. *Journal of Gansu Agricultural University* **55**, 121-126+133 (2020).
  263. Mrabet, R., Saber, N., El-Brahli, A., Lahlou, S. & Bessam, F. Total, particulate

- organic matter and structural stability of a Calcixeroll soil under different wheat rotations and tillage systems in a semiarid area of Morocco. *Soil Tillage Res.* **57**, 225-235 (2001).
264. Mujuru, L., Mureva, A., Velthorst, E. J. & Hoosbeek, M. R. Land use and management effects on soil organic matter fractions in Rhodic Ferralsols and Haplic Arenosols in Bindura and Shamva districts of Zimbabwe. *Geoderma* **209-210**, 262-272 (2013).
  265. Mujuru, L., Rusinamhodzi, L., Nyamangara, J. & Hoosbeek, M. R. Effects of nitrogen fertilizer and manure application on storage of carbon and nitrogen under continuous maize cropping in Arenosols and Luvisols of Zimbabwe. *The Journal of Agricultural Science* **154**, 242-257 (2016).
  266. Nacro, H. B., Benest, D. & Abbadie, L. Distribution of microbial activities and organic matter according to particle size in a humid savanna soil (Lamto, Côte d'Ivoire). *Soil Biol. Biochem.* **28**, 1687-1697 (1996).
  267. Nascente, A. S., Li, Y. C. & Crusciol, C. A. C. Cover crops and no-till effects on physical fractions of soil organic matter. *Soil Tillage Res.* **130**, 52-57 (2013).
  268. Nisar, S. & Benbi, D. K. Stabilization of organic C in an Indo-Gangetic alluvial soil under long-term manure and compost management in a rice–wheat system. *Carbon Manage.* **11**, 533-547 (2020).
  269. Obrycki, J. F., Karlen, D. L., Cambardella, C. A., Kovar, J. L. & Birrell, S. J. Corn stover harvest, tillage, and cover crop effects on soil health indicators. *Soil Sci. Soc. Am. J.* **82**, 910-918 (2018).
  270. Oduor, C. O., et al. Enhancing soil organic carbon, particulate organic carbon and microbial biomass in semi-arid rangeland using pasture enclosures. *BMC Ecol.* **18**, 45 (2018).
  271. Osburn, E. D., Hoch, P. J., Prather, C. M. & Strickland, M. S. Effects of micronutrient fertilization on soil carbon pools and microbial community functioning. *Appl. Soil Ecol.* **181**, 104664 (2023).
  272. Ovsepyan, L., Kurganova, I., de Gerenyu, V. L. & Kuzyakov, Y. Recovery of organic matter and microbial biomass after abandonment of degraded agricultural soils: the influence of climate. *Land Degradation & Development* **30**, 1861-1874 (2019).
  273. Ovsepyan, L. A., Kurganova, I. N., Lopes de Gerenyu, V. O., Rusakov, A. V. & Kuzyakov, Y. V. Changes in the fractional composition of organic matter in the

- soils of the forest–steppe zone during their postagrogenic evolution. *Eurasian Soil Sci.* **53**, 50-61 (2020).
274. Özbolat, O., et al. Long-term adoption of reduced tillage and green manure improves soil physicochemical properties and increases the abundance of beneficial bacteria in a Mediterranean rainfed almond orchard. *Geoderma* **429**, 116218 (2023).
  275. Pan, J., et al. Soil-resistant organic carbon improves soil erosion resistance under agroforestry in the Yellow River Flood Plain, of China. *Agrofor. Syst.* **96**, 997-1008 (2022).
  276. Pan, S., Shi, J., Peng, Y., Wang, Z. & Wang, X. Soil organic carbon pool distribution and stability with grazing and topography in a Mongolian grassland. *Agric. Ecosyst. Environ.* **348**, 108431 (2023).
  277. Panichini, M., et al. Carbon distribution in top- and subsoil horizons of two contrasting Andisols under pasture or forest. *Eur. J. Soil Sci.* **63**, 616-624 (2012).
  278. Patra, R., Saha, D. & Jagadamma, S. Winter wheat cover crop increased subsoil organic carbon in a long-term cotton cropping system in Tennessee. *Soil Tillage Res.* **224**, 105521 (2022).
  279. Paye, W. S., Lauriault, L. M., Acharya, P. & Ghimire, R. Soil carbon and nitrogen responses to dryland forage cropping systems following irrigation retirement. *Agron. J.* **116**, 489-503 (2023).
  280. Pendall, E., Osanai, Y., Williams, A. & Hovenden, M. J. Soil carbon storage under simulated climate change is mediated by plant functional type. *Glob. Change Biol.* **17**, 505-514 (2011).
  281. Peralta, A. L. & Wander, M. M. Soil organic matter dynamics under soybean exposed to elevated [CO<sub>2</sub>]. *Plant Soil* **303**, 69-81 (2008).
  282. Perry, S., Falvo, G., Mosier, S. & Robertson, G. P. Long-term changes in soil carbon and nitrogen fractions in *Switchgrass*, native grasses, and no-till corn bioenergy production systems. *Soil Sci. Soc. Am. J.* **87**, 1365-1375 (2023).
  283. Piano, J. T., et al. Soil organic matter fractions and carbon management index under integrated crop-livestock system. *Biosci. j.(Online)* **36**, 743-760 (2020).
  284. Pinheiro, É. F. M., de Campos, D. V. B., de Carvalho Balieiro, F., dos Anjos, L. H. C. & Pereira, M. G. Tillage systems effects on soil carbon stock and physical fractions of soil organic matter. *Agric. Syst.* **132**, 35-39 (2015).

285. Piva, J. T., et al. No-tillage and crop-livestock with silage production impact little on carbon and nitrogen in the short-term in a subtropical Ferralsol. *Revista Brasileira de Ciências Agrárias* **15**, e7057 (2020).
286. Poeplau, C., et al. Isolating organic carbon fractions with varying turnover rates in temperate agricultural soils – a comprehensive method comparison. *Soil Biol. Biochem.* **125**, 10-26 (2018).
287. Poeplau, C., Kätterer, T., Leblans, N. I. W. & Sigurdsson, B. D. Sensitivity of soil carbon fractions and their specific stabilization mechanisms to extreme soil warming in a subarctic grassland. *Glob. Change Biol.* **23**, 1316-1327 (2017).
288. Poeplau, C., Reiter, L., Berti, A. & Kätterer, T. Qualitative and quantitative response of soil organic carbon to 40 years of crop residue incorporation under contrasting nitrogen fertilisation regimes. *Soil Res.* **55**, 1-9 (2017).
289. Poeplau, C., Sigurdsson, P. & Sigurdsson, B. D. Depletion of soil carbon and aggregation after strong warming of a subarctic Andosol under forest and grassland cover. *SOIL* **6**, 115-129 (2020).
290. Poffenbarger, H. J., et al. Whole-profile soil organic matter content, composition, and stability under cropping systems that differ in belowground inputs. *Agric. Ecosyst. Environ.* **291**, 106810 (2020).
291. Prater, I., et al. How vegetation patches drive soil development and organic matter formation on polar islands. *Geoderma Regional* **27**, e00429 (2021).
292. Prater, I., et al. From fibrous plant residues to mineral-associated organic carbon – the fate of organic matter in Arctic permafrost soils. *Biogeosciences* **17**, 3367-3383 (2020).
293. Puissant, J., et al. Climate change effects on the stability and chemistry of soil organic carbon pools in a subalpine grassland. *Biogeochemistry* **132**, 123-139 (2017).
294. Qi, R., et al. Temperature effects on soil organic carbon, soil labile organic carbon fractions, and soil enzyme activities under long-term fertilization regimes. *Appl. Soil Ecol.* **102**, 36-45 (2016).
295. Qin, W., et al. Responses of soil carbon dynamics to precipitation and land use in an Inner Mongolian grassland. *Plant Soil* **419**, 85-100 (2022).
296. Quiroga, A., Fernández, R. & Noellemeyer, E. Grazing effect on soil properties in



- conventional and no-till systems. *Soil Tillage Res.* **105**, 164-170 (2009).
297. Rahmati, M., et al. Changes in soil organic carbon fractions and residence time five years after implementing conventional and conservation tillage practices. *Soil Tillage Res.* **200**, 104632 (2020).
  298. Rakkar, M. K., et al. Impacts of cattle grazing of corn residues on soil properties after 16 years. *Soil Sci. Soc. Am. J.* **81**, 414-424 (2017).
  299. Ramalho, B., et al. No-tillage and ryegrass grazing effects on stocks, stratification and lability of carbon and nitrogen in a subtropical Umbric Ferralsol. *Eur. J. Soil Sci.* **71**, 1106-1119 (2020).
  300. Ramifehiarivo, N., et al. Comparison of near and mid-infrared reflectance spectroscopy for the estimation of soil organic carbon fractions in Madagascar agricultural soils. *Geoderma Regional* **33**, e00638 (2023).
  301. Ramnarine, R., Voroney, R. P., Dunfield, K. E. & Wagner-Riddle, C. Characterization of the heavy, hydrolysable and non-hydrolysable fractions of soil organic carbon in conventional and no-tillage soils. *Soil Tillage Res.* **181**, 144-151 (2018).
  302. Ramos, M. L. G., et al. Carbon fractions in soil under no-tillage corn and cover crops in the Brazilian Cerrado. *Pesqui. Agropecu. Bras.* **55**, e01743 (2020).
  303. Rasmussen, C., et al. Controls on soil organic carbon partitioning and stabilization in the California sierra nevada. *Soil Systems* **2**, 41 (2018).
  304. Rasmussen, C. & White, D. A., II. Vegetation Effects on Soil Organic Carbon Quality in an Arid Hyperthermic Ecosystem. *Soil Sci.* **175**, 438-446 (2010).
  305. Rehman, S. u., et al. Soil organic carbon sequestration and modeling under conservation tillage and cropping systems in a rainfed agriculture. *Eur. J. Agron.* **147**, 126840 (2023).
  306. Ren, T., et al. Organic fertilization promotes the accumulation of soil particulate organic carbon in a 9-year plantation experiment. *Land Degradation & Development* **34**, 4741-4750 (2023).
  307. Rivero, C., et al. Nitrogen mineralized in anaerobiosis as indicator of soil aggregate stability. *Agron. J.* **112**, 592-607 (2020).
  308. Romaniuk, R., et al. Soil organic carbon, macro- and micronutrient changes in soil fractions with different lability in response to crop intensification. *Soil Tillage Res.*

**181**, 136-143 (2018).

309. Romero, C. M., et al. Tillage-residues affect mineral-associated organic matter on Vertisols in northern Mexico. *Geoderma Regional* **27**, e00430 (2021).
310. Rui, Y., et al. Persistent soil carbon enhanced in Mollisols by well-managed grasslands but not annual grain or dairy forage cropping systems. *Proc. Natl Acad. Sci. USA* **119**, e2118931119 (2022).
311. Sainju, U. M., Caesar-TonThat, T., Lenssen, A. W., Evans, R. G. & Kolberg, R. Long-term tillage and cropping sequence effects on dryland residue and soil carbon fractions. *Soil Sci. Soc. Am. J.* **71**, 1730-1739 (2007).
312. Sainju, U. M., Lenssen, A., Caesar-Thonthat, T. & Waddell, J. Carbon sequestration in dryland soils and plant residue as influenced by tillage and crop rotation. *J. Environ. Qual.* **35**, 1341-1347 (2006).
313. Sainju, U. M., et al. Tillage, crop rotation, and cultural practice effects on dryland soil carbon fractions. *Open J. Soil Sci.* **2**, 242-255 (2012).
314. Salonen, A.-R., et al. Assessing the effect of arable management practices on carbon storage and fractions after 24 years in boreal conditions of Finland. *Geoderma Regional* **34**, e00678 (2023).
315. Samal, S. K., et al. Five years' exposure of elevated atmospheric CO<sub>2</sub> and temperature enriched recalcitrant carbon in soil of subtropical humid climate. *Soil Tillage Res.* **203**, 104707 (2020).
316. Samson, M.-E., et al. Management practices differently affect particulate and mineral-associated organic matter and their precursors in arable soils. *Soil Biol. Biochem.* **148**, 107867 (2020).
317. Samson, V. M., et al. Evaluation of long-term organic carbon dynamics and organic matter stability in a cultivated paddy soil using a carbon and nitrogen stable isotopes-based model. *Soil Tillage Res.* **239**, 106040 (2024).
318. Santos, E. R. S., et al. Particulate soil organic matter in bahiagrass–rhizoma peanut mixtures and their monocultures. *Soil Sci. Soc. Am. J.* **83**, 658-665 (2019).
319. Sato, J. H., et al. Understanding the relations between soil organic matter fractions and N<sub>2</sub>O emissions in a long-term integrated crop–livestock system. *Eur. J. Soil Sci.* **70**, 1183-1196 (2019).
320. Schiedung, H., et al. Spatial controls of topsoil and subsoil organic carbon turnover

- under C<sub>3</sub>–C<sub>4</sub> vegetation change. *Geoderma* **303**, 44-51 (2017).
321. Schneckner, J., Borken, W., Schindlbacher, A. & Wanek, W. Little effects on soil organic matter chemistry of density fractions after seven years of forest soil warming. *Soil Biol. Biochem.* **103**, 300-307 (2016).
322. Schrumpf, M., et al. Storage and stability of organic carbon in soils as related to depth, occlusion within aggregates, and attachment to minerals. *Biogeosciences* **10**, 1675-1691 (2013).
323. Schulze, K., Borken, W., Muhr, J. & Matzner, E. Stock, turnover time and accumulation of organic matter in bulk and density fractions of a Podzol soil. *Eur. J. Soil Sci.* **60**, 567-577 (2009).
324. Semenov, V. M., et al. Pools and fractions of organic carbon in soil: structure, functions and methods of determination. *The Journal of Soils and Environment* **6**, 4-19 (2023).
325. Semenov, V. M., Lebedeva, T. N. & Pautova, N. B. Particulate organic matter in noncultivated and arable Soils. *Eurasian Soil Sci.* **52**, 396-404 (2019).
326. Semenov, V. M., et al. Measurement of the soil organic carbon pools isolated using bio-physical-chemical fractionation methods. *Eurasian Soil Sci.* **56**, 1327-1342 (2023).
327. Shang, W., et al. Soil organic matter fractions under different vegetation types in permafrost regions along the Qinghai-Tibet Highway, north of Kunlun Mountains, China. *J. Mountain Sci.* **12**, 1010-1024 (2015).
328. Shen, A., et al. Effects of desert plant communities on soil enzyme activities and soil organic carbon in the proluvial fan in the eastern foothills of the Helan Mountain in Ningxia, China. *J. Arid. Land* **16**, 725-737 (2024).
329. Shi, J., et al. Mechanisms controlling the stability and sequestration of mineral associated organic carbon upon erosion and deposition. *CATENA* **242**, 108119 (2024).
330. Shi, J., et al. Recalcitrant organic carbon plays a key role in soil carbon sequestration along a long-term vegetation succession on the Loess Plateau. *CATENA* **233**, 107528 (2023).
331. Silveira, M. L., Liu, K., Sollenberger, L. E., Follett, R. F. & Vendramini, J. M. B. Short-term effects of grazing intensity and nitrogen fertilization on soil organic carbon pools under perennial grass pastures in the southeastern USA. *Soil Biol.*

*Biochem.* **58**, 42-49 (2013).

332. Singh, A. K., et al. Tree growth rate regulate the influence of elevated CO<sub>2</sub> on soil biochemical responses under tropical condition. *J. Environ. Manage.* **231**, 1211-1221 (2019).
333. Sleutel, S., De Neve, S., Németh, T., Tóth, T. & Hofman, G. Effect of manure and fertilizer application on the distribution of organic carbon in different soil fractions in long-term field experiments. *Eur. J. Agron.* **25**, 280-288 (2006).
334. Smith Jacques, D. V., Strauss Johann, A. & Hardie Ailsa, G. Effects of long-term grazed crop and pasture systems under no-till on organic matter fractions and selected quality parameters of soil in the Overberg, South Africa. *S. Afr. J. Plant Soil* **37**, 1-10 (2020).
335. Somasundaram, J., Reeves, S., Wang, W., Heenan, M. & Dalal, R. Impact of 47 years of no tillage and stubble retention on soil aggregation and carbon distribution in a vertisol. *Land Degradation & Development* **28**, 1589-1602 (2017).
336. Song, B., et al. Light and heavy fractions of soil organic matter in response to climate warming and increased precipitation in a temperate steppe. *PLoS One* **7**, e33217 (2012).
337. Soong, J. L., et al. Soil properties explain tree growth and mortality, but not biomass, across phosphorus-depleted tropical forests. *Sci. Rep.* **10**, 2302 (2020).
338. Soucémarianadin, L. N., Quideau, S. A. & MacKenzie, M. D. Pyrogenic carbon stocks and storage mechanisms in podzolic soils of fire-affected Quebec black spruce forests. *Geoderma* **217-218**, 118-128 (2014).
339. Startsev, V. V., Khaydapova, D. D., Degteva, S. V. & Dymov, A. A. Soils on the southern border of the cryolithozone of European part of Russia (the Subpolar Urals) and their soil organic matter fractions and rheological behavior. *Geoderma* **361**, 114006 (2020).
340. Startsev, V. V., Mazur, A. S. & Dymov, A. A. The content and composition of organic matter in soils of the subpolar Urals. *Eurasian Soil Sci.* **53**, 1726-1734 (2020).
341. Stewart, C. E., Halvorson, A. D. & Delgado, J. A. Long-term N fertilization and conservation tillage practices conserve surface but not profile SOC stocks under semi-arid irrigated corn. *Soil Tillage Res.* **171**, 9-18 (2017).
342. Su, Y. Soil carbon and nitrogen sequestration following cropland to forage

- grassland conversion in the marginal land in the middle of Heihe River Basin, Northwest China. *Environmental Science* **27**, 1312-1318 (2006).
343. Su, Z., et al. Vegetation restoration altered the soil organic carbon composition and favoured its stability in a Robinia pseudoacacia plantation. *Sci. Total Environ.* **899**, 165665 (2023).
344. Sun, Q., Meyer, W. S., Koerber, G. R. & Marschner, P. Response of microbial activity to labile C addition in sandy soil from semi-arid woodland is influenced by vegetation patch and wildfire. *J. Soil Sci. Plant Nutr.* **17**, 62-73 (2017).
345. Sun, Q., et al. Responses of microbial necromass carbon and microbial community structure to straw-and straw-derived biochar in brown earth soil of northeast China. *Front. Microbiol.* **13**, 967746 (2022).
346. Sun, S., et al. Depth-dependent response of particulate and mineral-associated organic carbon to long-term throughfall reduction in a subtropical natural forest. *CATENA* **223**, 106904 (2023).
347. Sun, T., et al. Nitrogen addition increased soil particulate organic carbon via plant carbon input whereas reduced mineral-associated organic carbon through attenuating mineral protection in agroecosystem. *Sci. Total Environ.* **899**, 165705 (2023).
348. Sun, X., Niu, J. & Zhao, G. Effects of previous crop stubbles and nitrogen applied amount on summer maize yield and soil organic carbon pool at a semiarid loess site of China. *Agricultural Research in the Arid Areas* **36**, 19-27 (2018).
349. Surey, R., et al. Differences in labile soil organic matter explain potential denitrification and denitrifying communities in a long-term fertilization experiment. *Appl. Soil Ecol.* **153**, 103630 (2020).
350. Tang, H., et al. Interplay of soil characteristics and arbuscular mycorrhizal fungi diversity in alpine wetland restoration and carbon stabilization. *Front. Microbiol.* **15**, 1376418 (2024).
351. Teixeira, C. d. S., et al. Frequent defoliation of perennial legume-grass bicultures alters soil carbon dynamics. *Plant Soil* **490**, 423-434 (2023).
352. Teklay, T. & Chang, S. X. Temporal changes in soil carbon and nitrogen storage in a hybrid poplar chronosequence in northern Alberta. *Geoderma* **144**, 613-619 (2008).
353. Tian, J., Lu, S., Fan, M., Li, X. & Kuzyakov, Y. Integrated management systems

- and N fertilization: effect on soil organic matter in rice-rapeseed rotation. *Plant Soil* **372**, 53-63 (2013).
354. Tian, Q., et al. Variation of soil carbon accumulation across a topographic gradient in a humid subtropical mountain forest. *Biogeochemistry* **149**, 337-354 (2020).
  355. Tivet, F., et al. Soil organic carbon fraction losses upon continuous plow-based tillage and its restoration by diverse biomass-C inputs under no-till in sub-tropical and tropical regions of Brazil. *Geoderma* **209-210**, 214-225 (2013).
  356. Turchenek, L. W. & Oades, J. M. Fractionation of organo-mineral complexes by sedimentation and density techniques. *Geoderma* **21**, 311-343 (1979).
  357. van der Pol, L. K., et al. Addressing the soil carbon dilemma: Legumes in intensified rotations regenerate soil carbon while maintaining yields in semi-arid dryland wheat farms. *Agric. Ecosyst. Environ.* **330**, 107906 (2022).
  358. Veloso, M. G., Angers, D. A., Chantigny, M. H. & Bayer, C. Carbon accumulation and aggregation are mediated by fungi in a subtropical soil under conservation agriculture. *Geoderma* **363**, 114159 (2020).
  359. Viaud, V., Angers, D. A., Parnaudeau, V., Morvan, T. & Aubry, S. M. Response of organic matter to reduced tillage and animal manure in a temperate loamy soil. *Soil Use Manage.* **27**, 84-93 (2011).
  360. Vormstein, S., Kaiser, M., Piepho, H. P. & Ludwig, B. Aggregate formation and organo-mineral association affect characteristics of soil organic matter across soil horizons and parent materials in temperate broadleaf forest. *Biogeochemistry* **148**, 169-189 (2020).
  361. Wan, X., et al. Soil C:N ratio is the major determinant of soil microbial community structure in subtropical coniferous and broadleaf forest plantations. *Plant Soil* **387**, 103-116 (2015).
  362. Wander, M. M., Bidart, M. G. & Aref, S. Tillage impacts on depth distribution of total and particulate organic matter in three Illinois soils. *Soil Sci. Soc. Am. J.* **62**, 1704-1711 (1998).
  363. Wang, B., et al. Initial soil formation by biocrusts: nitrogen demand and clay protection control microbial necromass accrual and recycling. *Soil Biol. Biochem.* **167**, 108607 (2022).
  364. Wang, D., Wu, X., Cai, C. & Yang, W. Composition of organic carbon and their relationship with aggregate stability in red soil under different fertilizer application.

*Science of Soil and Water Conservation* **14**, 61-70 (2016).

365. Wang, F., Ma, R., Xia, K., Wen, Z. & Xu, X. Response of soil labile organic carbon fractions to forest conversions. *Research of Soil and Water Conservation* **30**, 233-240 (2023).
366. Wang, H., Wang, X. & Tian, X. Effect of straw-returning on the storage and distribution of different active fractions of soil organic carbon. *Chinese Journal of Applied Ecology* **25**, 3491-3498 (2014).
367. Wang, H., Wu, J., Li, G., Yan, L. & Liu, S. Effects of extreme rainfall frequency on soil organic carbon fractions and carbon pool in a wet meadow on the Qinghai-Tibet Plateau. *Ecol. Indic.* **146**, 109853 (2023).
368. Wang, M., et al. Effects of exogenous organic/inorganic nitrogen addition on carbon pool distribution and transformation in grassland soil. *Sci. Total Environ.* **858**, 159919 (2023).
369. Wang, R., et al. Response of soil carbon to nitrogen and water addition differs between labile and recalcitrant fractions: evidence from multi-year data and different soil depths in a semi-arid steppe. *CATENA* **172**, 857-865 (2019).
370. Wang, W., Wang, Q. & Lu, Z. Soil organic carbon and nitrogen content of density fractions and effect of meadow degradation to soil carbon and nitrogen of fractions in alpine Kobresia meadow. *Science in China Series D: Earth Sciences* **52**, 660-668 (2009).
371. Wang, X., et al. Effects of alternative fertilization practices on components of the soil organic carbon pool and yield stability in rain-fed maize production on the Loes Plateau. *Acta Prataculturae Sinica* **29**, 58-69 (2020).
372. Wang, X., Wanh, J., Liu, J. & Mao, N. Accumulation of soil black carbon and particulate organic carbon in the recovery stage of *Sea buckthorn* plantation on Loes Plateau. *J. Soil Water Conserv.* **27**, 250-254 (2013).
373. Wang, Y., et al. Mineral protection controls soil organic carbon stability in permafrost wetlands. *Sci. Total Environ.* **869**, 161864 (2023).
374. Wang, Y., Ruan, H., Huang, L., Feng, Q. & Qi, Y. Soil labile organic carbon of different land use types in a reclaimed land area of Taihu Lake. *Chinese Journal of Ecology* **29**, 741-748 (2010).
375. Wang, Y., et al. Effects of different soil conservation measures on soil organic carbon pools in *Nectarine* orchard. *Journal of Agro-Environment Science* **33**, 803-

809 (2014).

376. Wang, Y. & Zhang, M. Distribution characters of particulate organic carbon and black carbon in soils under different forestry vegetations. *Journal of Zhejiang University (Agriculture & Life Sciences)* **37**, 193-202 (2011).
377. Wei, C., et al. Soil aggregation accounts for the mineral soil organic carbon and nitrogen accrual in broadleaved forests as compared to that of coniferous forests in Northeast China: Cross-sites and multiple species comparisons. *Land Degradation & Development* **32**, 296-309 (2021).
378. Wei, H., et al. A quantitative study of the influence of soil organic carbon and pore characteristics on the stability of aggregates of the karst peak-cluster depression area in Southwest China. *J. Soils Sediments* **23**, 312-330 (2023).
379. Wei, H., et al. Grass cultivation alters soil organic carbon fractions in a subtropical orchard of southern China. *Soil Tillage Res.* **181**, 110-116 (2018).
380. Wen, Y., et al. Organic carbon preservation promoted by aromatic compound-iron complexes through manure fertilization in red soil. *J. Soils Sediments* **21**, 295-306 (2021).
381. Wenxiu, Z., et al. Effect of long-term application of organic manure in different amounts on the distribution of particulate organic matter and the contents of carbon and nitrogen in a mollisol. *Soils* **48**, 442-448 (2016).
382. Williams, E. K., Fogel, M. L., Berhe, A. A. & Plante, A. F. Distinct bioenergetic signatures in particulate versus mineral-associated soil organic matter. *Geoderma* **330**, 107-116 (2018).
383. Wu, J., Ai, L., Tian, Z. & Chang, X. The soil particulate organic carbon in different elevation and its relationship with vegetation in Qilian Mountain. *Ecology and Environment* **17**, 2358-2365 (2008).
384. Wu, J., et al. Responses of CH<sub>4</sub> flux and microbial diversity to changes in rainfall amount and frequencies in a wet meadow in the Tibetan Plateau. *CATENA* **202**, 105253 (2021).
385. Wu, P., Wang, J., Li, L. & Wang, X. Effects of organic materials applications on soil organic carbon fractions and nutrient contents in lime concretion black soil under chemical fertilizer reduction. *Acta Agriculturae Nucleatae Sinica* **36**, 2286-2294 (2022).
386. Wu, R., Wang, Y., Li, F. & Li, X. Effects of coupling film-mulched furrow-ridge



- cropping with maize straw soil-incorporation on maize yields and soil organic carbon pool at a semiarid loess site of China. *Acta Ecol. Sin.* **32**, 2855-2862 (2012).
387. Wu, X., Li, Y., Li, Z., Wang, Z. & Fan, M. Effects of land use type on soil total organic carbon and soil labile organic carbon in Naban River watershed. *Ecology and Environment* **22**, 6-11 (2013).
  388. Wu, Y., et al. Responses of soil nitrogen in different soil organic matter fractions to long-term nitrogen addition in a semi-arid grassland. *Chinese Journal of Plant Ecology* **45**, 790-798 (2021).
  389. Wu, Y., et al. The different factors driving SOC stability under different N addition durations in a *Phyllostachys edulis* forest. *Forests* **14**, 1890 (2023).
  390. Wyngaard, N., Echeverría, H. E., Rozas, H. R. S. & Divito, G. A. Fertilization and tillage effects on soil properties and maize yield in a southern Pampas Argiudoll. *Soil Tillage Res.* **119**, 22-30 (2012).
  391. Xi, D., Yu, Z., Xiong, Y., Liu, X. & Liu, J. Soil organic carbon fractions of evergreen broadleaved forests in Guanshan Mountain, Jiangxi, China, along altitude. *Chinese Journal of Applied Ecology* **31**, 3349-3356 (2020).
  392. Xiang, H., Zhang, L. & Wen, D. Change of soil carbon fractions and water-Stable aggregates in a forest ecosystem succession in South China. *Forests* **6**, 2703-2718 (2015).
  393. Xu, J., Gao, L., Sun, Y. & CUui, X. Distribution of mineral-bonded organic carbon and black carbon in forest soils of Great Xing'an Mountains, China and carbon sequestration potential of the soils *Acta Pedologica Sinica* **55**, 236-246 (2018).
  394. Xu, M., et al. Alteration in enzymatic stoichiometry controls the response of soil organic carbon dynamic to nitrogen and water addition in temperate cultivated grassland. *Eur. J. Soil Biol.* **101**, 103248 (2020).
  395. Xu, S., Lu, X., Zhou, M., Sui, Y. & Jiao, X. Effects of straw deep burial combined with nitrogen fertilizer on organic carbon components and nutrients in Bback soils. *Journal of Henan Agricultural Sciences* **51**, 63-72 (2022).
  396. Xu, W., et al. Distribution of organic carbon and particulate organic carbon in water-stable aggregates of paddy soil in black soil Aarea. *J. Soil Water Conserv.* **30**, 210-215 (2016).
  397. Xu, W., et al. Effects of cultivation on organic carbon fractionation and aggregate stability in Xinjiang oasis soils. *Acta Ecol. Sin.* **30**, 1773-1779 (2010).

398. Xu, X., Jin, Y., Xu, J., Zhang, Y. & Yang, J. Effects of herbaceous plant encroachment on the soil carbon pool in the shrub tundra of the Changbai mountains. *Forests* **16**, 197 (2025).
399. Xu, Y., et al. The efficiency and stability of soil organic carbon sequestration by perennial energy crops cultivation on marginal land depended on root traits. *Soil Tillage Res.* **235**, 105909 (2024).
400. Yan, M., Zhang, X., Liu, K., Lou, Y. & Wang, Y. Particle size primarily shifts chemical composition of organic matter under long-term fertilization in paddy soil. *Eur. J. Soil Sci.* **73**, e13170 (2022).
401. Yan, X. & An, H. Response of unprotected soil organic carbon to desertification in desert grassland. *Acta Ecol. Sin.* **38**, 2846-2854 (2018).
402. Yang, C., et al. Effects of management measures on organic carbon, nitrogen and chemical structure of different soil fractions in *Phyllostachys edulis* plantations. *Chinese Journal of Applied Ecology* **31**, 25-34 (2020).
403. Yang, K., et al. Effects of continuous nitrogen addition on microbial properties and soil organic matter in a *Larix gmelinii* plantation in China. *J. For. Res.* **29**, 85-92 (2018).
404. Yang, L., Song, X., Lyu, S., Shen, W. & Gao, Y. Dynamics and fractions of soil organic carbon in response to 35 years of afforestation in subtropical China. *Plant Soil* **500**, 481-494 (2024).
405. Yang, W., et al. Natural revegetation over ~ 160 years alters carbon and nitrogen sequestration and stabilization in soil organic matter on the Loess Plateau of China. *CATENA* **220**, 106647 (2023).
406. Yang, X. M. & Kay, B. D. Impacts of tillage practices on total, loose- and occluded-particulate, and humified organic carbon fractions in soils within a field in southern Ontario. *Can. J. Soil Sci.* **81**, 149-156 (2001).
407. Yang, Y., et al. Responses of soil particulate organic carbon and nitrogen along an altitudinal gradient on the Helan Mountain, Inner Mongolia. *Acta Prataculturae Sinica* **21**, 54-60 (2012).
408. Yeasmin, S., et al. Effect of land use on organic carbon storage potential of soils with contrasting native organic matter content. *Int. J. Agron.* **2020**, 8042961 (2020).

409. Yeasmin, S., Singh, B. P., Johnston, C. T., Hua, Q. & Sparks, D. L. Changes in particulate and mineral-associated organic carbon with land use in contrasting soils. *Pedosphere* **33**, 421-435 (2023).
410. Yin, Y., et al. Contents of soil organic carbon and components in three types of forests in the mountain area of Eastern Liaoning. *Chinese Journal of Ecology* **37**, 2100 (2018).
411. Yonekura, Y., et al. Soil organic matter dynamics in density and particle-size fractions following destruction of tropical rainforest and the subsequent establishment of Imperata grassland in Indonesian Borneo using stable carbon isotopes. *Plant Soil* **372**, 683-699 (2013).
412. Yu, M., et al. Soil organic carbon stabilization Is dominated by non-sorptive process among the subsoils from different parent material. *J. Geophys. Res.: Biogeosci.* **128**, e2022JG007286 (2023).
413. Yu, Q., et al. Secondary shrubs promoted the priming effect by increasing soil particle organic carbon mineralization. *Front. For. Global Change* **6**, 1288259 (2023).
414. Yuan, M.-t., et al. Effects of swine manure biochar application on the content and chemical structure of particulate and mineral-associated organic carbon in acidic and calcareous paddy soils. *Journal of Plant Nutrition and Fertilizers* **30**, 441-456 (2024).
415. Yuan, X., et al. Plant and microbial regulations of soil carbon dynamics under warming in two alpine swamp meadow ecosystems on the Tibetan Plateau. *Sci. Total Environ.* **790**, 148072 (2021).
416. Yuan, X., et al. Sensitivity of soil carbon dynamics to nitrogen and phosphorus enrichment in an alpine meadow. *Soil Biol. Biochem.* **150**, 107984 (2020).
417. Yuan, Y., et al. Effects of amendments on labile organic carbon and soil enzymes activities in upland eed soil. *Soils* **49**, 909-918 (2017).
418. Yuan, Z., et al. Tree diversity increases soil C and N stocks of secondary forests in subtropical China. *CATENA* **222**, 106812 (2023).
419. Yuan, Z.-Q. & Jiang, X.-J. Vegetation and soil covariation, not grazing exclusion, control soil organic carbon and nitrogen in density fractions of alpine meadows in a Tibetan permafrost region. *CATENA* **196**, 104832 (2021).
420. Yuan, Z.-Q., et al. Pasture degradation impact on soil carbon and nitrogen fractions

- of alpine meadow in a Tibetan permafrost region. *J. Soils Sediments* **20**, 2330-2342 (2020).
421. Yue, Y., Men, X., Sun, Z. & Chen, X. Exploring the role of stumps in soil ecology: a study of microsite organic carbon and enzyme activities in a *Larix olgensis* Henry plantation. *Forests* **14**, 1027 (2023).
  422. Zagal, E., Córdova, C., Sohi, S. P. & Powlson, D. S. Free and intra-aggregate organic matter as indicators of soil quality change in volcanic soils under contrasting crop rotations. *Soil Use Manage.* **29**, 531-539 (2013).
  423. Zagal, E., Muñoz, C., Quiroz, M. & Córdova, C. Sensitivity of early indicators for evaluating quality changes in soil organic matter. *Geoderma* **151**, 191-198 (2009).
  424. Zhang, A., et al. Biochar more than stubble management affected carbon allocation and persistence in soil matrix: a 9-year temperate cropland trial. *J. Soils Sediments* **23**, 3018-3028 (2023).
  425. Zhang, B., et al. Response of soil organic carbon and its fractions to natural vegetation restoration in a tropical karst area, southwest China. *Front. For. Global Change* **6**, 1172062 (2023).
  426. Zhang, J., Zhang, F. & Chang, H. Duration of continuous cropping with straw return affects soil organic carbon. *Soil Use Manage.* **39**, 1096-1108 (2023).
  427. Zhang, J., Zhang, F. & Yang, L. Continuous straw returning enhances the carbon sequestration potential of soil aggregates by altering the quality and stability of organic carbon. *J. Environ. Manage.* **358**, 120903 (2024).
  428. Zhang, J., et al. Nitrogen deposition enhances soil organic carbon and microbial residual carbon in a tropical forest. *Plant Soil* **484**, 217-235 (2023).
  429. Zhang, L., et al. Infrared spectroscopy prediction of organic carbon and total nitrogen in soil and particulate organic matter from diverse Canadian agricultural regions. *Can. J. Soil Sci.* **98**, 77-90 (2018).
  430. Zhang, M., Xin, Y. & Zhao, Y. Impact of burning on soil organic carbon fractions in *Pinus sylvestris* var. *mongolica* natural forest of Great Xing'an Mountains. *J. Soil Water Conserv.* **30**, 322-326 (2016).
  431. Zhang, P., Li, X., Li, y. & Yin, P. Effects of vegetation restoration on soil organic carbon and total nitrogen contents in the alpine agro-pastoral ecotone. *Journal of Gansu Agricultural University* **42**, 98-102 (2007).

432. Zhang, S., et al. Effects of conservation tillage on active soil organic carbon composition. *J. Soil Water Conserv.* **29**, 226-231+252 (2015).
433. Zhang, X., et al. Change of soil organic carbon fractions at different successional stages of *Betula platyphylla* forest in Changbai Mountains. *Chinese Journal of Ecology* **35**, 282-289 (2016).
434. Zhang, X., et al. Responses of soil organic carbon and its labile fractions to nitrogen and phosphorus additions in *Cunninghamia lanceolata* plantations in subtropical China. *Chinese Journal of Applied Ecology* **28**, 449-455 (2017).
435. Zhang, Y., et al. Differential effects of forest-floor litter and roots on soil organic carbon formation in a temperate oak forest. *Soil Biol. Biochem.* **180**, 109017 (2023).
436. Zhang, Y., Zeng, D., Lei, Z., Li, X. & Lin, G. Microbial properties determine dynamics of topsoil organic carbon stocks and fractions along an age-sequence of Mongolian pine plantations. *Plant Soil* **483**, 441-457 (2023).
437. Zhang, Y.-H., Li, Y., Zhou, Y., Chen, Y.-J. & An, S.-S. Changes of soil nutrients and organic carbon fractions in *Caragana korshinskii* forests with different restoration years in mountainous areas of southern Ningxia, China. *The journal of applied ecology* **35**, 639-647 (2024).
438. Zhang, Z., et al. The effect of thinning intensity on the soil carbon pool mediated by soil microbial communities and necromass carbon in coastal zone protected forests. *Sci. Total Environ.* **881**, 163492 (2023).
439. Zhang, Z., Kaye, J. P., Bradley, B. A., Amsili, J. P. & Suseela, V. Cover crop functional types differentially alter the content and composition of soil organic carbon in particulate and mineral-associated fractions. *Glob. Change Biol.* **28**, 5831-5848 (2022).
440. Zhao, G., et al. Elevated CO<sub>2</sub> decreases soil carbon stability in Tibetan Plateau. *Environ. Res. Lett.* **15**, 114002 (2020).
441. Zhao, P., Chen, X. & Wang, E. Responses of accumulation-loss patterns for soil organic carbon and its fractions to tillage and water erosion in black soil area. *Chinese Journal of Applied Ecology* **28**, 3634-3642 (2017).
442. Zhao, Q., et al. Asymmetric effects of litter removal and litter addition on the structure and function of soil microbial communities in a managed pine forest. *Plant Soil* **414**, 81-93 (2017).

443. Zhao, Y., et al. Sphagnum increases soil's sequestration capacity of mineral-associated organic carbon via activating metal oxides. *Nat. Commun.* **14**, 5052 (2023).
444. Zhao, Y., Zhang, W., Hu, P., Xiao, J. & Wang, K. Responses of soil organic carbon fractions to different vegetation restoration in a typical karst depression. *Acta Ecol. Sin.* **41**, 8535-8544 (2021).
445. Zhao, Z., Zhao, Z., Fu, B., Wang, J. & Tang, W. Characteristics of soil organic carbon fractions under different land use patterns in a tropical area. *J. Soils Sediments* **21**, 689-697 (2021).
446. Zheng, Y., et al. Nitrogen addition increases the glucose-induced priming effect of the particulate but not the mineral-associated organic carbon fraction. *Soil Biol. Biochem.* **184**, 109106 (2023).
447. Zhong, Y., Yan, W. & Shangguan, Z. Soil carbon and nitrogen fractions in the soil profile and their response to long-term nitrogen fertilization in a wheat field. *CATENA* **135**, 38-46 (2015).
448. Zhou, Y., Zhang, Z., Zhang, J., Zhao, M. & He, N. Changes in soil particulate organic carbon and their response to changing environments on the Tibetan Plateau, Mongolian Plateau, and Loess Plateau, China. *J. Soil Sci. Plant Nutr.* **23**, 420-430 (2023).
449. Zou, Z., et al. Decadal application of mineral fertilizers alters the molecular composition and origins of organic matter in particulate and mineral-associated fractions. *Soil Biol. Biochem.* **182**, 109042 (2023).